1997

# Direct methods for dynamic monitoring of secretions from single cells by capillary electrophoresis and microscopy with laser-induced native fluorescence detection

Wei Tong
*Iowa State University*

# INFORMATION TO USERS

This manuscript has been reproduced from the microfilm master. UMI films the text directly from the original or copy submitted. Thus, some thesis and dissertation copies are in typewriter face, while others may be from any type of computer printer.

**The quality of this reproduction is dependent upon the quality of the copy submitted.** Broken or indistinct print, colored or poor quality illustrations and photographs, print bleedthrough, substandard margins, and improper alignment can adversely affect reproduction.

In the unlikely event that the author did not send UMI a complete manuscript and there are missing pages, these will be noted. Also, if unauthorized copyright material had to be removed, a note will indicate the deletion.

Oversize materials (e.g., maps, drawings, charts) are reproduced by sectioning the original, beginning at the upper left-hand corner and continuing from left to right in equal sections with small overlaps. Each original is also photographed in one exposure and is included in reduced form at the back of the book.

Photographs included in the original manuscript have been reproduced xerographically in this copy. Higher quality 6" x 9" black and white photographic prints are available for any photographs or illustrations appearing in this copy for an additional charge. Contact UMI directly to order.

**UMI**

A Bell & Howell Information Company
300 North Zeeb Road, Ann Arbor MI 48106-1346 USA
313/761-4700 800/521-0600

# Direct methods for dynamic monitoring of secretions from single cells by capillary electrophoresis and microscopy with laser-induced native fluorescence detection

by

Wei Tong

A dissertation submitted to the graduate faculty

in partial fulfillment of the requirements for the degree of

DOCTOR OF PHILOSOPHY

Major: Analytical Chemistry

Major Professor: Edward S. Yeung

Iowa State University

Ames, Iowa

1997

Graduate College
Iowa State University

This is to certify that the Doctoral dissertation of

Wei Tong

has met the dissertation requirements of Iowa State University

Signature was redacted for privacy.

Major Professor

Signature was redacted for privacy.

For the Major Program

Signature was redacted for privacy.

For the Graduate College

# TABLE OF CONTENTS

## ABSTRACT

Microscale separation and detection methods for real-time monitoring of dynamic cellular processes (e.g., secretion) by capillary electrophoresis (CE) and microscopic imaging were developed. Ultraviolet laser-induced native fluorescence (LINF) provides simple, sensitive and direct detection of neurotransmitters and proteins without any derivatization.

An on-column CE-LINF protocol for quantification of the release from single cell was demonstrated. Quantitative measurements of both the amount of insulin released from and the amount remaining in the cell (βTC3) were achieved simultaneously.

Secretion of catecholamines (norepinephrine (NE) and epinephrine (E)) from individual bovine adrenal chromaffin cells was determined using the on-column CE-LINF. No apparent relationship was found between the ratio of NE/E released and the original ratio of NE/E in the cell. Temporal information about the release was traced out with a dynamic stimulating method by pumping secretagogue continuously passing the cell with the aid of electroosmotic flow and measuring the peak broadening of the released catecholamines in the electropherogram.

Direct visualization of the secretion process of individual bovine adrenal chromaffin cells was achieved by LINF imaging microscopy with high temporal and spatial resolution. Large variations were found among cells in the amount of catecholamines secreted and the rate of secretion. Local heterogeneity in the rate of secretion was also found.

The secretion of serotonin from individual leech Retzius neurons was directly characterized by LINF microscopy with high spatial resolution. The results from images of co-cultured pressure sensory (P) (non-serotonergic) and Retzius (serotonergic) cells, as well as capillary electrophoresis, suggested that the major native fluorescence excited by the laser was derived from intracellular serotonin. A much more substantial release of serotonin was

found at the axon stump left during cell isolation, a preferred region for synapse formation. The release of serotonin was also characterized to be calcium dependent.

# GENERAL INTRODUCTION

## Dissertation Organization

This dissertation begins with a general introduction of recent progress in the area of single-cell chemical analysis with a list of cited references. The following chapters are arranged in such a way that published papers or manuscripts submitted or in preparation to be submitted are each presented as separate chapters. These chapters are followed by a general conclusion. References for each paper and manuscript are at the end of the chapter in which they are cited.

## Single-Cell Chemical Analysis

In recent years, single-cell chemical analysis has received considerable interest. Because of the ultrasmall sample volume and the concomitantly low absolute amount of analyte involved, chemical analysis of single cells is challenging for analytical chemist. Since some of the early work in late 80's and early 90's [1-5], a number of review articles [6-13] have been published summarizing the separation based and voltammetric or amperometric microelectrode based methods for single-cell chemical analysis.

There are several reasons that single-cell analysis is considered important. First, because of the high heterogeneity among individual cells, it is important to understand the variability between cells, from chemical composition to physiological response. This is then related to their overall biological functionality. Second, cells, especially endocrine and neurological cells, also exist in an extremely heterogeneous environment: the cells we are interested in usually coexist with other cells and therefore are exposed to a mixture of hormones and neurotransmitters released from neighboring cells. Single-cell analysis has the inherent advantage that it provides a controlled environment precluding the influence of other

cells. This is extremely important for the understanding of the dynamic cellular processes such as secretion, uptake and metabolism. Third, single-cell analysis is also potentially useful as a powerful early diagnostic tool. It is well known that if cells are analyzed individually, the chance of finding abnormal cells or the cells that carry certain biological markers for certain diseases is substantially greater. This a big advantage over conventional bulk analysis where a large population of cells is used. The effect of the lower number of abnormal cells present at the early stages of diseases are usually masked by the majority healthy cells.

Although membrane capacitance measurements with the patch-clamp technique [14] provides a fast means to measure the extent of exocytosis by measuring the change of surface area caused by fusion of secretory vesicles with cell membrane, it is a physical or indirect method and therefore will not be discussed further here. Separation-based methods (microcolumn liquid chromatography and capillary electrophoresis), electrochemical methods using microelectrodes (amperometry and fast scan voltammetry) and microscopic imaging methods are among the most common methods used for single-cell chemical analysis. In the remainder of this introduction, the recent advances and future prospects in these areas are discussed.

**Separation-Based Methods**

Microcolumn separation methods, especially capillary electrophoresis (CE) are well suited for single-cell analysis because: 1) the small dimension of the capillary column is compatible with the small "sample" volume of a single cell and dilution by the running buffer is avoided; 2) the extremely high separation efficiency ($10^5$ - $10^6$ theoretical plates) and fastness allows for the separation of complex constituents from inside a single cell in a short time scale; 3) the capillary column itself can be used as the site of single-cell manipulation,

such as derivatization of cellular components or physiological stimulation (secretion or uptake), prior to detection.

Electrochemical detection provides sensitive detection for electroactive cellular species [9]. Many works on single-cell analysis were performed using amperometric detection after microcolumn LC and CE separation. A species is detected if it is oxidized at the potential of the electrode and results in a current response. The detection limit is as low as attomole to zeptomole level. Neurotransmitters were quantitatively analyzed in cytoplasmic injections from single neurons in pond snail *Planorbis corneus* and land snail *Helix aspersa* using microcolumn LC and CE with electrochemical detections [1, 2, 6, 15-17]. Catecholamines in single mammalian adrenal medullary cells as well as their secretion were quantified by microcolumn LC with electrochemical detection [18, 19]. Analysis of single neurons in *P. corneus* by CE with electrochemical detection was used to provide evidence supporting a two-compartment model for neurotransmitters in single nerve cells [20]. CE with scanning electrochemical detection was also used to identify the identity of the species by its voltammetric characteristics [16, 21]. Derivatization with naphthalene-2,3-dicarboxaldehyde (NDA) prior to analysis extends the scope of electrochemical detection to some non-electroactive species such as some amino acids with attomole detection limits [22].

Laser-induced fluorescence (LIF) is another well-established detection mechanism for single-cell analysis [23]. Many biomolecules including biogenic amines, some proteins, alkaloids, vitamins and steroids will fluoresce naturally when excited with suitable wavelengths [24]. Many proteins (such as hemoglobin, methemoglobin, carbonic anhydrase, hemoglobin variants and insulin, etc.) that have tryptophan and/or tyrosine residues can be quantified at the single cell level by CE using UV laser (usually 275 nm) excited native fluorescence detection [5, 25-28]. Cellular neurotransmitters (such as catecholamine, serotonin) and steroids were also detected using CE and laser-induced native fluorescence

(LINF) [29, 30]. Since LINF is a direct detection method, it avoids the problem of incomplete derivatization reactions or slow derivatization kinetics and therefore extremely useful for dynamic monitoring of single cell events such as secretion or uptake. Exocytotic release of serotonin, insulin and catecholamine from single mast cells, pancreatic β-cells and adrenal chromaffin cells were quantitatively monitored by CE-LINF [31-33]. Although the quantum efficiency of native fluorescence is usually low, by selecting the appropriate pH and avoiding band broadening plus the sensitivity of LIF, one can still achieve detection limits in the range of $10^{-10}$ M or $10^{-19}$ mole.

However, for the majority of biomolecules which cannot fluoresce naturally, derivatization with a fluorophore is often used either in pre-column, on-column or post-column mode with detection limits as low as $10^{-18}$ - $10^{-21}$ moles [34]. Pre-column derivatization of single cells with NDA was used to identify several amine containing analytes in individual snail neurons [2] and bovine adrenal medullary cells [35]. On-column derivatization uses the inlet end of the capillary as the reaction chamber. Thiols inside single human red blood cells were derivatized on-column with monobromobimane (mBBr) transported through the cell membrane [5]. Individual pheochromocytoma (PC12) cells were analyzed by CE after on-column derivatization with NDA [36]. The advantage of on-column derivatization over pre-column derivatization is that the sample dilution is limited by the size of the capillary and the only source of dilution is the diffusion of the analytes along the capillary bore which is usually very small. Post-column derivatization is one of the ways to solve the multiple labeling problem associated with pre-column derivatization. Derivatization reagents (such as o-phthaldialdehyde (OPA), fluorescamine and NDA with 3-mercaptoethanol) that can react rapidly are preferred for post-column derivatization. Amino acids from homogenates of *Planorbis corneus* neurons and hemoglobin in a single human erythrocyte were analyzed after post-column derivatization with NDA [37]. OPA post-

column derivatization using a coaxially connected capillary for the determination of hemoglobin and carbonic anhydrase in single human erythrocytes was also demonstrated [38]. Peptides labeled with fluorescamine [39] and fluorescein isothiocyanate (FITC) [40] were analyzed in single neuron cells. Some of the problems associated with derivatization procedures include: extensive sample handling which can cause loss of analytes and/or contamination; dilution of reaction products which may cause diminished sensitivity; slow reaction kinetics which may cause incomplete reactions and lead to irreproducibility; and, multiple labeling of solutes with several functional groups [34]. A way to circumvent these problems is to use indirect fluorescence detection [41] for non-fluorescent ionic analytes. Intracellular $K^+$, $Na^+$ [5, 42], lactate and pyruvate [43] in single human erythrocytes were all monitored by indirect fluorescence detection.

CE-based enzyme assays are useful for the detection of sub-attomole levels of intracellular species because of the large amplification factors provided by enzymatic reactions [44]. The use of LIF detection further lowers the detection limit and is demonstrated useful for the analysis of LDH isoenzymes in single human erythrocytes [45]. The LIF enzyme assay detection limit for LDH-1 was down to $10^{-21}$ mol (800 molecules). The enzyme assay protocol was applicable to the study of LDH activity, a possible marker for leukemia, in lymphocytes [46]. A particle-counting immunoassay using antibody coated latex particles was miniaturized for capillary electrophoresis to analyze glucose-6-phosphate dehydrogenase (G6PDH) using laser scattering detection [47]. In fact, the activity and concentration of G6PDH from a single human erythrocytes was determined simultaneously with this method [48]. The detection limit of this method is $10^{-21}$ mol of G6PDH (600 molecules). A CE-based immunoassay with LIF detection was used to determine insulin content and secretion from a single islet of Langerhans [49], and an on-line competitive assay system was built to monitor the insulin secretion from a single islet [50].

Radiochemical detection methods involve culturing isolated cells in $^{35}$S-methionine and then detecting the newly synthesized methionine-containing peptides which have incorporated the radiolabel [11]. Peptides in single *Aplysia* neurons, as well as their release, were measured with HPLC methods [51-55]. A postcolumn radionuclide detection method for CE was also developed [56] and applied to measure the neuropeptides in single buccal cells of *Aplysia californica* [57].

Optical detection usually provides relatively little information about the chemical identity of analytes (unless the migration times can be correlated with standards). Mass spectrometry (MS) can provide chemical analysis at the single cell level with the benefit of unsurpassed chemical specificity. Recent developments in CE, electrospray ionization (ESI) and Fourier transform ion cyclotron resonance (FTICR) MS have made direct analysis of cellular proteins possible [58]. In one early report, CE-ESI-FTICR was used to analyze both the $\alpha$ and the $\beta$ chains of hemoglobin acquired from 10 human erythrocytes (corresponding to 4.5 fmol of hemoglobin) [58]. Later, selective ion accumulation techniques based on quadrupolar excitation (QE) was incorporated and the hemoglobin from a single human erythrocytes ($\approx$450 amol) was characterized [59]. Using CE-ESI-FTMS with an ultralow flow rate ($\leq$ 4nL/min), a resolving power of about 60,000 for injection of 0.7 to 3 attomole of 8- to 29-kDalton proteins with errors of <1Dalton was achieved [60]. Single human erythrocytes were also analyzed by microspot matrix-assisted laser desorption ionization (MALDI) MS even without separation [61].

**Electrochemical Methods Using Microelectrodes**

Amperometric and fast scan voltammetric methods using microelectrodes provide millisecond time resolution for fast cellular events like exocytosis as well as spatial resolution for measurements in intracellular compartments [62]. The earliest uses of

microelectrodes were for *in vivo* neurochemical measurements [62]. Since that time, many new developments have been made to follow the exocytosis at the single cell level in real time [6, 12, 63, 64]. Several neurotransmitters like catecholamine, serotonin, certain amino acids and peptides are electroactive and can be oxidized or reduced at reasonable potentials. The most widely used microelectrodes were made of carbon fiber constructed both in disk [63] or cylindrical [65] shape with the diameters close to that of a single cell (15-20μm).

Exocytosis from single bovine adrenal chromaffin cells was monitored in this way [66-68]. This method can discriminate the release of single secretory granules of catecholamine from single cells through a series of amperometrically measured current "spikes". Each "spike" observed on the current vs. time plot corresponded to catecholamine release from a single granule within the cell. Using Nafion-coated carbon fiber microelectrodes, this method was used to identify the released catecholamines as epinephrine (E) and norepinephrine (NE) [69]. Integration of the current observed for each spike provided an estimate of catecholamine content equaling 5 - 8 amol for each granule using Faraday's Law [66]. Catecholamine release from PC12 cells was also monitored with microelectrode amperometry at the zeptomole level [70]. Other electroactive species such as serotonin, histamine [71, 72], oxygen [73] and tryptophan- or tyrosine-containing peptides [74] were also monitored at the single cell level.

Although voltammetric methods usually provide a relatively narrow electrode potential window to identify different electroactive species, such characterization ability is still useful for identification in single-cell analysis. Epinephrine and norepinephrine released from single cells was differentiated using background subtracted fast-scan cyclic voltammetry (CV) at 800V/s by scanning to sufficiently high voltage (> 1V) to observe a second oxidative wave for E [75]. Histamine and serotonin were discriminated similarly during the course of the forward and the reverse CV scan [71]. In addition, Nafion-coated microelectrodes were

often used to screen out the most common interferate ascorbate and DOPAC [76-78]. Poly pyrrole-coated electrodes were used to increase catecholamine sensitivity [79]. However, the additional layer decreases the temporal response. Also, high-pass filtering is also used to discriminate against ascorbic acid, DOPAC and acidic pH changes [80].

By using a smaller size microelectrodes, the intracellular compartments were individually and selectively measured. The penetration of electroactive drugs into neurons of the marine snail, *Aplysia californica* was monitored with intracellular voltammetry [81]. Carbon ring electrodes were used to monitor dopamine in the cytoplasm of single neurons of *Planorbis corneus* [82, 83].

Many biologically important species are not as easy to detect even though their oxidation or reduction is thermodynamically favored. Chemically-modified electrodes (CME) can solve some of these problems by using mediators modified at the electrode surface to shuffle electrons between analytes and the electrode surface [13]. Exocytotic release of insulin from single pancreatic β-cells was monitored using polynuclear ruthenium oxide modified microelectrodes [84, 85]. Enzyme-modified microelectrodes were used for monitoring the excitatory neurotransmitter glutamate [86] and glucose transients at the single cell level [87,88].

Amperometry using microelectrodes has found wide application in characterizing the exocytosis process. For example, neurotransmitter release from endocrine cells was speculated to be much slower than in the peripheral or the central nervous system. It was initially suggested that this could be due to diffusional broadening [89]. However, after analyzing the spike width and the pre-spike feature at different pH and temperature values, it was subsequently argued that the factors involved in the exocytotic processes, such as pH-dependent conformation and $Ca^{2+}$-dependent binding affinity of chromogranin A (a major protein in the vesicles), are not negligible [90-92]. However, the combination of

amperometry and capacitance measurements suggested that the persistence of secretion after depolarization is due to diffusion of $Ca^{2+}$ between channels and release sites, implying that $Ca^{2+}$ channels and secretory vesicles are not colocalized [93, 94]. Similar method with isolated mast cells and chromaffin cells also showed that when photolysis of caged $Ca^{2+}$ was used to stimulate secretion there is a delay between increases in capacitance and the release of oxidizable transmitters. The increases in capacitance that are not resolved as steps cannot be readily interpreted as secretory events unless they are confirmed independently [95]. Careful analysis of amperometric spikes shows that about 70% are preceded by a small "foot" (the trickle of transmitters out of the early fusion pore). 20-50% of the foot signals exhibit rapid fluctuations that are interpreted as flickering of the fusion pore and those "stand-alone" foot signals may reflect transient fusions (vesicles do not collapse completely into the plasma membrane) [96]. Using smaller size microelectrodes (1μm radius), some spatial resolution of exocytotic release sites was achieved and results showed that release sites are spatially localized on endocrine cells [97].

**Fluorescence Imaging Microscopy**

Microscopic imaging techniques can obtain spatial and temporal resolution of cellular processes simultaneously. In fact, the goal of research on and application of fluorescence microscopy is to *watch* in greater detail (i.e., improve spatial resolution); to *measure* more specifically, sensitively and quickly (i.e., improve spectroscopic information and temporal resolution); and to *manipulate* more precisely (i.e., improve control) simultaneously at the intact single cell level [98]. Fluorescence imaging as well as confocal fluorescence imaging microscopy have become conventional tools in biological Sciences [98, 99]. Usually, some fluorescent dyes are used as intracellular probes in fluorescence microscopy for certain intracellular species such as calcium and some other ions. Alternatively, chemiluminescence

microscopy is also used for some species [100]. However, similar problems as mentioned in derivatization detection of CE and LC also exist. Direct microscopic imaging will be addressed in the remainder of this introduction.

Exocytotic events were quantitatively counted by observing the cell under differential interference contrast (DIC) or Nomarski optics with video-microscopy [101, 102]. However, these methods do not provide any chemical information. As mentioned above, LINF is a powerful method for direct fluorescence measurement of some biomolecules. In fact, autofluorescence from NAD(P)H (excitation: 360 nm; emission: 400-500 nm) was used as an intrinsic probe to study cellular metabolism by fluorescence microscopy in the late 50's [103]. The uptake of serotonin by single living astrocytes was first monitored by LINF imaging microscopy with simultaneous high temporal and spatial resolution [104]. Later, the exocytotic release of serotonin from single astrocytes [105], mast cells [106], as well as the release of catecholamine from single adrenal chromaffin cells [107] were also studied through LINF microscopy. Simultaneously achieved spatial and temporal resolution in LINF microscopy enables one to find the local heterogeneity in neurotransmitter release kinetics for different areas of neuroendocrine cells much more easily [105-107] as compared to amperometric methods using smaller sized microelectrodes [97].

Although UV-excited autofluorescence of NAD(P)H was developed into a non-invasive optical method to monitor cellular respiration [108], photobleaching of the autifluorescence as well as chromatic aberration between the UV excitation and the visible fluorescence in confocal microscopy remained serious problems. Two-photon excitation applied to laser scanning microscopy was demonstrated to solve some of these problems [109]. Recently, three-photon excitation was reported to excite short wavelength UV fluorescence of tryptophan and serotonin, and serotonin distribution in living rat basophilic leukemia (RBL-2H3) cells was measured [110]. This technique circumvents the limitation imposed by

photodamage, scattering and discriminates against the background encountered in other UV microscopies.

The spatial resolution of conventional optical techniques mentioned above is limited by diffraction limit ($\lambda/2$, where $\lambda$ is the wavelength). The realization of better resolution by subwavelength light sources has led to the concept of near-field optics (NFO) and near-field scanning optical microscopy (NSOM) [111]. Some recent review articles summarized the development and application of this technique [112-114].

In conclusion, chemical analysis at the single-cell level is becoming a mature and conventional technique not only for analytical chemists, but also for biologists. While the development of more sensitive detection schemes for single-cell analysis is very important, better spatial and temporal resolution in direct dynamic monitoring of cellular processes is another equally exciting direction.

## References


1. Wallingford, R. A.; Ewing, A. G. *Anal. Chem.* **1988**, *60*,1972-1975.
2. Kennedy, R. T.; Oates, M. D.; Cooper, B. R.; Nickerson, B.; Jorgenson, J. M. *Science* **1989**, *246*, 57-63.
3. Olefirowicz, T. M.; Ewing, A. G. *Anal. Chem.* **1990**, *62*, 1872-1876.
4. Olefirowicz, T. M.; Ewing, A. G. *Chimia*, **1991**, *45*, 106-108.
5. Hogan, B. L.; Yeung, E. S. *Anal. Chem.* **1992**, *66*, 2841-2845.
6. Ewing, A. G.; Strein, T. G.; Lau, Y. Y. *Acc. Chem. Res.* **1992**, *25*, 440-447.
7. Hayes, M. A.; Gilman, S. D.; Ewing, A. G. in *Capillary Electrophoresis Technology*, Chapter 28, Guzman, N. A. Ed. New York: Marcell Dekker, **1993**: 753-793.
8. Yeung, E. S. *Acc. Chem. Res.* **1994**, *27*, 409-414.

9. Ewing, A. G.; Mesaros, J. M.; Gavin, P. F. *Anal. Chem.* **1994**, *66*, 527A-537A.

10. Gilman, S. D.; Ewing, A. G. *J. Cap. Electrophor.* **1995**, *2*, 1-13.

11. Jankowski, J. A.; Tracht, S.; Sweedler, J. V. Trends *Anal. Chem.* **1995**, *14*, 170-176.

12. Wightman, R. M.; Finnegan, J. M.; Pihel, K. Trends *Anal. Chem.* **1995**, *14*, 154-158.

13. Huang, L.; Kennedy, R. T. Trends *Anal. Chem.* **1995**, *14*, 158-164.

14. Penner, R. Neher, E. *Trends in Neurosci.* **1989**, *12*, 159-163.

15. Ewing, A. G. *J. Neurosci. Meth.* **1993**, *48*, 215-224.

16. Kennedy, R. T.; St. Claire III, R. L.; White, J. G.; Jorgenson, J. W. *Mikrochim. Acta* **1987**, *11*, 37-45.

17. Kennedy, R. T.; Jorgenson, J. W. *Anal. Chem.* **1989**, *61*, 436-441.

18. Cooper, B. R.; Jankowski, J. A.; Leszczyszyn, D. J.; Wightman, R. M.; Jorgenson, J. W. *Anal. Chem.* **1992**, *64*, 691-694.

19. Cooper, B. R.; Wightman, R. M.; Jorgensom, J. W. *J. Chromatogr. B* **1994**, *653*, 25-34.

20. Kristensen, H. K.; Lau, Y. Y.; Ewing, A. G. *J. Neurosci. Meth.* **1994**, *51*, 183-148.

21. Swanek, F. D.; Chen, G.; Ewing, A. G. *Anal. Chem.* **1994**, *68*, 3912-3916.

22. Oates, M. D.; Cooper, B. R.; Jorgenson, J. W. *Anal. Chem.* **1990**, *62*, 1537-1577.

23. Yeung, E. S. Optical Detectors for Capillary Electrophoresis, in *Advances in Chromatography*, Vol. 35, Brown, P. R. and Grushka, E. Eds., Marcel Dekker, New York, **1995**, pp.20-31.

24. Schnepel, F.-H. in *Fluorometric Analysis in Biomedical Chemistry,* Winefordner, J. D. Ed., John Wiley & Sons, New York, **1991**, pp.69-106.

25. Lee, T. T.; Yeung, E. S. *Anal. Chem.* **1992**, *64*, 3045-3051.

26. Lee, T. T.; Lillard, S. J.; Yeung, E. S. *Electrophoresis*, **1993**, *14*, 429-438.

27. Lillard, S. J.; Yeung, E. S.; Lautamo, R. M. A.; Mao, D. T. *J. Chromatogr. A* **1995**, *718*, 397-404.

28. Tong, W.; Yeung, E. S. *J. Chromatogr. B* **1996**, *685*, 35-40.

29. Chang, H.-T.; Yeung, E. S. *Anal. Chem.* **1995**, *67*, 1079-1083.

30. Malek, A.; Khaledi, M. G. *Ninth International Symposium on High Performance Capillary Electrophoresis and Related Microscale Techniques (HPCE'97)*, Anaheim, CA, 1997, p.136.

31. Lillard, S. J.; Yeung, E. S.; McCloskey, M. A. *Anal. Chem.* **1996**, *68*, 2879-2904.

32. Tong, W.; Yeung, E. S. *J. Chromatogr. B* **1997**, *689*, 321-325.

33. Tong, W.; Yeung, E. S. *J. Neurosci. Meth.* in press.

34. Hietpas, P. B.; Ewing, A. G. *J. Liq. Chromatogr.* **1995**, *18*, 3557-3576.

35. Hoyt, A. M. Jr.; Beale, S. C.; Larmann, J. P. Jr.; Jorgenson, J. W. *J. Microcolumn Sepa.* **1993**, *5*, 325-330.

36. Gilman, S. D.; Ewing, A. G. *Anal. Chem.* **1995**, *34*, 58-64.

37. Gilman, S. D.; Ewing, A. G. *Anal. Meth. Instrum.*, **1995**, *2*, 133-141.

38. Zhang, L.; Yeung, E. S. *J. Chromatogr. A* **1996**, *734*, 331-337.

39. Shippy, S.; Jankowski, J. A.; Sweedler, J. V. *Anal. Chim. Acta* **1995**, *307*, 163-171.

40. Liu, Y.-M.; Sweedler, J. V. *Anal. Chem.* **1996**, *68*, 3928-3933.

41. Yeung, E. S.; Kuhr, W. G. *Anal. Chem.* **1991**, *63*, 275A-282A.

42. Li, Q.; Yeung, E. S. J. Capillary Electrophor. **1994**, *1*, 55-61.

43. Xue, Q.; Yeung, E. S. *J. Chromatogr. A* **1994**, *661*, 287-295.

44. Regnier, F. E.; Patterson, D. H.; Harmon, B. J. *Trends Anal. Chem.* **1995**, *14*, 177-181.

45. Xue, Q.; Yeung, E. S. *Anal. Chem.* **1994**, *66*, 1175-1178.

46. Xue, Q.; Yeung, E. S. *J. Chromatogr. B* **1996**, *677*, 233-240.

47. Rosenzweig, Z.; Yeung, E. S. *Anal. Chem.* **1994**, *66*, 1771-1776.

48. Tan, W.; Yeung, E. S. *Anal. Biochem.* **1995**, *226*, 74-79.

49. Schultz, N. H.; Huang, L.; Kennedy, R. T. *Anal. Chem.* **1995**, *67*, 924-929.

50. Tao, L.; Kennedy, R. T. *Anal. Chem.* **1996**, *68*, 3899-3906.

51. Lloyd, P. E.; Schacher, S.; Kufermann, I.; Weiss, K. R. *Proc. Natl. Acad. Sci. USA* **1986**, *83*, 9794-9798.

52. Hall, J. D.; Lloyd, P. E. *J. Neurobiol.* **1991**, *22*, 583-589.

53. Church, P. J.; Lloyd, P. E. *J. Neurosci.* **1991**, *11*, 618-625.

54. Whim, M. D.; Lloyd, P. E. *J. Neurosci.* **1992**, *12*, 3545-3553.

55. Whim, M. D.; Lloyd, P. E. *J. Neurosci.* **1994**, *14*, 4244-4251.

56. Tracht, S. E.; Toma, V.; Sweedler, J. V. *Anal. Chem.*. **1994**, *66*, 2382-2389.

57. Tracht, S. E.; Cruz, L.; Stobba-Wiley, C. M.; Sweedler, J. V. *Anal. Chem.* **1996**, *68*, 3922-3927.

58. Hofstadler, S. A.; Swanek, F. D.; Gale, D. C.; Ewing, A. G.; Smith, R. D. *Anal. Chem.* **1995**, *67*, 1477-1480.

59. Hofstadler, S. A.; Severs, J. C.; Smith, R. D.; Swanek, F. D.; Ewing, A. G. *Rapid Commun. Mass Spectrom.* **1996**, *10*, 919-922.

60. Valaskovic, G. A.; Kelleher, N. L.; McLafferty, F. W. *Science* **1996**, *273*, 1199-1202.

61. Li, L.; Golding, R. E.; Whittal, R. M. *J. Am. Chem. Soc.* **1996**, *118*, 11662-11663.

62. Adams, R. N. *Anal. Chem.* **1976**, *48*, 1128A-1138A.

63. Whightman, R. M.; May, L. J.; Michael, A. C. *Anal. Chem.* **1988**, *60*, 769A-779A.

64. Stamford, J. A.; Justice, J. B., Jr. *Anal. Chem.* **1996**, *68*, 359A-363A.

65. Ponchon, J.-L.; Caspuglio, R.; Gonon, F.; Jouvat, M.; Pujol, I. F. *Anal. Chem.* **1979**, *51*, 1483-1486.

66. Leszczyszyn, D. J.; Jankowski, J. A.; Viveros, O. H.; Diliberto, E. J., Jr.; Near, J. A.; Wightman, R. M. *J. Biol. Chem.* **1990**, *265*, 14736-14737.

67. Leszczyszyn, D. J.; Jankowski, J. A.; Viveros, O. H.; Diliberto, E. J., Jr.; Near, J. A.; Wightman, R. M. *J. Neurochem.* **1991**, *56*, 1855-1863.

68. Wightman, R. M.; Jankowski, J. A.; Kennedy, R. T.; Kawagoe, K. T.; Schroeder, T. J.; Leszczyszyn, D. J.; Near, J. A.; Diliberto, E. J., Jr.; Viveros, O. H. *Proc. Natl. Acad. Sci. USA* **1991**, *88*, 10754-10758.

69. Ciolkowski, E. L.; Cooper, B. R.; Jankowski, J. A.; Jorgenson, J. W.; Wightman, R. M. *J. Am. Chem. Soc.* **1992**, *114*, 2815-2821.

70. Chen, T. K.; Luo, G.; Ewing, A. G. *Anal. Chem.* **1994**, *66*, 3031-3035.

71. Pihel, K.; Hsieh, S.; Jorgenson, J. W.; Wightman, R. M. *Anal. Chem.* **1995**, *67*, 4514-4521.

72. Alvarez de Toledo, G.; Fernandez-Chacon, R.; Fernandez, J. M. *Nature* **1993**, *363*, 554-558.

73. Lau, Y. Y.; Abe, T.; Ewing, A. G. *Anal. Chem.* **1992**, *64*, 1702-1705.

74. Paras, C. D.; Kennedy, R. T. *Anal. Chem.* **1995**, 67, 3633-3637.

75. Pihel, K.; Schroeder, T. J.; Wightman, R. M. *Anal. Chem.* **1994**, *66*, 4532-4537.

76. Brazell, M. P.; Kasser, R. J.; Renner, K. J.; Feng, J.; Moghaddam, B.; Adams, R. N. *J. Neurosci. Meth.* **1987**, *22*, 167-172.

77. Garris, P. A.; Ciolkowski, E. L.; Wightman, R. M. *Neuroscience* **1994**, *59*, 417-427.

78. Kawagoe, K. T.; Garris, P. A.; Wightman, R. M. *J. ElectroAnal. Chem.* **1993**, *359*, 193-207.

79. Pihel, K.; walker, Q. D.; Wightman, R. M. *Anal. Chem.* **1996**, *68*, 2084-2089.

80. Cahill, P. S.; Walker, Q. D.; Finnegan, J. M.; Mickelson, G. E.; Travis, E.R.; Wightman, R. M. *Anal. Chem.* **1996**, *68*, 3180-3186.

81. Meulemans, A.; Poulain, B.; Baux, G.; Tauc, L.; Henzel, D. *Anal. Chem.* **1986**, *58*, 2088-2092.

82. Chien, J. B.; Wallingford, R. A.; Ewing, A. G. *J. Neurochem.* **1990**, *54*, 633-638.

83. Lau, Y. Y.; Chien, J. B.; Wong, D. K. Y.; Ewing, A. G. *Electroanalysis* **1991**, *3*, 87-95.

84. Kennedy, R. T.; Huang, L.; Atkinson, M. A.; Dush, P. *Anal. Chem.* **1993**, *65*, 1882-1887.

85. Kennedy, R. T.; Huang, L.; Aspinwall, C. A. *J. Am. Chem. Soc.* **1996**, *118*, 1795-1796.

86. Pantano, P.; Hellman, M.; Kuhr, W. G. *J. Am. Chem. Soc.* **1991**, *113*, 1832-1833.

87. Abe, T.; Lau, Y. Y.; Ewing, A. G. *J. Am. Chem. Soc.* **1991**, *113*, 7421-7423.

88. Abe, T.; Lau, Y. Y.; Ewing, A. G. *Anal. Chem.* **1992**, *64*, 2160-2163.

89. Schroeder, T. J.; Jankowski, J. A.; Kawagoe, K. T.; Wightman, R. M. *Anal. Chem.* **1992**, *64*, 3077-3083.

90. Jankowski, J. A.; Schroeder, T. J.; Ciolkowski, E. L.; Wightman, R. M. *J. Biol. Chem.* **1993**, *268*, 14694-14700.

91. Walker, A.; Glavinovic, M. I.; Trifaró, J.-M. *Pflügers Arch.* **1996**, *431*, 729-735.

92. Walker, A.; Glavinovic, M. I.; Trifaró, J.-M. *Pflügers Arch.* **1996**, *432*, 729-735.

93. Chow, R. H.; Klingauf, J.; Neher, E. *Proc. Natl. Acad. Sci. USA* **1994**, *91*, 12765-12769.

94. Chow, R. H.; Klingauf, J.; Heinemann, C.; Zucker, R. S.; Neher, E. *Neuron* **1996**, *16*, 369-376.

95. Oberhauser, A. F.; Robinson, I. M.; Fernandez, J. M. *Biophys. J.* **1996**, *71*, 1131-1139.

96. Zhou, Z.; Misler, S.; Chow, R. H. *Biophys. J.* **1996**, *70*, 1543-1552.

97. Schroeder, T. J.; Jankowski, J. A.; Senyshyn, J.; Holz, R. W.; Wightman, R. M. *J. Biol. Chem.* **1994**, *269*, 17215-17220.

98. Wang, X. F.; Herman, B. *Fluorescence Imaging Spectroscopy and Microscopy*, John Wiley & Sons, Inc. New York, **1996**.

99. Foskett, J. K.; Grinstein, S. *Noninvasive Techniques in Cell Biology*, Wiley-Liss, New York, **1990**.

100. Suzaki, E.; Kawai, E.; Kodama, Y.; Suzaki, T.; Masujima, T. *Biochim. Biophys. Acta* **1994**, *1201*, 328-332.

101. Edwards, C.; Englert, D.; Lotshaw, D.; Ye, H. Z. *Cell Motility* **1984**, *4*, 297-303.

102. Tarakawa, S.; Fan, J.-H.; Kumakura, K.; Ohara-Imaizumi, M. *Neurosci. Lett.* **1991**, *123*, 82-86.

103. Chance, B.; Thorell, B. *J. Biol. Chem.* **1959**, *234*, 3044-3050.

104. Tan, W.; Parpura, V.; Haydon, P. G.; Yeung, E. S. *Anal. Chem.* **1995**, *67*, 2575-2579.

105. Tan, W.; Haydon, P. G.; Yeung, E. S. *Appl. Spectr.* in press.

106. Lillard, S. L.; Yeung, E. S. *J. Neurosci. Meth.* in press.

107. Tong, W.; Yeung, E. S. *Appl. Spectr.* submitted.

108. Chance, B.; Lieberman, M. *Exp. Eye Res.* **1978**, *26*, 111-117.

109. Denk, W.; Strickler, J. H.; Webb, W. W. *Science* **1990**, *248*, 73-76.

110. Maiti, B.; Shear, J. B.; Williams, R. M.; Zipfel, R. R.; Webb, W. W. *Science* **1997**, *275*, 530-532.

111. Betzig, E.; Trautman, J. K.; Harris, T. D.; Weiner, J. S.; Kostelak, R. L. *Science* **1991**, *251*, 1468-1470.

112. Betzig, E.; Trautman, J. K. *Science* **1992**, *257*, 189-195.

113. Kopelman, R.; Tan, W. in *Spectroscopic and Microscopic Imaging of Chemical State*, Morris, M. D., Ed., Dekker, New York, **1993**, p.227.

114. Tan, W.; Kopelman, R. in *Fluoresence Imaging Spectroscopy and Microscopy*, Wang, X. F.; Herman, B., Ed., John Wiley & Sons, Inc., New York, **1996**, p.407.

# CHAPTER 1

## MONITORING SINGLE-CELL PHARMACOKINETICS BY CAPILLARY ELECTROPHORESIS AND LASER-INDUCED NATIVE FLUORESCENCE

A paper published in the Journal of Chromatography B: Biomedical Applications[1]

Wei Tong and Edward S. Yeung

## ABSTRACT

The quantification of insulin released from single cells of the insulin-secreting cell line βTC3 permeabilized by digitonin is demonstrated. A simple method for monitoring the on-column release process by using capillary electrophoresis and laser-induced native fluorescence detection is described. Quantitative measurements of both the amount of insulin released and the amount remaining in the cell can be achieved simultaneously. This protocol provides an alternative approach to the study of cell secretion in the field of neuroscience and endocrinology.

---

# INTRODUCTION

Capillary electrophoresis (CE), with its compatibility with extremely small sample volume, high separation efficiency and multiple analytes determination, has become a powerful tool for single-cell analysis [1-3]. Various chemical species, from inorganic ions to neurotransmitters to proteins, have been analyzed at the level of a single mammalian cell [4-21]. Electrochemical [4,7-10] and laser-induced native fluorescence (LINF) detection schemes [13,20] have proven to be the most direct techniques for single-cell analysis with CE, since they measure the native properties of the analytes. This avoids problems with incomplete reaction or slow kinetics.

While the quantitation of the total amount of intracellular components is very important, in some cases, however, monitoring the dynamic chemical changes of a single cell (e.g., exocytosis, endocytosis, metabolism and ion regulation) is more relevant to the understanding of the interaction of the cell with its environment. In many living organisms, the cellular environment is highly heterogeneous. The cells one is interested in usually coexist with other cells and therefore is exposed to a mixture of hormones and neurotransmitters released from neighboring cells. Dynamic monitoring of single cells has the inherent advantage that it provides a controlled environment and precludes the influences of other cells. This is very important in the understanding of cell biology and the pathogenesis of certain kinds of diseases. Intracellular fluorescent probes have been developed to measure the level of calcium and other ions inside the single cells [22-24]. Microelectrodes are also used to measure the release of oxidizable compounds [25-29]. Recently, neurotransmitter uptake has been imaged in single living astrocytes using a UV laser-based optical microscope and CCD detection system [30].

In most of the above methods, it is difficult to perform quantitative measurement of the absolute amount of species secreted or uptaken. It is also difficult to simultaneously measure

the amount of analytes secreted and the amount remaining in the cell after release, which are pertinent information for pharmakokinetic studies. The quantitation nature of CE makes it an interesting alternative approach to the study of the single cell secretion.

Kristensen et al. [16] used CE with amperometric detection to directly identify and measure the neurotransmitter, dopamine, in two vesicular compartments in a single nerve cell of *Planorbis corneus*. Insulin is traditionally determined by radioimmunoassay (RIA) and enzyme-linked immunosorbent assay (ELISA) [31,32]. CE-based immunoassay have also been used for insulin analysis [33,34]. However, the CE-LINF method we recently developed for the analysis of insulin in single pancreatic cells [35] is more suitable for studying release because it is a direct method that does not involve derivatization. In the present work, we have developed an on-column protocol to simultaneously monitor the release of insulin from a single βTC3 cell and the residual amount of insulin in the same cell. Insulin is selected here because type II diabetes is characterized by improper insulin release from the pancreatic β-cells. The underlying causes of this improper release is still not clear. Digitonin is used in the present work to cause the insulin release. Digitonin reacts with cholesterol in the cell membrane to permeate the cell by producing pores on the membrane. Digitonin has been used to cause the release of catecholamines from adrenal medullary cells [29].

## EXPERIMENTAL

### CE Apparatus

The CE setup was laboratory-made and similar to that described previously [12]. Briefly, a high-voltage power supply (Series MJ, 0-30kV, Glassman High Voltage, Whitehouse Station, NJ, USA) was used to drive the electrophoresis. A 22 μm I.D,.360 μm O.D. fused-silica capillary (Polymicro Technologies, Phoenix, AZ, USA) was used for

separation. The total length was 63 cm, and the detection window was 46 cm from the injection end. For single-cell measurements, a bare capillary was used after rinsing with 0.1 M NaOH for 5 min and equilibrating with running buffer for 10 min. For lysed cell measurements, a non-bonded poly(ethylene oxide) (PEO) coated capillary was used. The capillary was treated with 0.1 M HCl, 0.2% PEO (in 0.1 M HCl) for 5 min, respectively, before finally being flushed with the running buffer. The entire electrophoresis and detection system was enclosed in a sheet-metal box with HV interlocks. The buffer reservoir at the high-voltage end was enclosed in a plexiglass box.

The 275-nm line from an Ar ion laser (Model 2045, Spectra Physics, Mountain View, CA, USA) was isolated from other lines with an external prism and focused with a 1-cm focal length quartz lens onto the detection window of the capillary. One WG-305 (Melles Griot, Irvine, CA) and one UG-1 filter (ESCO, Oak Ridge, NJ) were used to block the scattered light and room light from reaching the photomultiplier tube. A low pass (1 Hz) filter was employed to limit the output signal bandwidth. Data were collected at 5 Hz by a 24-bit A/D conversion interface (ChromPerfect, Justice Innovation, Palo Alto, CA, USA). The data was stored in an IBM/PC-compatible computer.

**Reagents**

A balanced salt solution (PBS) was composed of 136 mM NaCl, 5.4 mM KCl, 0.5 mM $NaH_2PO_4$, 0.34 mM $Na_2HPO_4$, 0.8 mM $MgSO_4$, 1.3 mM $CaCl_2$ and 10 mM HEPES and adjusted to pH 7.4 with NaOH. Bovine insulin and tricine were purchased from Sigma (St. Louis, MO, USA). Digitonin was obtained from Fluka (Ronkonkoma, NY, USA) and poly(ethylene oxide) of $M_r$ 8,000,000 was from Aldrich (Milwaukee, WI, USA). All other chemicals were purchased from Fisher (Fair Lawn, NJ, USA).

**Methods**

Because of the difficulties in isolating large numbers of highly purified pancreatic β-cells, insulin-producing β-cell lines are usually used as a model for wild type pancreatic β-cells [36]. βTC3 cells [37] were generous gifts from Dr. W. Hsu, College of Veterinary Medicine, Iowa State University. Before analysis, the cells were washed five times with 5-ml portions of balanced salt solution. Hydrodynamic injection similar to that described in [12] was used to inject a single cell into the end of the capillary. Once the cell adheres to the capillary wall (Fig.1A), 20 μM digitonin (dissolved in the balanced salt solution) is hydrodynamically injected by lifting the injection end in the digitonin vial 20 cm above the ground buffer reservoir for 1 min. This corresponds to a 3.2-mm plug of digitonin, which is enough to cover the whole cell. The injection end of the capillary is then put back to the running buffer reservoir and let incubate for 15 min (Fig.1B). During this time, the digitonin will dissolve the cholesterol in the cell membrane and permeable pores are produced. The insulin-containing granules permeate through the pores and give off their insulin. The release process is not linear with respect to time. A 15-min time period was chosen to produce sufficient material for quantitation yet allow experiments to proceed at a convenient pace. Then, CE is run at 3 kV for 5 min to separate the released insulin zone from the cell (Fig.1C). Alternatively, balanced salt solution is introduced into the capillary hydrodynamically to achieve the same separation. Finally, the running voltage was increased to 30 kV. The cell will lyse and give off the rest of the insulin. Two separated insulin zones will then migrate towards the detection windows with the aid of the electroosmotic flow (Fig.1D). Quantitation is achieved by measuring the peak areas and comparing them with those obtained for calibration runs with standard solutions of insulin between cell injections.

In the off-column experiment, two equal portions of cell suspensions are used. One portion of cells is incubated with digitonin for 15 min and the other portion is just incubated

Figure 1. Schematic diagram of on-column monitoring of insulin release from a single cell.

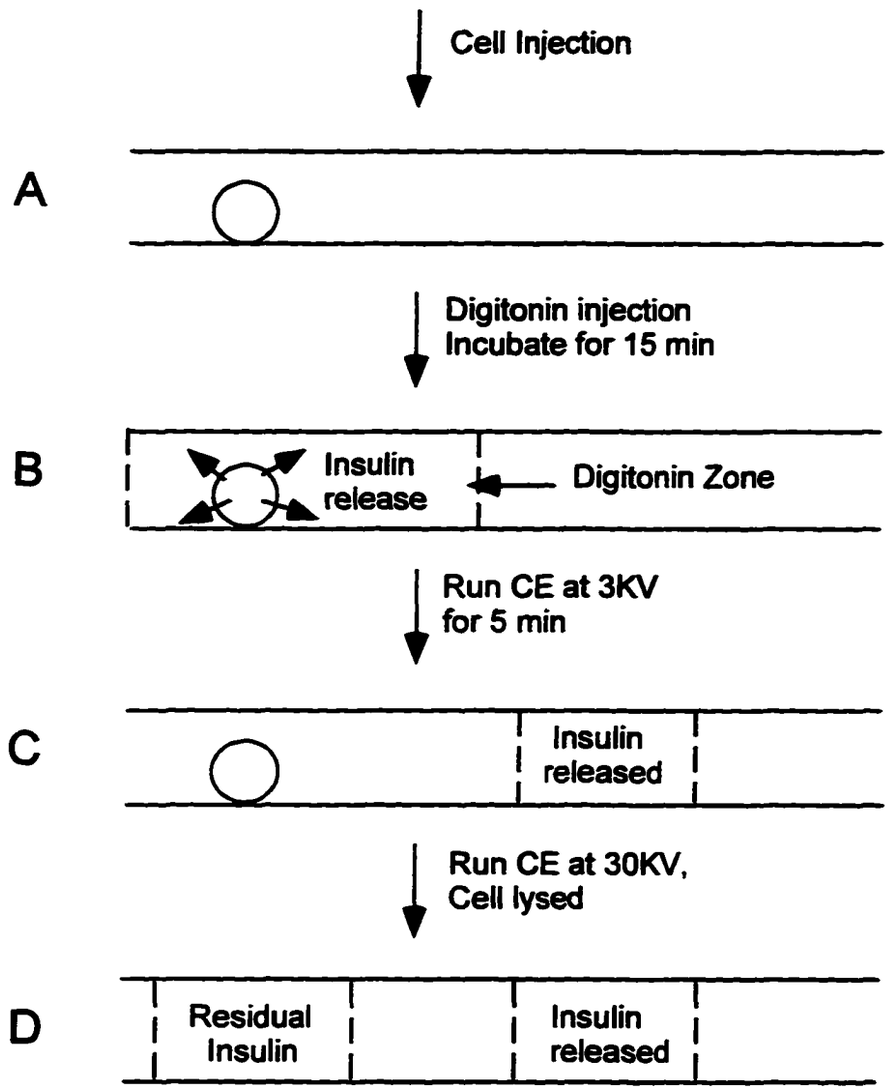
Cell Injection
A
Digitonin injection
Incubate for 15 min
B
Insulin
release
Digitonin Zone
Run CE at 3KV
for 5 min
C
Insulin
released
Run CE at 30KV,
Cell lysed
D
Residual
Insulin
Insulin
released

with the balanced salt solution. The cells are then spun down and lysed ultrasonically in $H_2O$. The two lysates, which correspond to the average amount of insulin left in the cells and total amount of insulin, are analyzed with CE-LINF.

## RESULTS AND DISCUSSION

The key aspects of this work are the processes of injection, on-column releasing, and on-column lysis of the single cells. The adhesion of the cell to the capillary wall soon after injection helps to prevent the cell from further migration down the capillary, so that the later on injected releasing reagent can pass and cover the whole cell. The cell is rather rugged and remains unlysed in 20 μM digitonin for at least 30 min. This is probably because the cell membrane is relatively poor in cholesterol [38].

Fig. 2B is a typical electropherogram obtained with the present protocol for a single β TC3 cell. Since we run CE at 3kV for 5 min to separate the released insulin zone from the intact cell, the released insulin peak (peak 1) should separate from the residual insulin (peak 2) by 0.5 min (electromigration at 30 kV). However, the peak separation here is only about 0.2 min. The time is also not reproducible from run to run. This is because the cell will sometimes moves or even lyse during the 3kV CE step, as confirmed by monitoring under a microscope. As a result, the peak for the residual insulin actually reaches the detection window earlier than expected.

Hydrodynamic flow experiments can be used to confirm that peak 1 and 2 correspond to the released insulin and residual insulin (Fig. 2C). In this experiment, after incubate the cell with digitonin, the injection end of the capillary is lifted by 30 cm for 15 min. The cell will not lyse or move during this period. The calculated peak separation for peaks 1 and 2 is about 0.5 min, which is very close to the experimental result. For a set of five experiments, the temporal separation is (0.57±0.04) min. In addition, if the cell is not incubated with

Figure 2. Electropherograms of insulin standard (A) and insulin from a single βTC3 cell (B and C). (A) Normal CE-LINF, 30kV, 500 amol insulin injected; (B) On-column release CE-LINF; peak 1: insulin released from the cell due to digitonin; peak 2: residual insulin, which is released due to lysis. The two peaks are separated electrophoretically after release. (C) Same as (B), except that the two peaks are separated hydrodynamically after release. Running buffer: 20 mM tricine (pH 8.5).

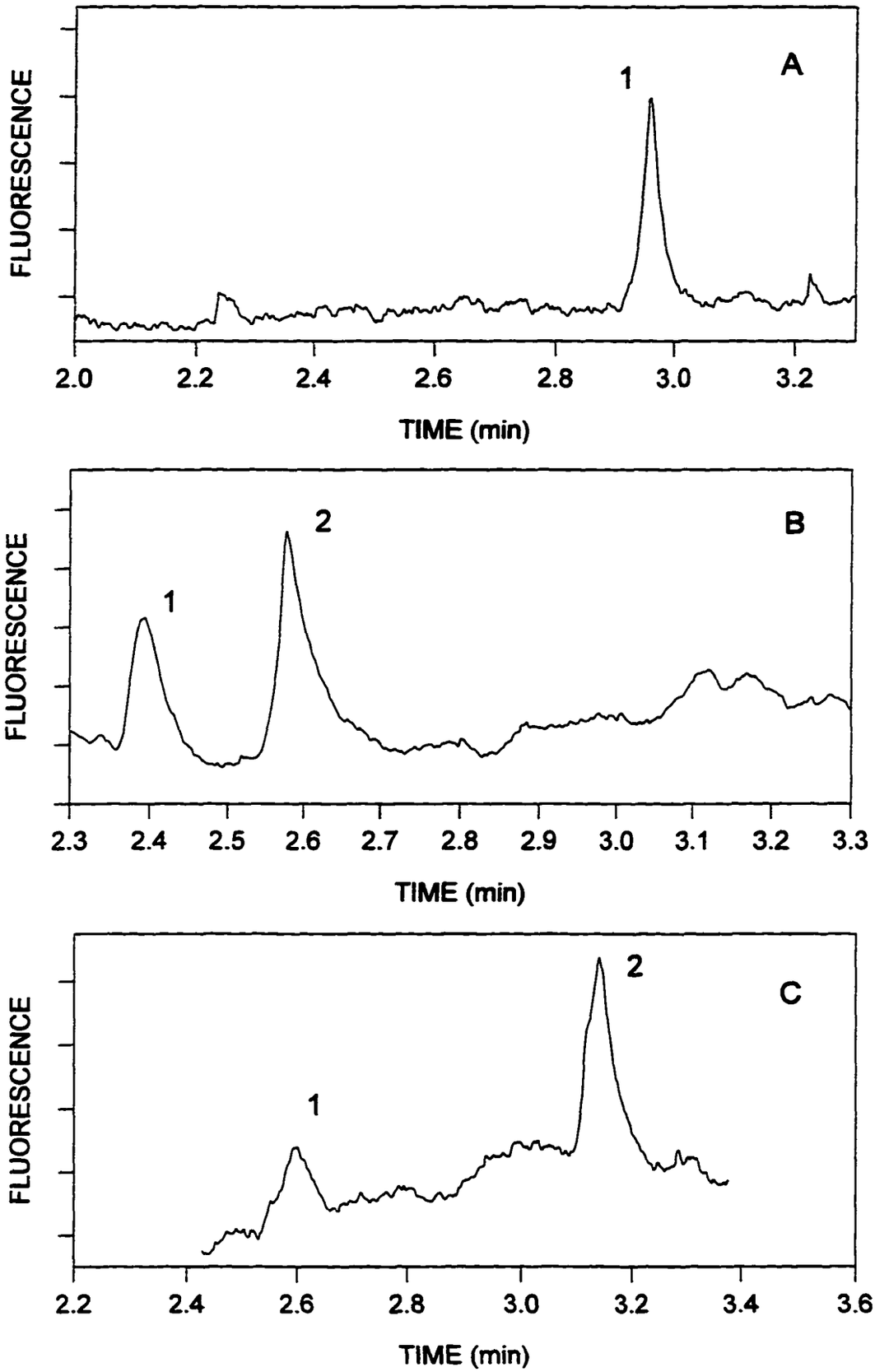
A
1
FLUORESCENCE
2.0
2.2
2.4
2.6
2.8
3.0
3.2
TIME (min)
B
1
2
FLUORESCENCE
2.3
2.4
2.5
2.6
2.7
2.8
2.9
3.0
3.1
3.2
3.3
TIME (min)
C
1
2
FLUORESCENCE
2.2
2.4
2.6
2.8
3.0
3.2
3.4
3.6
TIME (min)

digitonin and simply run CE at 30 kV after cell injection or if hydrodynamically flow is applied for the same amount of time at the same height, we only observe peak 2 (at about 3 min with a larger peak area). The migration times for single-cell analysis are not highly reproducible. This is because the cellular species may adsorb on the capillary wall and change the rate of the electroosmotic flow [13].

Table 1 summarizes the fraction of insulin released by digitonin for several batch of cells from different culture dishes, as determined by CE-LINF. On the average, 41% and 21% of insulin are released for batches 1 and 2, respectively. These are smaller percentages compared to the 59% and 47% release obtained by off-column measurements. Apparently, the spinning process caused some additional intracellular insulin to leak out to distort the measured release percentage. This highlights the importance of studying release on column and on a single-cell basis. In general, Table 1 shows that the inter-batch variations are larger than the intra-batch variation, This is ecpected from cultured cells.

Other chemicals (e.g., glucose, KCl and carbachol) which stimulate the physiological release of insulin are also tested. Off-column experiments showed insulin release of less than 15% [39]. We have not been able to reliably quantify such small amount of release by the present on-column protocol due to the marginal signal-to-noise ratio. Further improvements in instrumentation will be needed for such studies..

## CONCLUSION

A simple method for monitoring the release of insulin from single cells by using capillary electrophoresis and laser-induced native fluorescence is demonstrated. Quantitative measurements of the amount of species released and residual amount in the cell can be performed simultaneously. This will provide a useful alternative approach to the quantitative study of cell secretion in the field of neuroscience, pharmacokinetics and endocrinology.

Table 1. On-column insulin release determined by CE-LINF.

| Cell No. | Peak 1 (Area) | Peak 2 (Area) | Insulin Released (%) |
|---|---|---|---|
| *Batch 1* | | | |
| 1 | 2027 | 2821 | 41.8 |
| 2 | 2087 | 3210 | 40.2 |
| *Batch 2* | | | |
| 3 | 1712 | 6376 | 21.2 |
| *Batch 3* | | | |
| 4 | 1336 | 787 | 62.9 |
| *Batch 4* | | | |
| 5 | 1971 | 3660 | 35.0 |
| 6 | 3076 | 3642 | 45.8 |
| 7 | 2524 | 4843 | 34.3 |

## ACKNOWLEDGMENTS

The authors thank Dr. W. H. Hsu for generous gift of βTC3 cells. We also thank Dr. T.-H. Chen for help in preparing the cells. The Ames Laboratory is operated for the U.S. Department of Energy by Iowa State University under the contract No. W-7405-Eng-82. This work was supported by the Director of Energy Research, Office of Basic Energy Sciences, Division of Chemical Sciences.

## REFERENCES

1. E. S. Yeung, *Acc. Chem. Res.*, 27, (1994) 409.
2. A. G. Ewing, J. M. Mesaros, P. F. Gavin, *Anal. Chem.*, 66, (1994) 527A.
3. P. B. Hietpas, A. G. Ewing, *J. Liq. Chromatogr.*, 18, (1995) 3557.
4. R. A. Wallingford, A. G. Ewing, *Anal. Chem.*, 60, (1988) 1972.
5. R. T. Kennedy, M. D. Oates, B. R. Cooper, B. Nickerson, J. W. Jorgenson, *Science*, 246, (1988) 57.
6. R. T. Kennedy, J. W. Jorgenson, *Anal. Chem.*, 61, (1989) 432.
7. J. B. Chien, R. A. Wallingford, A. G. Ewing, *J. Neurochem.*, 54, (1990) 633.
8. T. M. Olefirowicz, A. G. Ewing, *Anal. Chem.*, 62, (1990) 1872.
9. T. M. Olefirowicz, A. G. Ewing, *J. Neurosci. Methods*, 34, (1990) 11.
10. T. M. Olefirowicz, A. G. Ewing, *Chimica*, 45, (1991) 106.
11. A. G. Ewing, T. G. Strein, Y. Y. Lau, *Acc. Chem. Res.*, 25, (1992) 440.
12. B. L. Hogan, E. S. Yeung, *Anal. Chem.*, 64, (1992) 2841.
13. T. T. Lee, E. S. Yeung, *Anal. Chem.*, 64, (1992) 3045.
14. Q. Xue, E. S. Yeung, *J. Chromatogr.*, 661, (1994) 287.
15. Q. Xue, E. S. Yeung, *Anal. Chem.*, 66, (1994) 1175.

16. H. K. Kristensen, Y. Y. Lau, A. G. Ewing, *J. Neurosci. Methods*, 51, (1994) 183.

17. Z. Rosenzweig, E. S. Yeung, *Anal. Chem.*, 66, (1994) 1771.

18. Q. Li, E. S. Yeung, *J. Capillary Electrophor.*, 1, (1994) 55.

19. S. D. Gilman, A. G. Ewing, *Anal. Chem.*, 67, (1995) 58.

20. H. T. Chang, E. S. Yeung, *Anal. Chem.*, 67, (1995) 1079.

21. S. A. Hofstadler, F. D. Swanek, D. C. Gale, A. G. Ewing, R. D. Smith, *Anal. Chem.*, 67, (1995) 1477.

22. G. Gryznkiewicz, M. Poenie, R. Y. Tsien, J. Biol. Chem., 260, (1985) 3440.

23. J. K. Foskett, S. Grinstein, *Noninvasive Techniques in Cell Biology*, Wiley-Liss, NY 1990.

24. R. Y. Tsien, *C&E News*, 72(29) (1994) 34.

25. G. Alvarez de Toledo, R. Fernandez-Chacon, J. M. Fernandez, *Nature*, 363, (1993) 554.

26. D. J. Leszczyszyn, J. A. Jankowski, O. H. Viveros, E. J. Diliberto,Jr., J. A. Near, R. M. Wightman, *J. Biol. Chem.*, 265, (1990) 14736.

27. R. H. Chow, L. von Ruden, E. Neher, *Nature*, 356, (1992) 60.

28. R. T. Kennedy, L. Huang, M. A. Atkinson, P. Dush, *Anal. Chem.*, 65, (1993) 1882.

29. P. S. Cahill, R. M. Wightman, *Anal. Chem.*, 67, (1995) 2599.

30. W. Tan, V. Parpura, P. G. Haydon, E. S. Yeung, *Anal. Chem.*, 67, (1995) 2575.

31. R. S. Yalow, S. A. Berson, *Clin. Invest.*, 39, (1960) 1157.

32. J. Kekow, K. Ulrichs, W. Muller-Ruchholtz, W. L. Gross, *Diabetes*, 37, (1988) 321.

33. N. M. Schultz, R. T. Kennedy, *Anal. Chem.*, 65, (1993) 3161.

34. N. M. Schultz, L. Huang, R. T. Kennedy, *Anal. Chem.*, 67, (1995) 924.

35. W. Tong, E. S. Yeung, *J. Chromatogr.* B, 685 (1996) 35.

36. C. B. Wollheim, P. Meda, P. A. Halban, *Methods in Enzymol.*, 192, (1990) 223.

37. S. Efrat, M. Leiser, M. Surana, D. Tal and N. Fleischer, *Diabetes*, 42, (1993) 901.

38. W. Montague, *Diabetes and the Endocrine Pancreas*, p.26, Oxford University Press, NY 1983.

39. R. D'Ambra, M. Surana, S. Efrat, R. G. Starr, N. Fleischer, *Endocrinology*, 126, (1990) 2815.

# CHAPTER 2

## ON-COLUMN MONITORING OF SECRETION OF CATECHOLAMINES FROM SINGLE BOVINE ADRENAL CHROMAFFIN CELLS BY CAPILLARY ELECTROPHORESIS

A paper accepted by the Journal of Neuroscience Methods

Wei Tong and Edward S. Yeung

## ABSTRACT

The secretion of catecholamines from individual bovine adrenal medullary cells was quantitatively monitored by capillary electrophoresis with laser-induced native fluorescence detection. By using a physiological balanced-salt solution as the running buffer for CE, the amount of norepinephrine (NE) and epinephrine (E) secreted by their physiological secretagogue, acetylcholine, and the amount remaining in a single cell can be simultaneously quantified. Among the six different glands (from separate cows) studied, a predominance of E-rich cells were found. There was no apparent relationship between the ratio of NE/E released and the original NE/E content in the cell. The secretion process was also monitored dynamically with this method by continuously passing acetylcholine over the cell during stimulation. From the peak width and shape of the released material, one can estimate the time scale of the release process.

## INTRODUCTION

Monitoring the dynamic chemical changes of a single cell (e.g., secretion, uptake, metabolism, and ion regulation) has become increasingly important in the understanding of the interaction of the cell with its environment. Exocytosis, the process by which the intracellular vesicles fuse with the inner surface of the plasma membrane and release their contents into the surrounding medium, is the mechanism underlying the secretion of many physiologically important mediators such as hormones, enzymes, and neurotransmitters. A number of technical approaches have been developed to provide detailed insight into the process. Membrane capacitance measurement with whole-cell patch-clamp technique[1,2] has allowed determination of the extent of exocytotic membrane fusion. Intracellular fluorescent probes have been developed to measure the level of calcium and other ions inside single cells.[3-5] Amperometry and fast scan voltammetry using microelectrodes are also used to measure the release of oxidizable compounds.[6-10] Recently, neurotransmitter uptake has been imaged in single living astrocytes using a UV laser-based optical microscope and CCD detection system.[11]

Among the above methods, membrane capacitance measurements and intracellular fluorescent probes can follow the time course of secretion indirectly. However, it is difficult to perform quantitative determinations. Electrochemical methods using microelectrodes provide fast time resolution and good sensitivity at a single-point.[10,12] To quantify the total amount of released material over time, other approaches have been developed. With its high separation efficiency, quantitative determination of multiple compounds released from the cell can be achieved simultaneously by capillary electrophoresis (CE). CE has been used[13] with amperometric detection to directly identify and measure the neurotransmitter, dopamine (DA), in two vesicular compartments in a single nerve cell of *Planorbis corneus*. Recently,

we have developed an on-column CE protocol to measure the secretion of insulin and serotonin from single permeabilized βTC3 cells and mast cells, respectively[14,15]

The chromaffin cells of the adrenal medulla are innervated neuroendocrine cells that primarily secrete catecholamines, norepinephrine (NE) and epinephrine (E), into blood. Norepinephrine and epinephrine are well recognized as activators of physiological responses to emergency situations. There are several well-established clinical disorders of adrenomedullary hyperfunction and hypofunction including pheochromocytoma and insulin-dependent diabetes mellitus (IDDM).[16,17] In order to elucidate the molecular mechanism of neurotransmitter secretion at the nerve terminal, chromaffin cells have been used as "model nerve terminals".[18-20] Electrochemical detection using microelectrodes has been the main method for monitoring the exocytosis of chromaffin cells directly.[6,7] Off-column secretion of NE and E from individual cultured chromaffin cells have been quantified by microcolumn HPLC.[21] We have also demonstrated the determination of NE and E in single bovine adrenal chromaffin cells by CE with laser-induced native fluorescence detection (CE-LINF).[22] In the present study, we describe an on-column CE method to simultaneously monitor the secreted amount of NE and E from single bovine adrenal chromaffin cells and the residual amount of NE and E in the same cell. By passing the secretagogue dynamically over the cell in the capillary with the aid of electroosmotic flow, temporal information about the release process can also be obtained through the extent of broadening of the release peaks.

## EXPERIMENTAL

### CE Apparatus

The home-made CE setup was similar to that described previously.[23] A 21 μm i.d., 360 μm o.d. fused-silica capillary (Polymicro Technologies, Phoenix, AZ) was used for on-

column secretion, separation and detection. The total length was 65 cm, and the detection window was 47.5 cm from the injection end. A high-voltage power supply (Glassman High Voltage, Inc., Whitehouse Station, NJ; Series MJ, 0-30 kV) was used to drive the electrophoresis. The capillary was rinsed with deionized water, 0.1 M HCl, and running buffer for 10 min, sequentially, before use. The entire electrophoresis and detection system was enclosed in a sheet-metal box with HV interlocks. The running buffer reservoir at the high-voltage end was further enclosed in a plexiglass box.

The 275-nm line from an Ar ion laser (Spectra Physics, Mountain View, CA, Model 2045) was isolated from other lines with an external prism and focused with a 1 cm focal length quartz lens onto the detection window of the capillary. Fluorescence was collected with a 10× microscope objective (Edmund Scientific, Barrington, NJ) and passed through a WG-305 (Melles Griot, Irvine, CA) and one UG-1 filter (ESCO, Oak Ridge, NJ) onto a photomultiplier tube. A low pass (2 Hz) filter was employed to limit the output signal bandwidth. Data was collected at 5 Hz with a 24-bit A/D interface (ChromPerfect, Justice Innovation, Palo Alto, CA) and stored in an IBM/PC-compatible computer. Peak integration and deconvolution were performed with commercial software (Peakfit, Jandel Scientific, San Rafael, CA).

**Reagents**

Unless otherwise noted, all chemicals were purchased from Fisher Scientific (Fair Lawn, NJ). Catecholamine (DA, NE and E) (Sigma, St. Louis, MO) stock solutions were prepared in 0.1 M perchloric acid and stored in a refrigerator. Hank's balanced-salt solution, bovine serum albumin (BSA) (Fraction V), and acetylcholine were obtained from Sigma. Collagenase (Type I) was purchased from Worthington Biochemical (Freehold, NJ).

**Cell Isolation**

Bovine adrenal medullary cells were isolated according to that reported by Livett[24] with some modifications. Bovine adrenal glands were obtained from the local slaughter house where they were excised soon after death and freed from adhering fat. The glands were perfused through the adrenal vein with 15-ml of ice-cold Hank's balanced-salt solution containing 0.1% BSA (pH 7.4) (buffer A) and transported back to the laboratory on ice. The glands were then perfused again through the adrenal vein with ice-cold buffer A until the perfusate was free of erythrocytes and plasma. 4 ml of 0.05% collagenase (in buffer A) was injected into each gland through the adrenal vein. The glands were put in a plastic beaker and incubated in 37°C water bath for 30 min, by which time the consistency of the medullary tissue became flaccid. The adrenal cortex, which is visually distinguishable from the medulla, was then dissected away and discarded. The medullae obtained were minced finely on ice with a pair of sharp scissors and any obvious islands of cortical tissue were removed. A further portion (5 ml) of 0.05% collagenase (in buffer A) per gland was added to the chopped medullae for digestion in a plastic beaker with gentle agitation for 15 min at 37°C. The mixture was then diluted with ice-cold buffer A and filtered through 200-μm and 50-μm nylon mesh, respectively, to remove undigested material. The crude suspension of medullary cells was chilled on ice and then centrifuged at 50 g for 2 min. The cell pellet was washed with 10 ml of buffer A by gently drawing up and down through a wide bore (4 mm i.d.) plastic pipette and centrifuged again. The cell pellet was then resuspended in a buffer consisting of 150 mM NaCl, 4.2 mM KCl, 1.0 mM $Na_2HPO_4$, 0.7 mM $MgCl_2$, 2 mM $CaCl_2$, 11.2 mM glucose, 10 mM HEPES, and 0.5% BSA (pH 7.4) (buffer B). The cell suspension was incubated at 37°C for 1.5 h. After incubation, the cells were centrifuged and resuspended in buffer B (without BSA). The cells were used as soon as possible. If it was

necessary to keep them for a long time (hours) before use, the cell suspension in buffer B was chilled on ice and re-equilibrated to 37°C for 10 min before use.

**CE Methods**

Buffer B (without BSA) was used as the CE running buffer to ensure that the cell remained viable throughout. Hydrodynamic injection similar to that described in ref. 23 was used to inject a single cell into the inlet end of the capillary. Once the cell adhered to the capillary wall, pressure was applied at the outlet end of the capillary to push the extracellular buffer (introduced during the cell injection procedure) out of the capillary. This also served to confirm cell adhesion to the capillary wall. For release in static experiments, $5 \times 10^{-4}$ M acetylcholine (ACh) (in buffer B without BSA) is hydrodynamically injected by lifting the injection end (ACh vial) 20 cm above the outlet buffer reservoir for 1 min. This corresponds to a 2.8 mm long plug of ACh, which is enough to cover the whole cell. The injection end was then returned to the same level as the outlet end and the cell was incubated for 5 min. During this time, ACh will stimulate the exocytosis of catecholamines (CA). The inlet end of the capillary was then switched back to the buffer vial containing only buffer B (without BSA). CE was run at 3 kV for 5 min to migrate the released NE and E zones away from the cell. Electrophoresis was stopped, the capillary was put under a microscope, and 0.1% SDS in buffer B (without BSA) was introduced into the capillary by applying a vacuum at the outlet end. As confirmed visually through the microscope, the cell will lyse and give off the remaining NE and E. The capillary was then returned to the buffer B (without BSA and ACh) vial and CE was continued at 18 kV. Two sets of doublets were usually obtained in the electropherograms which corresponded to the released and residual NE and E. Quantitation was achieved by measuring the peak area and comparing them with those obtained for calibration runs with standard solution of NE and E between cell injection.

For dynamic release experiments, the inlet end of the capillary was put back to the buffer vial containing $5 \times 10^{-4}$ M ACh (in buffer B without BSA) after cell injection. CE was run at a relatively lower voltage (3 kV or 6 kV) for 10 min to migrate the ACh past the cell and stimulate the release. CA were migrated away from the cell immediately after they were released. This dynamic release process will cause the broadening of the doublet corresponding to the released NE and E. Electrophoresis was then stopped and the same procedures as in the static experiments were followed to lyse the cell and to run CE at a normal voltage (18 kV). From the extra peak broadening of the released NE and E peaks, the time scale of the secretion process can be elucidated.

## RESULTS AND DISCUSSION

### Separation of CA in Physiological Buffer and Treatment of Capillary

Although catecholamines have closely related structures, they can be well separated by CE under acidic conditions.[22] At higher pH, they cannot be resolved by CE.[25] We found that in physiological buffer treatment of the capillary is very important for catecholamine separation. Figure 1 shows the electropherograms of CA when the capillary was treated differently. The resolution of CA improved dramatically when the capillary was pre-treated with 0.1 M HCl. Treatment with HCl presumably removes all potential ion-exchange sites on the capillary wall. In practice, 10 min of treatment with 0.1 M HCl followed by 10 min equilibration with the running buffer can make the capillary last for a few hours without significant loss of resolution.

As seen from the experimental procedures above, it is very important for the cell to adhere to the capillary wall. This not only ensures the viability of the cell, but also helps to prevent the cell from further migration down the capillary so that the subsequent on-column procedures (introduction of secretagogue, migration of released zones and lysing of the cell)

Figure 1. Separation of catecholamines in physiological buffer B (without BSA) with differently treated capillaries. (A) new capillary equilibrated with running buffer for 15 min; (B) capillary flushed with 0.1 M NaOH for 15 min and equilibrated with running buffer for 15 min; (C) capillary flushed with 0.1 M HCl for 15 min and equilibrated with running buffer for 15 min. 4 fmol of each CA is injected; capillary length: 65 cm, 46 cm to detector; running voltage: 18 kV.

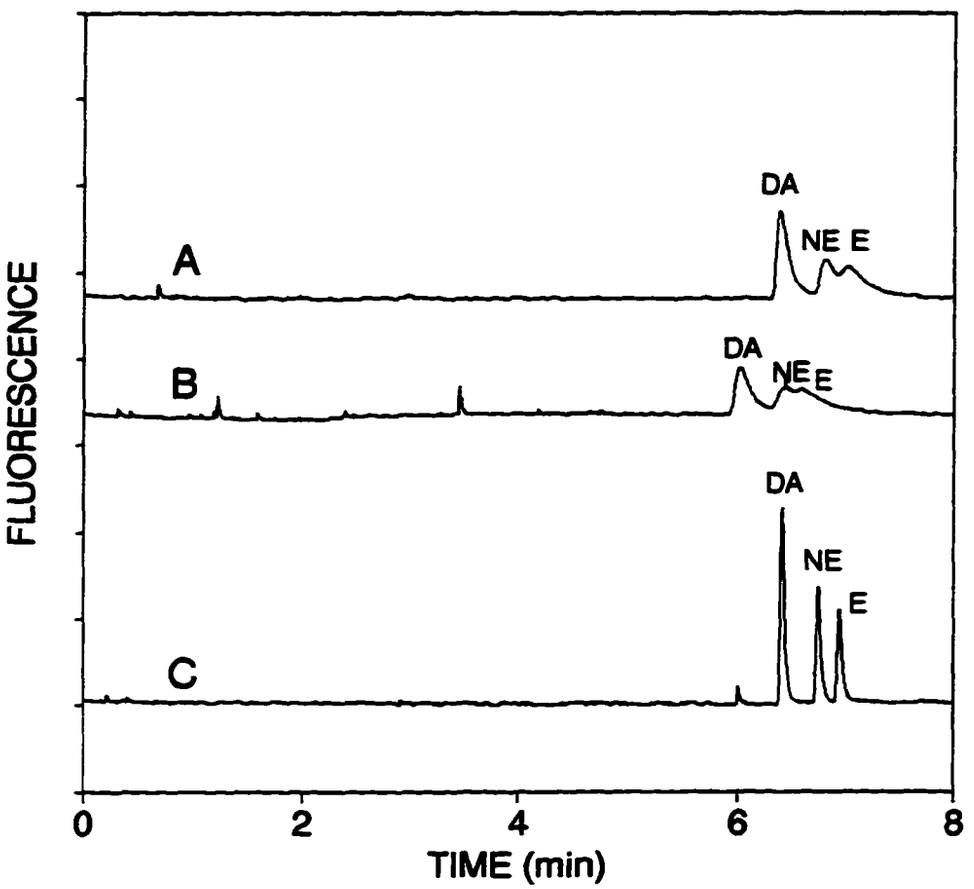
FLUORESCENCE
A
B
C
DA
NE
E
0
2
4
6
8
TIME (min)

can be implemented. We have found that treating the capillary with NaOH can help cell adhesion to the capillary wall.[14,15] However, NaOH treatment deteriorates the resolution of CA (Fig. 1B). This problem was solved by treating only a small length of the inlet end of the capillary with NaOH. In practice, a ~6 mm plug of 0.1 M NaOH was injected into the inlet end and the capillary was incubated for 5 min. The NaOH plug was then pushed out by applying pressure at the outlet end of the capillary.

**Quantitation of Release from Single Cells in Static Experiments**

Secretion of many neurotransmitters, hormones, and enzymes seems to occur in two stages. The substances to be released are first packaged into vesicles within the cell, and the contents of those vesicles are subsequently released into the external medium via exocytosis. In other words, the secretion of a cell is a biphasal process corresponding to the existence of two storage compartments of the substances to be released. It is known that activation of a number of receptors (e.g., nicotinic, cholinergic and muscarinic receptors, etc.[18,26]) on chromaffin cells will stimulate catecholamine secretion. Under physiological conditions catecholamine is released from chromaffin cells in response to stimulation of the splanchnic nerve, and the immediate stimulus to catecholamine secretion is acetylcholine released during splanchnic nerve activity. Therefore, acetylcholine was used here as the secretagogue. Bulk release experiments[24,27] have shown that the secretion of chromaffin cells is a transient process. The first phase of release is fast as studied by membrane capacitance, fluorescent probes, and electrochemical measurements.[6,7,28,29]

The experimental protocol for release experiments is shown in Figure 2. Figure 3 is a typical electropherogram obtained from static release experiments for single adrenal chromaffin cells. Earlier studies[21,22] showed that NE and E are the only natively fluorescent species present in any significant amount in these chromaffin cells. The first two

Figure 2. **Schematic diagram of on-column release and lysis processes for a single cell.**

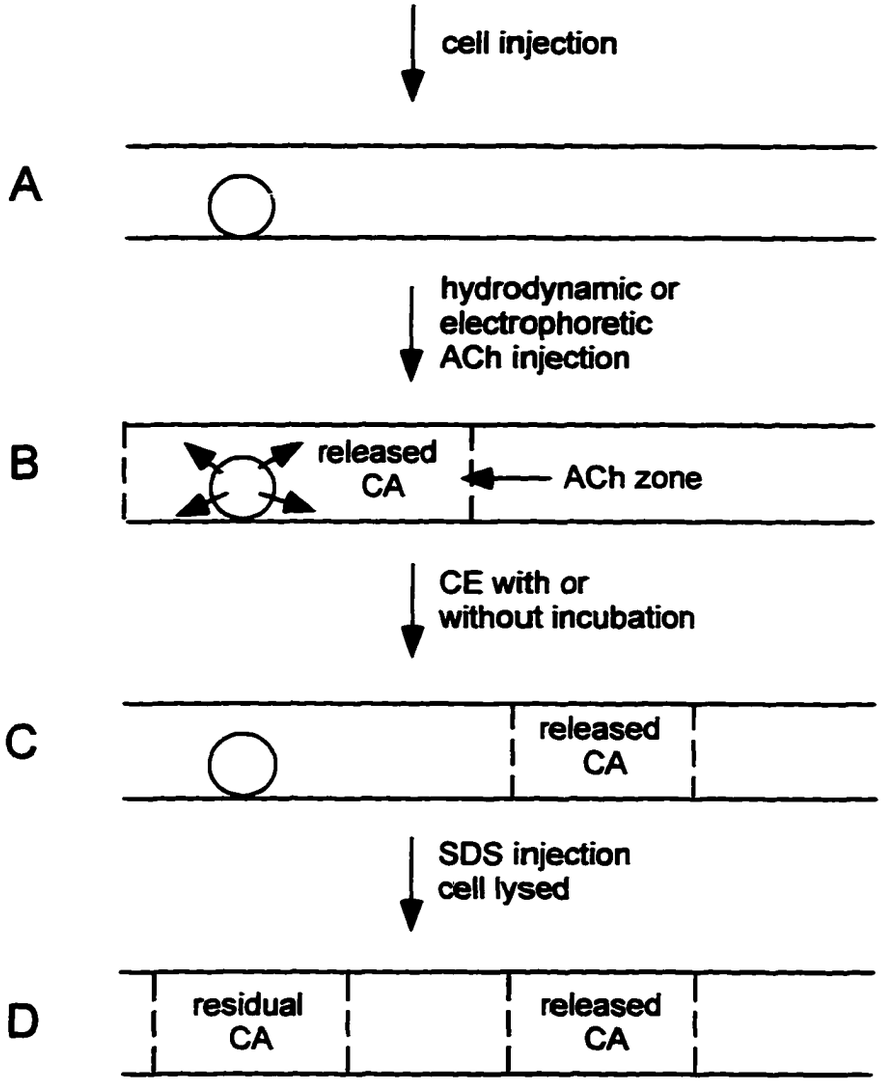
cell injection
A
hydrodynamic or
electrophoretic
ACh injection
B
released
CA
ACh zone
CE with or
without incubation
C
released
CA
SDS injection
cell lysed
D
residual
CA
released
CA

Figure 3. Electropherogram from on-column static release from a single adrenal chromaffin cell. Peaks 1 and 2 correspond to the released NE and E, respectively. Peaks 3 and 4 represent the residual NE and E inside the cell after secretion. The ordinate has been expanded to highlight peaks 1-3.

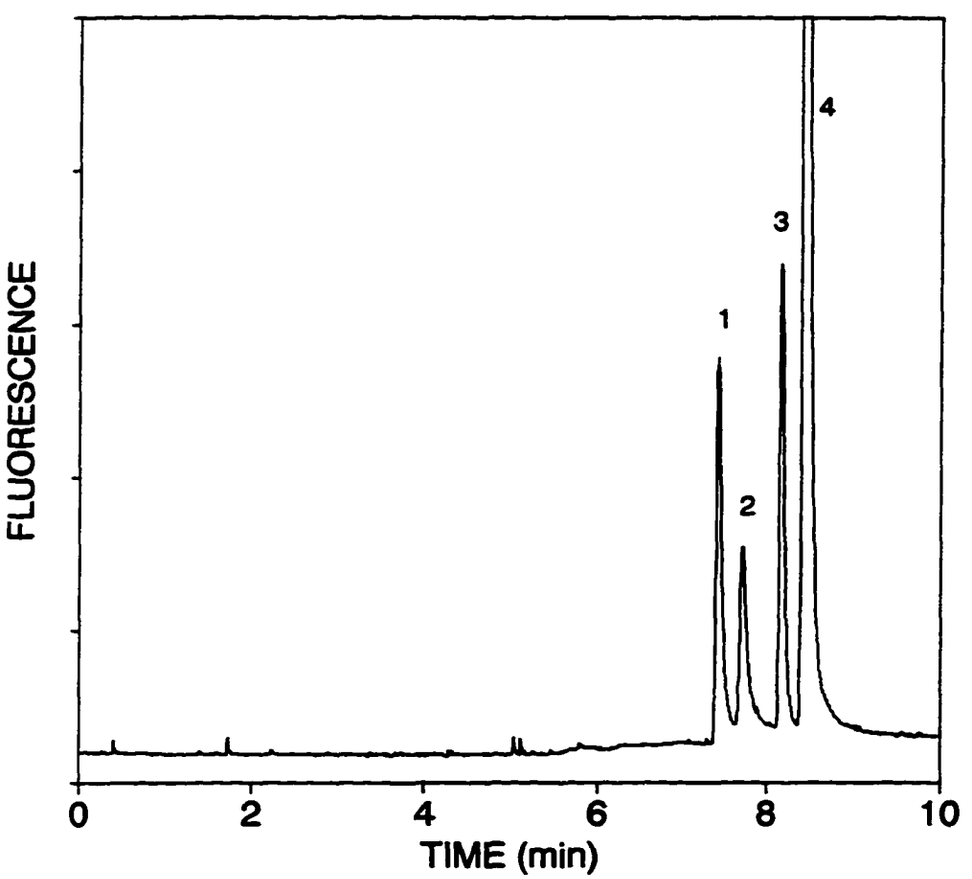
FLUORESCENCE
1
2
3
4
0
2
4
6
8
10
TIME (min)

peaks correspond to NE and E released during the 5 min incubation with ACh, respectively. These extra peaks were absent if ACh was not present. The last two peaks represent the residual NE and E in the cell after secretion (as a result of cell lysis). Since the released NE and E zones were migrated away from the cell at 3 kV for 5 min after incubation, the corresponding migration time difference between the release peak and the lysis peak due to electrophoresis at 18 kV for both NE and E should be 50 s. The actual measured values for 17 cells are (45.3 ± 10.8) s for NE and (46.3 ± 10.9) s for E. This also confirmed that the first two peaks are the released NE and E. Since the separation between NE and E is constant, we can conclude that the small amount of SDS injected did not lead to micelle formation to affect electrophoresis. The quantitative results from static release experiments on 17 individual adrenal chromaffin cells are summarized in Table 1.

Table 1 shows large variations among the cells with respect to catecholamine content as well as released amounts. Immunocytochemical studies have confirmed the existence of two distinct chromaffin cell populations that differ by the presence (epinephrine-rich cells) or absence (norepinephrine-rich cells) of phenylethanolamine N-methyltransferase (PNMT), the enzyme that converts NE to E.[30] As seen from the last column in Table 1, only one of the 17 cells can be considered to be NE-rich. Most of them (10) are E-rich. There are many cells (6) that cannot be regarded as NE- or E-dominant. No detectable dopamine was found in these cells. These results are somewhat different from those obtained by microcolumn HPLC,[21] where cultured cells were studied. It is not clear whether our isolation procedure or whether culturing the cells biased the results.

In agreement with our bulk release studies and literature reports,[31] on the average, a higher percentage of the total NE (34 ± 21%) was released than E (25 ± 23%) on the average when the cells are stimulated by ACh. This may be explained by the biosynthetic processes of NE and E. NE is synthesized from DA within intracellular secreting vesicles. The

Table 1. On-column static release of NE and E from individual adrenal chromaffin cells determined by CE-LINF

| Cell # | NE | | | E | | | NE/E | |
|---|---|---|---|---|---|---|---|---|
| | Released (fmol) | Total* (fmol) | Released (%) | Released (fmol) | Total* (fmol) | Released (%) | Released Ratio | Total Ratio |
| 1 | 19 | 62 | 31 | 185 | 310 | 60 | 0.10 | 0.20 |
| 2 | 1.7 | 23 | 7.4 | 1.6 | 7.5 | 21 | 1.05 | 3.02 |
| 3 | 1.8 | 4.9 | 36 | 2.6 | 3.5 | 75 | 0.67 | 1.39 |
| 4 | 2.8 | 90 | 3.1 | 12.1 | 220 | 5.4 | 0.23 | 0.40 |
| 5 | 25 | 203 | 10.8 | 57 | 280 | 20 | 0.43 | 0.81 |
| 6 | 2.5 | 7.0 | 36 | 3.6 | 94 | 3.9 | 0.69 | 0.07 |
| 7 | 3.4 | 8.9 | 38 | 15.9 | 61 | 26 | 0.22 | 0.15 |
| 8 | 4.1 | 13 | 31 | 16.6 | 240 | 7.0 | 0.25 | 0.06 |
| 9 | 46 | 90 | 51 | 42 | 370 | 11.2 | 1.09 | 0.24 |
| 10 | 5.2 | 49 | 10.5 | 9.2 | 370 | 2.5 | 0.57 | 0.13 |
| 11 | 2.5 | 6.2 | 40 | 8.5 | 61 | 14.0 | 0.29 | 0.10 |
| 12 | 2.6 | 12 | 22 | 9.9 | 190 | 5.2 | 0.27 | 0.06 |
| 13 | 13.9 | 24 | 57 | 1.0 | 145 | 0.7 | 14.5 | 0.17 |
| 14 | 9.8 | 26 | 37 | 54 | 103 | 27 | 0.18 | 0.13 |
| 15 | 9.4 | 19 | 50 | 80 | 210 | 38 | 0.12 | 0.09 |
| 16 | 53 | 250 | 21 | 270 | 390 | 70 | 0.19 | 0.63 |
| 17 | 25 | 28 | 94 | 13.4 | 32 | 42 | 1.89 | 0.84 |
| Mean | 13.4 | 55 | 34 | 46 | 190 | 25 | 1.34 | 0.50 |

* Total amounts are calulated from the sum of areas of the release and lysis peaks

biosynthetic steps leading to NE occur in all the adrenal chromaffin cells. However, the conversion of NE to E by PNMT occurs in cytoplasm. Therefore, NE must return to the cytoplasm, the location of PNMT, to be converted to E, which is then transported by an energy-dependent process back to the vesicles to be ready for release.[16,17] As a result, NE is more readily released by exocytosis than E, and a higher percentage of the total NE is thus released. However, differential release of NE and E may also depend on the type of secretagogues used.[32] There are reports which concluded that all E is secreted from E-rich cells and that all NE is secreted from NE-rich cells.[32,33] It is interesting to note that in this study (Table 1, last 2 columns) there seems to be no apparent relationship between the ratio of NE/E released and the original ratio of NE/E in the cell, even for cells from the same adrenal gland (cells 6 and 7, cells 8 and 9, cells 12 and 13, and cells 14 to 16).

Differential secretion of NE and E is regulated by stimulus pattern,[34] frequency of stimulation[35] and differential expression of receptor types on the surface of NE- or E-rich cells.[36] In the future, it will be interesting to determine intracellular calcium changes in the subpopulation of E- and NE-rich cells when stimulated with different secretagogues, to define to what extent these changes parallel the data on differential secretion of NE and E.[37] However, current cell isolation and separation techniques for adrenal chromaffin cells[38] do not provide pure E- or NE-rich cells for such experiments. Besides, as revealed by this and previous studies,[7,21] there are also some cells that cannot be regarded as E- or NE-rich. It is therefore important to study individual cell function and determine the cell identity simultaneously, as is done in this work.

**Peak Broadening in Static Experiments**

For Gaussian peaks, the peak variance or dispersion ($\sigma^2$) in static on-column release experiments can be expressed as:

$$\sigma^2 = \sigma^2_d + \sigma^2_e \qquad (1)$$

in which $\sigma^2_d$ corresponds to the peak broadening caused by axial diffusion, and $\sigma^2_e$ corresponds to the extra peak broadening caused by on-column manipulation (e.g., introduction of SDS to lyse the cell and the migration of the released zones during injection of the secretagogue). The extra peak broadening depends on the ruggedness of the cell towards SDS and its sensitivity to stimulation, and therefore varies from cell to cell. $\sigma^2_d$, on the other hand, can be calculated according to the following equation:

$$\sigma^2_d = 2Dt \qquad (2)$$

in which D is the diffusion coefficient for NE and E ($D = 6 \times 10^{-6}$ cm$^2$/s) and t is the time NE and E spend in the capillary before they reach the detection window. If we assume that lysing of the cell by SDS is instantaneous (confirmed by observation with a microscope), $\sigma^2_e$ for the lysis peak for NE and E can be regarded as zero. Therefore, the peak width (FWHM = $2\sigma$) for the lysis peaks can be considered as caused only by diffusion. This is a reasonable approximation since the peak width for injection of NE and E standard solutions (0.23 mm long plugs) are (4.6 ± 1.7) s and (5.4 ± 2.7) s, and the peak width for residual NE and E (on lysis) for 17 cells (Table 2) are (5.4 ± 2.5) s and (4.9 ± 2.1) s. There are only a few exceptions to this in Table 2, where the width of the lysis peak was substantially broader than expected from diffusion alone, indicating some problems with hydrodynamic manipulation of the cell. On the other hand, released NE and E spend more time in the capillary (5 min incubation, 5 min CE at 3 kV). Table 2 shows that the release peaks are typically broader than the lysis peaks. The width difference between the release peak and the corresponding

Table 2. Peak widths (s, full width at half maximum) for the release and lysis peaks for NE and E in static experiments

| | NE | | E | | Width from $\sigma_e^{2*}$ | |
|---|---|---|---|---|---|---|
| cell # | release | lysis | release | lysis | NE | E |
| 1 | 14.8 | 14.6 | 8.2 | 4.6 | 0 | 3.4 |
| 2 | 6.7 | 3.9 | 6.4 | 4.8 | 2.3 | 0 |
| 3 | 6.9 | 4.5 | 8.2 | 9.1 | 1.9 | 0 |
| 4 | 8.1 | 3.8 | 8.1 | 3.8 | 4.0 | 4.0 |
| 5 | 8.3 | 10.2 | 11.6 | 10.3 | 0 | 0 |
| 6 | 11.6 | 3.8 | 9.6 | 3.3 | 7.7 | 6.1 |
| 7 | 9.9 | 6.3 | 8.9 | 5.9 | 3.3 | 2.7 |
| 8 | 5.4 | 3.4 | 5.8 | 3.4 | 1.2 | 1.7 |
| 9 | 5.2 | 4.2 | 8.6 | 3.4 | 0 | 4.9 |
| 10 | 9.7 | 4.0 | 6.9 | 4.7 | 5.5 | 1.6 |
| 11 | 5.1 | 3.8 | 4.0 | 3.5 | 0 | 0 |
| 12 | 7.8 | 5.0 | 7.3 | 3.6 | 2.3 | 3.3 |
| 13 | 9.8 | 4.8 | 5.6 | 3.3 | 4.8 | 1.7 |
| 14 | 5.4 | 4.8 | 5.9 | 3.3 | 0 | 2.2 |
| 15 | 5.1 | 5.4 | 7.1 | 3.5 | 0 | 3.3 |
| 16 | 8.3 | 5.4 | 10.5 | 8.0 | 2.4 | 2.0 |
| 17 | 4.5 | 4.8 | 6.2 | 4.0 | 0 | 1.6 |
| mean | 7.8 | 5.4 | 7.6 | 4.9 | 2.1 | 2.3 |

*Release time corresponds to the extra peak width for release compared to lysis.

Values that are < 1 s have been set to zero.

lysis peak is therefore caused by the combination of on-column manipulation, release time, and additional diffusional broadening. As expected, the average peak widths for the corresponding release peak and lysis peak for NE and E are similar.

By correcting for diffusional broadening, the contribution of other peak broadening factors to the width of the release peak can be calculated. For the 17 cells studied, the average extra peak widths (according to Eq. 1) of the released NE and E are 2.1 s and 2.3 s, respectively. These extra peak widths provide insight into the release process. Since we injected a 2.8 mm plug of ACh to stimulate release, the width of this zone corresponds to an elution time of 2.5 s for electrophoresis at 18 kV (0.11 cm $s^{-1}$). This implies that virtually the entire ACh zone contains released CA. Release thus occurs throughout the 1 min interval when ACh is being introduced in addition to the localized process during the incubation period.

**Dynamic Release Experiments**

To learn more about the time scale of the release process, a low voltage (3 kV or 6 kV) is used to drive the ACh continuously past the cell immobilized on the capillary wall. The released NE and E will migrate away from the cell immediately after release. Because release consists of exocytosis over a relatively long time, this will make the release peaks for NE and E even broader than those in the static experiments. Figure 4 shows the electropherograms for dynamic release experiments for single chromaffin cells. As can be seen, at 6 kV the release peaks are broader relative to the release peaks at 3 kV. This is expected because the released CA are spread further axially at 6 kV (0.035 cm $s^{-1}$) than at 3 kV (0.018 cm $s^{-1}$) for identical release times. The absolute migration times are not very reproducible from cell to cell due to capillary contamination as mentioned above. However, the peak separations between the released and residual species were reproducible. The

Figure 4. Electropherograms from on-column dynamic release from single adrenal chromaffin cells. (A) 3 kV is applied when stimulated with ACh; (B) 6 kV is applied when stimulated with ACh. Peak identities are the same as in Figure 2. The ordinate has been expanded to highlight peaks 1-3.

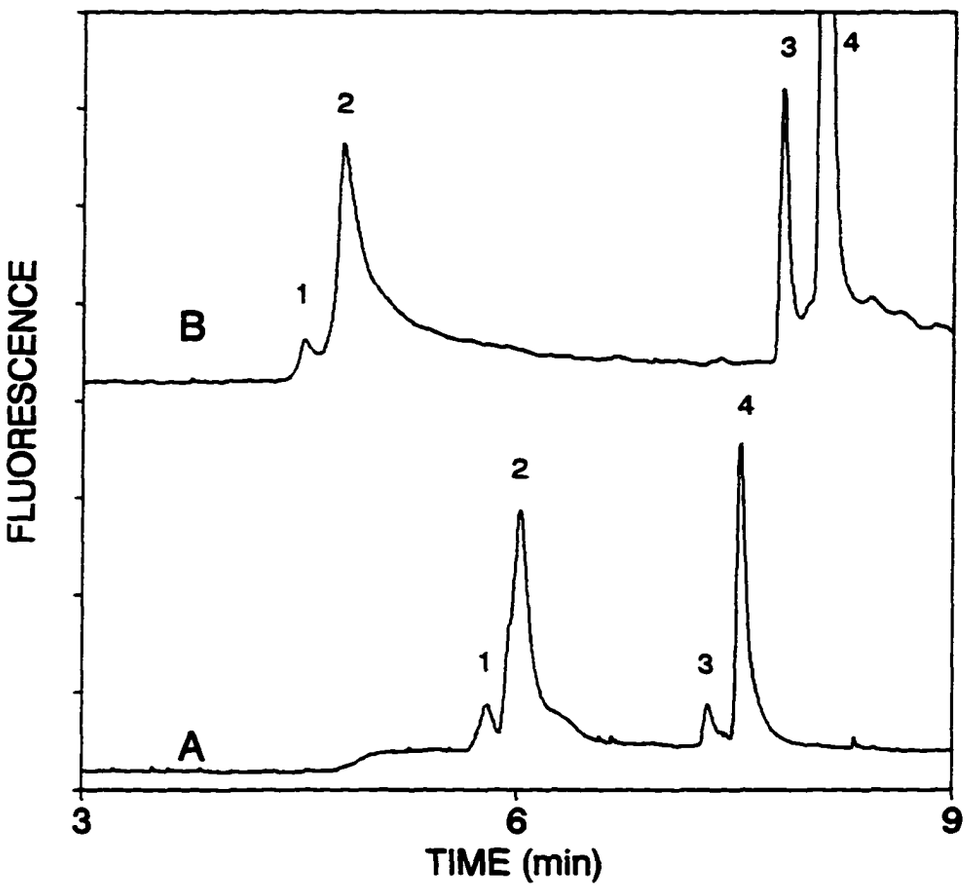
FLUORESCENCE
B
A
1
2
3
4
3
6
9
TIME (min)

theoretical peak separations between the release peak and the lysis peak are 1.67 min and 3.33 min for the application of 3 kV and 6 kV during stimulation, respectively. The experimental results are (1.57 ± 0.10) min and (2.96 ± 0.28) min for two sets of 5 cells.

Peak widths (FWHM) for 3 kV and 6 kV dynamic release experiments are summarized in Table 3. Extra peak widths after correction for on-column manipulation and diffusion can be calculated as in the static experiments. When 3 kV was applied during release, the average extra peak widths for a set of 5 cells for NE and E are 4.2 s and 5.9 s, which are larger than those in the static release experiments. When 6 kV was applied during release, the average extra peak widths for another set of 5 cells are 13 s and 14 s, which are larger than both the static release and the 3 kV release experiments. In fact, there should be a monotonic relationship between the peak widths and the linear velocities of the solution flow during stimulation.

Close examination of Figure 4 reveals that the release peaks are highly skewed rather than Gaussian-shaped. The application of Eq. 1 unduly oversimplifies the information. Indeed, the actual peak shape traces out the time course of release during dynamic stimulation at low voltage. It should be noted that since electrophoresis was run at 18 kV, the time axis in Figure 4 should be scaled 6× and 3× for 3 kV and 6 kV stimulation, respectively. We can conclude that release occurs over the entire 10-min stimulation period, with the majority of the material being produced early on in a 90 s interval.

## CONCLUSIONS

We have demonstrated the application of on-column CE-LINF for quantitative monitoring the total secretion of catecholamines from individual bovine adrenal chromaffin cells. For 17 individual cells analyzed, the average percentage of norepinephrine and epinephrine released were (34 ± 21)% and (25 ± 23)%, respectively. No obvious relationship

Table 3. **Peak widths (s, full width at half maximum) for the release and lysis peaks for NE and E in dynamic experiments**

| | NE | | E | | Width from $\sigma_e^{2*}$ | |
|---|---|---|---|---|---|---|
| cell # | release | lysis | release | lysis | NE | E |
| 3 kV | | | | | | |
| 18 | 7.4 | 5.5 | 8.1 | 5.3 | 1.2 | 2.3 |
| 19 | 17 | 3.7 | 23 | 3.1 | 13 | 20 |
| 20 | 8.4 | 5.2 | 8.7 | 4.4 | 2.8 | 4.1 |
| 21 | 6.0 | 3.4 | 6.1 | 3.4 | 2.1 | 2.2 |
| 22 | 8.0 | 5.8 | 8.2 | 6.4 | 1.7 | 1.0 |
| mean | 9.3 | 4.7 | 11 | 4.5 | 4.2 | 5.9 |
| 6 kV | | | | | | |
| 23 | 14 | 3.6 | 13 | 3.8 | 10.3 | 9.1 |
| 24 | 5.9 | 4.4 | 4.5 | 3.6 | 0 | 0 |
| 25 | 43 | 5.8 | 53 | 7.3 | 38 | 46 |
| 26 | 18 | 4.5 | 12 | 4.4 | 14 | 7.6 |
| 27 | 9.5 | 3.9 | 11 | 3.9 | 5.4 | 6.9 |
| mean | 18 | 4.4 | 19 | 4.6 | 13 | 14 |

*Release time corresponds to the extra peak width for release compared to lysis.

Values that are < 1 s have been set to zero.

between the ratio of NE/E released and the original ratio of NE/E in the cells was found. This approach provides a direct method for the quantitation of the differential secretion behavior among different cell types. Temporal information was also obtained by applying a low voltage continuously during the secretion process. The observed peak shape maps out the exact time scale of the release process. The time resolution is in the 1 s range. This is not fast enough to depict individual exocytotic events. However, the integrated release over this time scale is exactly what is needed to elucidate the effects of hormonal secretion and cell signaling. The direct quantitative results from LINF make this method a powerful alternative to the study of pharmacokinetics in neuroscience and endocrinology.

## ACKNOWLEDGMENTS

The authors thank Drs. W. H. Hsu and T.-H. Chen for guidance in cell isolation, and Mr. R. Anderson for the generous gift of bovine adrenal glands. The Ames Laboratory is operated for the U.S. Department of Energy by Iowa State University under Contract No. W-7405-Eng-82. This work was supported by the Director of Energy Research, Office of Basic Energy Science, Division of Chemical Sciences.

## REFERENCES

1. Neher, E.; Marty, A. Discrete changes of cells membrane capacitance observed under conditions of enhanced secretion in bovine adrenal chromaffin cells. *Proc. Natl. Acad. Sci. USA* **1982,** *79,* 6712-6716.
2. Penner, R.; Neher, E. The patch-clamp technique in the study of secretion. *Trends in Neurosci.* **1989**, *12*, 159-163.

3. Gryznkiewicz, G.; Poenie, M.; Tsien, R. Y. A new generation of $Ca^{2+}$ indicators with greatly improved fluorescence properties. *J. Biol. Chem.* **1985**, *260*, 3440-3450.

4. Foskett, J. K.; Grinstein, S. *Noninvasive Techniques in Cell Biology* **1990**, Wiley-Liss, NY.

5. Tsien, R. Y. Fluorescence imaging creates a window on the cell. *C&E News* **1994**, *72(29)*, 34-44.

6. Leszczyszyn, D. J.; Jankowski, J. A.; Viveros, O. H.; Diliberto, Jr., E. J.; Near, J. A.; Wightman, R. M. Nicotinic receptor-mediated catecholamine secretion from individual chromaffin cells. *J. Biol. Chem.* **1990**, *265*, 14736-14737.

7. Ciolkowski, E. L.; Cooper, B. R.; Jankowski, J. A.; Jorgensen, J. W.; Wightman, R. M. Direct observation of epinephrine and norepinephrine cosecretion from individual adrenal medullary chromaffin cells. *J. Am. Chem. Soc.* **1992**, *114*, 2815-2821.

8. Chow, R. H.; von Ruden, L.; Neher, E. Delay in vesicle fusion revealed by electrochemical monitoring of single secretory events in adrenal chromaffin cells. *Nature* **1992**, *356*, 60-63.

9. Alvarez de Toledo, G.; Fernandez-Chacon, R.; Fernandez, J. M. Release of secretory products during transient vesicle fusion. *Nature* **1993**, *363*, 554-558.

10. Pihel, K.; Showchien, H.; Jorgensen, J. W.; Wightman, R. M. Electrochemical detection of histamine and 5-hydroxytryptamine at isolated mast cells. *Anal. Chem.* **1995**, *67*, 4514-4521.

11. Tan, W.; Parpura, V.; Haydon, P. G..; Yeung, E. S. Neurotransmitter imaging in living cells based on native fluorescence detection. *Anal. Chem.* **1995**, *67*, 2575-2579.

12. Schroeder, T. J.; Jankowski, J. A.; Kawagoe, K. T.; Wightman, R. M. Analysis of diffusional broadening of vesicular packets of catecholamines released from biological cells during exocytosis. *Anal. Chem.* **1992**, *64*, 3077-3083.

13. Kristensen, H. K.; Lau, Y. Y.; Ewing, A. G. Capillary electrophoresis of single cells: observation of two compartments of neurotransmitter vesicles. *J. Neurosci. Methods* **1994**, *51*, 183-188.

14. Tong, W.; Yeung, E. S. Monitoring single-cell pharmacokinetics by capillary electrophoresis and laser-induced native fluorescence. *J. Chromatogr. B*, **1997**, *689*, 321-325.

15. Lillard, S. J.; Yeung, E. S.; McCloskey, M. A. Monitoring exocytosis and release from individual mast cells by capillary electrophoresis with laser-induced native fluorescence detection. *Anal. Chem.* **1996**, 68, 2897-2904.

16. Malven, P. V. *Mammalian Neuroendocrinology*, Chapter 13: Adrenal medulla, 1993, CRC Press, FL.

17. Cryer, P. E. The adrenal medullae, in *The Adrenal Gland,* James, V. H. T., Ed., pp. 465-489, 1992, Raven Press, NY.

18. Burgoyne, R. D. Control of exocytosis in adrenal chromaffin cells. *Biochim. Biophys. Acta* **1991**, *1071*, 174-202.

19. Burgoyne, R. D.; Morgan, A. Regulated exocytosis. *Biochem. J.* **1993**, *293*, 305-316.

20. Burgoyne, R. D. Mechanisms of catecholamine secretion from adrenal chromaffin cells. *J. Physiol. Pharmacol.* **1995**, *46*, 273-283.

21. Cooper, B. R.; Wightman, R. M.; Jorgensen, J. W. Quantitation of epinephrine and norepinephrine secretion from individual adrenal medullary cells by microcolumn high-performance liquid chromatography. *J. Chromatogr. B.* **1994**, *653*, 25-34.

22. Chang, H. T.; Yeung, E. S. Determination of catecholamines in single adrenal medullary cells by capillary electrophoresis and laser-induced native fluorescence. *Anal. Chem.* **1995**, *67*, 1079-1083.

23. Hogan, B. L.; Yeung, E. S. Determination of intracellular species at the level of a single erythrocyte via capillary electrophoresis with direct and indirect fluorescence detection. *Anal. Chem.* **1992**, *64*, 2841-2845.

24. Fenwick, E. M.; Fajdiga, P. B.; Howe, N. B. S.; Livett, B. G. Functional and morphological characterization of isolated bovine adrenal medullary cells. *J. Cell Biol.* **1978**, *76*, 12-30.

25. Wallingford, R. A.; Ewing, A. G. Retention of ionic and non-ionic catechols in capillary zone electrophoresis with micellar solutions. *J. Chromatogr.* **1988**, *441*, 299-309.

26. Burgoyne, R. D. Mechanism of secretion from adrenal chromaffin cells. *Biochim. Biophys. Acta* **1984**, *779*, 201-216.

27. Knight, D. E.; Baker, P. F. Stimulus-secretion coupling in isolated bovine adrenal medullary cells. *Quart. J. Exp. Physiol.* **1983**, *68*, 123-143.

28. Cheek, T. R.; Jackson, T. R.; O'Sullivan, A. J.; Moreton, R. B.; Berridge, M. J.; Burgoyne, R. D. Simultaneous measurements of cytosolic calcium and secretion in single bovine adrenal chromaffin cells by fluorescent imaging of fura-2 in cocultured cells. *J. Cell Biol.* **1989**, *109*, 1219-1227.

29. Finnegan, J. M.; Wightman, R. M. Correlation of real-time catecholamine release and cytosolic $Ca^{2+}$ at single bovine chromaffin cells. *J. Biol. Chem.* **1995**, *270*, 5353-5359.

30. Goldstein, M.; Fuxe, K., Hökfelt, T.; Joh, T. H. Immunohistochemical studies of phenylethanolamine N-methyltransferase, dopa decarboxylase and dopamine b-hydroxylase. *Experitia Basel*, **1971**, *27*, 951-952.

31. Greenberg, A.; Zinder, O. a- and b-receptor control of catecholamine secretion from isolated adrenal medulla cells. *Cell Tissue Res.* **1982**, *226*, 655-665.

32. Kilpatrick, D. L.; Ledbetter, F. H.; Carson, K. A.; Kirshner, A. G.; Slepetis, R.; Kirshner, N. Stability of bovine adrenal medulla cells in culture. *J. Neurochem.* **1980**, *35*, 679-692.

33. Marley, P. D.; Livett, B. G. Differences between the mechanisms of adrenaline and noradrenaline secretion from isolated bovine adrenal chromaffin cells. *Neurosci. Lett.* **1987**, *77*, 81-86.

34. Bereiter, D. D.; Engeland, W. C.; Gann, D. S. Adrenal secretion of epinephrine after stimulation of trigeminal nucleus caudalis depends on stimulus pattern. *Neuroendocrinology* **1987**, *45*, 54-61.

35. Mirkin, B. L. Factors influencing the selective secretion of adrenal medullary hormones. *J. Pharmacol Exp. Ther.* **1961**, *132*, 218-225.

36. Choi, A. Y.; Cahill, A. L.; Perry, B. D.; Perlman, R. L. Histamine evokes greater increase in phosphatidylinositol metabolism and catecholamine secretion in epinephrine-containing than norepinephrine-containing chromaffin cells. *J. Neurochem.* **1993**, *61*, 541-549.

37. Nunez, L.; Fuente, M. T. DeLa, García, A. G.; García-Sancho, J. Differential $Ca^{2+}$ responses of adrenergic and noradrenergic chromaffin cells to various secretagogues. *Am. J. Physiol.* **1995**, *269*, C1540-C1546.

38. Moro, M. A.; López, M. G.; Gandía, L.; Michelena, P.; García, A. G. Separation and culture of living adrenaline- and noradrenaline-containing cells from bovine adrenal medullae. *Anal. Biochem.* **1990**, *185*, 243-248.

# CHAPTER 3

# DIRECT VISUALIZATION OF SECRETION OF SINGLE BOVINE ADRENAL CHROMAFFIN CELLS BY LASER-INDUCED NATIVE FLUORESCENCE IMAGING MICROSCOPY

A manuscript submitted to Applied Spectroscopy

Wei Tong and Edward S. Yeung

## ABSTRACT

Direct visualization of the secretion process of individual bovine adrenal chromaffin cells was achieved with laser-induced native fluorescence imaging microscopy. By monitoring the native fluorescence of catecholamines excited by the 275-nm laser line with an intensified CCD camera, good temporal and spatial resolution were obtained simultaneously without using additional fluorescent probes. Large variations were found among individual cells in terms of the amount of catecholamines secreted and the rates of secretion. Different regions of a cell also behave differently during the secretion process. However, the degree of this local heterogeneity is smaller than in neurons and neuroglia. The influence of deep-UV laser excitation on cells is also discussed. This quantitative native fluorescence imaging technique provides a useful non-invasive approach for the study of dynamic cellular changes and the understanding of the molecular mechanisms of the secretory processes.

## INTRODUCTION

The high degree of heterogeneity of the nervous and endocrine systems makes it extremely important for real-time monitoring of dynamic chemical changes at single-cell level to gain a better understanding of the interaction of cells with their environment. Secretion mediated by exocytosis is one of the fundamental phenomena whose mechanism mimics the release of neurotransmitters at synaptic sites. Although the regulation of the secretory pathway has been studied extensively, its molecular mechanism is still not clear [1]. To further elucidate this mechanism, many real-time methods have been developed to monitor the process. Membrane capacitance measurement with patch-clamp technique [2] provides a fast but indirect means to measure the extent of exocytosis. Recent study has shown that there is a considerable delay between increase in capacitance and the release of the secretory products [3]. Amperometry and fast scan voltammetry using microelectrodes are fast and direct methods that can provide chemical information about the secretion process [4,5]. However, because microelectrodes are inherently single-point sensors, either one location of the cell or the whole cell is monitored. Some fluorescent dyes have been used successfully as intracellular fluorescent probes in microscopic imaging, although applications are limited to a few intracellular species such as calcium and other ions [6]. The combination of electrochemical methods and intracellular fluorescent probes was also possible to provide correlation of real-time release and cytosolic $Ca^{2+}$ signal [7]. Exocytotic events can also be quantitatively counted by observing the cells under a Normarski microscope through a CCD camera and an imaging processor [8].

It is important to develop methods that can follow the real-time secretory process with both high temporal and high spatial resolution. The native fluorescence of some proteins and neurotransmitters excited by a deep-UV laser has been shown to be a powerful probe for single-cell analysis with capillary electrophoresis (CE) [9, 10]. The advantages of direct

native fluorescence detection include: (1) no chemical derivatization with fluorescent dyes is needed so no contamination or additional background will be introduced; (2) uncertainties about the efficiencies of the derivatization reactions are eliminated to ensure fast and quantitative response, without influences from slow reaction kinetics or incomplete equilibrium; and (3) the biological integrity of the cells will not be unnecessarily disturbed by having additional reagents or from exposure to artificial environments. We have reported the coupling of laser-induced native fluorescence detection with CE to quantitatively monitor the secretion of insulin, serotonin and catecholamine from single cells [11-13]. The uptake of serotonin by single living astrocytes was also recorded by native fluorescence imaging microscopy [14].

The catecholamine (mainly epinephrine and norepinephrine) secreting adrenal chromaffin cells have been used as "model nerve terminals" to elucidate the molecular mechanism of neurotransmitter secretion at the nerve terminal [15, 16]. Although epinephrine and norepinephrine are fluorescent when excited with a 275-nm line from an $Ar^+$ laser, the fluorescence wavelength is in the deeper UV region (310 nm) compared to that for serotonin (350 nm). This leads to additional challenges for detection. Conventional microscopes with glass optics are no longer applicable. In the present study, we used a modified microscope with quartz lenses to achieve sensitive detection. The *in vitro* dynamics of catecholamine release from bovine adrenal chromaffin cells was monitored with both high spatial and high temporal resolution.

## EXPERIMENTAL SECTION

### Instrumentation and Imaging

A conventional upright laboratory microscope (American Optics) was used for imaging. To facilitate transmission of the deep-UV fluorescence, the original glass tube lens of the microscope was replaced with a quartz lens and the extra glass optics inside the microscope was removed. The imaging system setup is similar to our previous report [14]. An intensified CCD (ICCD) camera (Princeton Instruments) was mounted on the top port of the microscope with a home-made adapter. The 275-nm laser line from an $Ar^+$ laser (Model 2045, Spectra Physics) was isolated with an external quartz prism. It was directed with a pair of right angle quartz prism (Edmund Scientific) to the microscope sample stage. The total laser power is 150 mW. However, the power of the 275-nm line actually hit the cell was only about 1 mW. The angle of incidence was approximately 30°. An external mechanical shutter (IES004, Melles Griot) controlled by the synchronous pulse output from the ICCD system was used to ensure that the cells were exposed to laser light only during data collection. The native fluorescence was collected through a 40× quartz microscope objective (N.A. = 0.65, Carl Zeiss) and passed through a WG-305 (Melles Griot) and a UG-1 (ESCO) filters before hitting the ICCD camera.

A flow-through perfusion system similar to one described previously [17] was controlled by a syringe pump for imaging. It consisted of a plastic plate with a hole drilled at the center as the flow-through chamber, with two inlets and one outlet connected to the chamber. Two quartz cover slides (Quartz Scientific) were used to seal the chamber with the help of a thin film of vacuum grease (Apeizon). One of the cover slides was pre-coated with poly-L-lysine and mounted onto the flow chamber initially. 2μL of cell suspension was placed on the cover slide and the cells were allowed to adhere. The other cover slide was then mounted and the flow cell was filled with physiological buffer solution (PBS) through one of the inlets. The flow cell was flipped over carefully and taped onto the sample stage of the microscope to avoid movement during the experiment. Acetylcholine (ACh) ($5\times10^{-4}$ M

in PBS) was then pumped through the other inlet to stimulate cell secretion. The secretory process of the chromaffin cells was monitored by taking a sequence of "movies" with the ICCD camera. Unless otherwise stated, the exposure time for each frame was 150 ms. This allowed us to determine the release of catecholamine as a function of time based on the change in fluorescence intensity. Background variations due to the changes in laser intensity and light collection for each cell sample were normalized by dividing each data set by the background intensity (non-cell region) in the corresponding images.

### Cell Isolation and Reagents

The same bovine adrenal medullary cell isolation procedures as previously reported [13] were used. The cell viability was > 95% as assessed by trypan blue exclusion. Unless otherwise noted, all chemicals were purchased from Fisher Scientific. The PBS used for imaging experiment consists of 150 mM NaCl, 4.1 mM KCl, 1.0 mM $Na_2HPO_4$, 0.7 mM $MgCl_2$, 2 mM $CaCl_2$, 11.2 mM glucose and 10 mM HEPES. Catecholamines, epinephrine (E) and norepinephrine (NE) (Sigma, St. Louis, MO), were prepared in 0.1 M perchloric acid and stored in a refrigerator. Hank's balanced-salt solution, bovine serum albumin (BSA) (Fraction V), and acetylcholine were obtained from Sigma. Collagenase (Type I) was purchased from Worthington Biochemical (Freehold, NJ).

## RESULTS AND DISCUSSION

### Selectivity of Native Fluorescence Microscopy

Many biomolecules including biogenic amines and proteins will fluoresce naturally when excited with 275-nm laser line [18]. It is known that the adrenal chromaffin granules contain several proteins [19-21]. The wavelengths of native fluorescence of proteins excited

by 275-nm laser are at about 350 nm and 310 nm, which are primarily contributions from tryptopan and tyrosine residuals, respectively. Figure 1 shows the close resemblance in fluorescence spectra of the catecholamines and the SDS lysates of the adrenal chromaffin cells in PBS. Both exhibits fluorescence maxima at about 310 nm. No substantial amount of fluorescence is observed in the vicinity of 350 nm for cell lysates. This indicates that the proteins in chromaffin cells either do not fluoresce substantially or the amounts of proteins are so low that their fluorescence (at least by tryptopan residuals) is neglectable. This is also in agreement with our CE experiments [10, 13], where the main peaks detected using 275-nm laser excitation were NE and E. In addition, here we are looking at a time-dependent fluorescence change. Contributions from stray light and fluorescence from the background matrix, cell membrane, and cell nuclei are canceled out in the process. For these reasons, we can interpret the decrease of the fluorescence intensities as being due to the release of catecholamines and the co-release of some granular proteins. However, since the fluorescence spectra of NE and E are so similar (data not shown), it is not possible to distinguish between the release of NE vs. E.

**Catecholamine Secretion Dynamics**

Figure 2 shows some selected images for adrenal chromaffin cells when stimulated with ACh. The first image is the normal transmission optical image before stimulation and the sixth image is the transmission optical image after the experiment. The location, size and shape of each cell did not change dramatically. After the laser experiment, the cells were still viable and were not stained by trypan blue. The second to fifth images correspond to the first, 24th, 48th and 72nd frame after stimulation with ACh. The frame rate of the image sequence is 8.8 s/frame. The interval could be much shorter, but the release process under study was relatively slow.

Figure 1. Fluorescence spectra of catecholamines (NE and E) and SDS lysates of bovine adrenal chromaffin cells. Excitation wavelength: 275 nm.

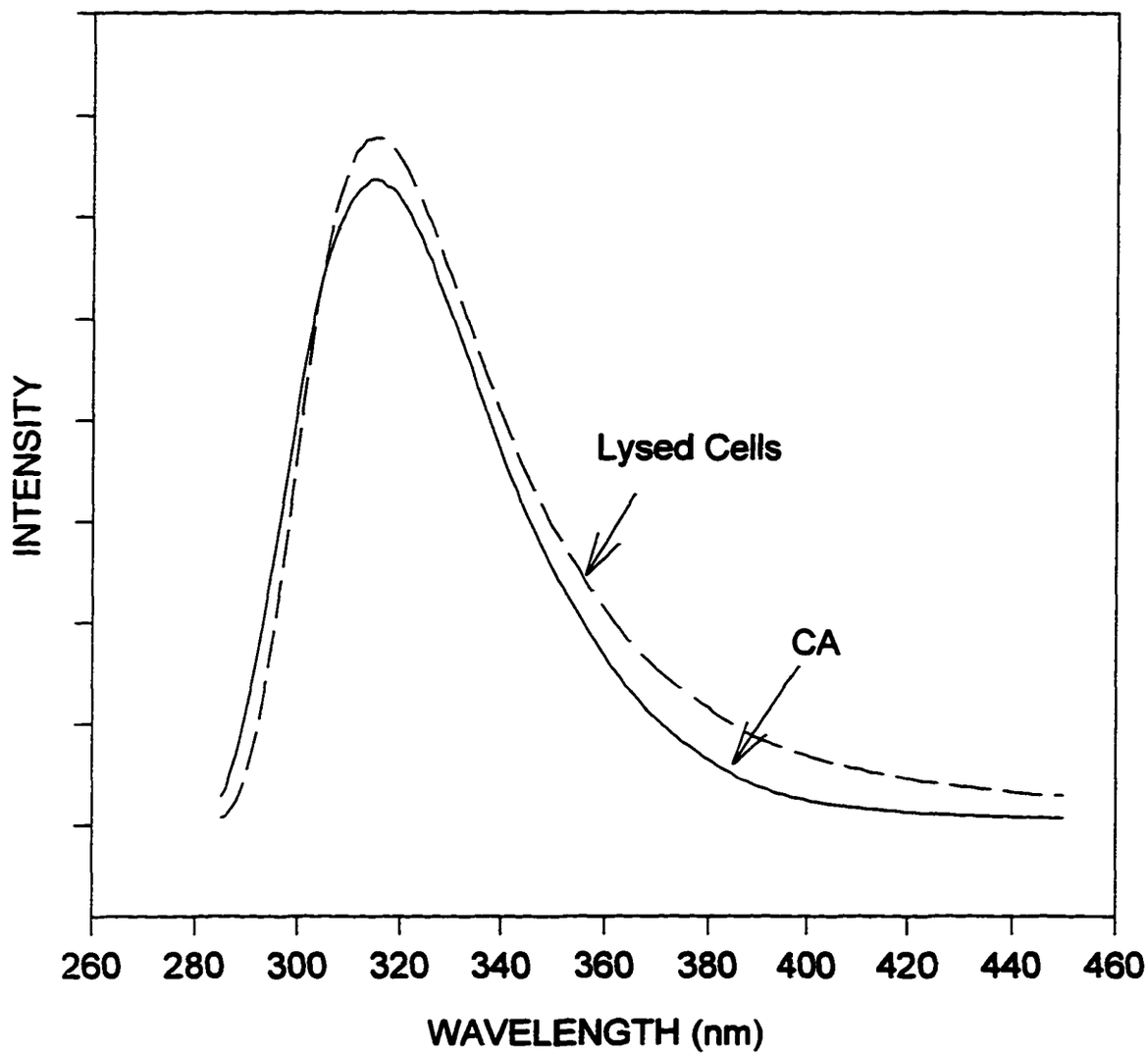
INTENSITY
Lysed Cells
CA
260
280
300
320
340
360
380
400
420
440
460
WAVELENGTH (nm)

Figure 2. Images of bovine adrenal chromaffin cells at different stages after stimulation. (1) transmission optical image of the cells before stimulation; (2) UV fluorescence image of the cells at the point of stimulation (0 sec); (3) - (5) UV fluorescence images of the cells at 211.2, 422.4 and 633.6 s after stimulation (i.e., the 24th, 48th and 72nd frames); and (6) transmission optical image of the cells after release and laser exposure.

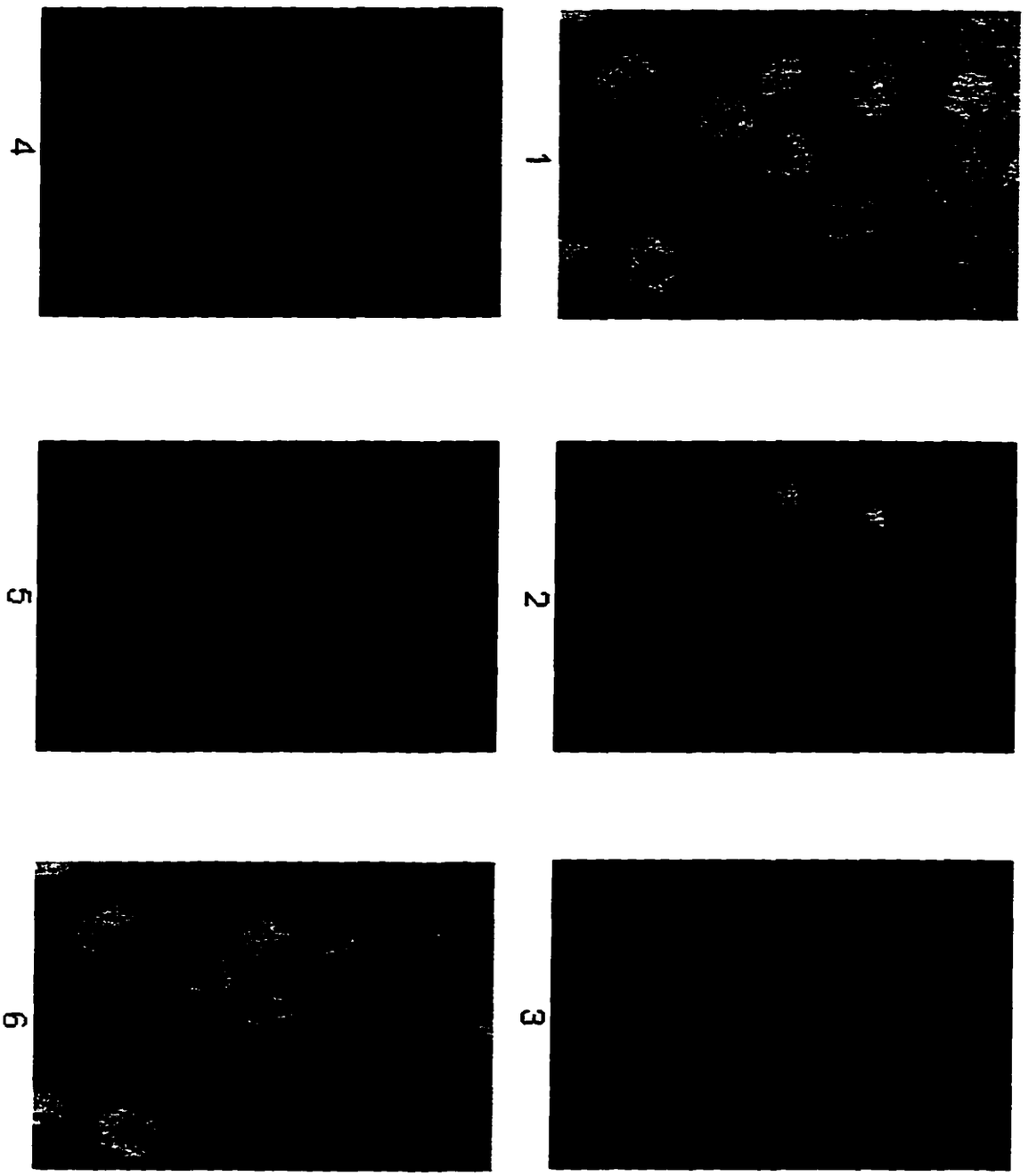
4
1
5
2
6
3

Quantitative profiles of the release process could be obtained by integrating the fluorescence intensities of each cell in each frame, and then plotting these against the time. Some typical release profiles are shown in Figure 3. The slope of the profiles reflect the rate of release at that particular time. Figure 4A shows the rate of release for the cells in Figure 3 during different time periods. As expected, there are large variations in the catecholamine content as well as the secretion kinetics among different cells. Generally, the rate of release is faster at the early stages of stimulation and slows down or even stops later on. This is in agreement with our results from dynamic release experiments in CE [13]. Bulk release experiments with many cells have shown the same trend with time [22, 23]. A plot of the average of 31 cells also shows the same trend (see Figure 4B). This can be explained by desensitization of receptors and channels and the rapid termination of the intracellular $Ca^{2+}$ signal [24, 25]. The large error bars in Fig. 4B are not due to experimental errors. They reflect actual variations among individual cells. There are also relatively large variations during the first minute, reflecting the large asynchronous release behavior at the early stages of stimulation. We also observed similar phenomena for mast cells [26].

To further prove the decrease of the UV fluorescence intensities of the cells is not due to the bleaching of catecholamine by laser exposure, we also did control experiments with catecholamine solutions and chromaffin cells without ACh stimulation. As shown in Figure 5, neither the catecholamine solution ($1.25\times10^{-3}$ M, NE/E = 1/4) nor the cells were bleached during laser exposure at the level used in this study. It is interesting to note that release here and in astrocytes [14, 17] is reflected by a decrease in fluorescence intensity, while release in mast cells [26] causes an increase in fluorescence intensity. This is because serotonin in mast cell granules are so densely packed that fluorescence quenching is the dominant relaxation process. Only when the granules are dissolved in the surrounding fluid will the native fluorescence of serotonin be observable.

Figure 3. Typical kinetics of catecholamine secretion from several adrenal chromaffin cells. The integrated fluorescence intensities of the cells were normalized to the corresponding non-cell regions.

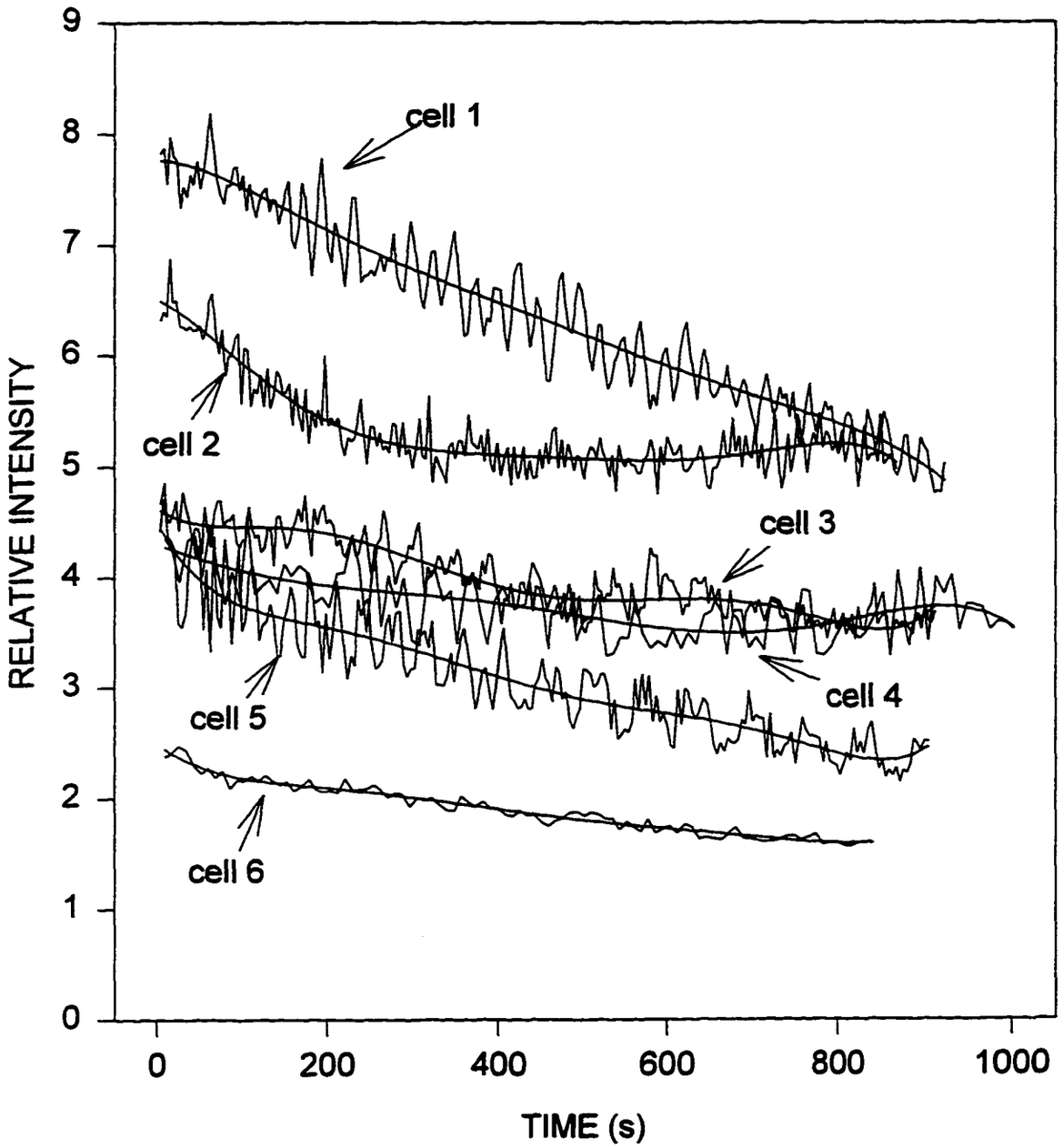
RELATIVE INTENSITY
TIME (s)
cell 1
cell 2
cell 3
cell 4
cell 5
cell 6
0
1
2
3
4
5
6
7
8
9
0
200
400
600
800
1000

Figure 4. The rates (slopes of the plots in Fig. 3) of secretion during different time periods. Time periods 1 to 5 represent intervals between 0 - 60 s, 61 - 180 s, 181 -360 s, 361 - 600 s and 601 - 900 s, respectively. (A) rates of secretion for cells 1 - 6 in Fig. 3; (B) averaged rate of secretion among all 31 cells.

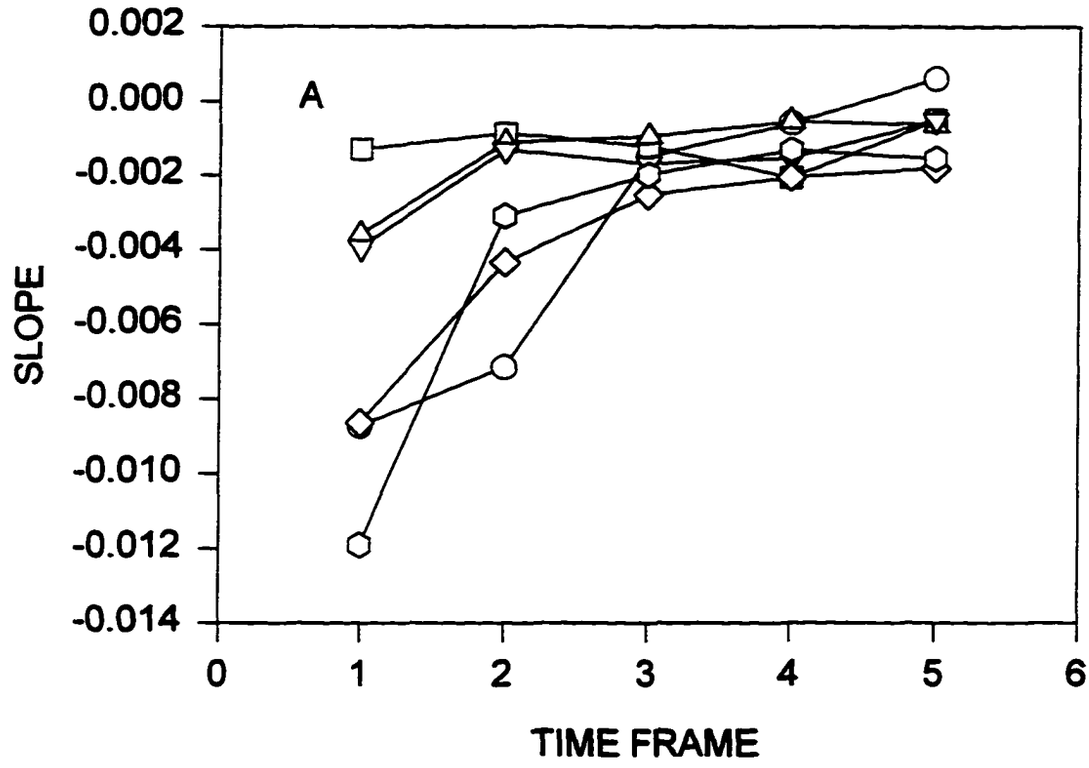
A
0.002
0.000
-0.002
-0.004
-0.006
-0.008
-0.010
-0.012
-0.014
SLOPE
0
1
2
3
4
5
6
TIME FRAME

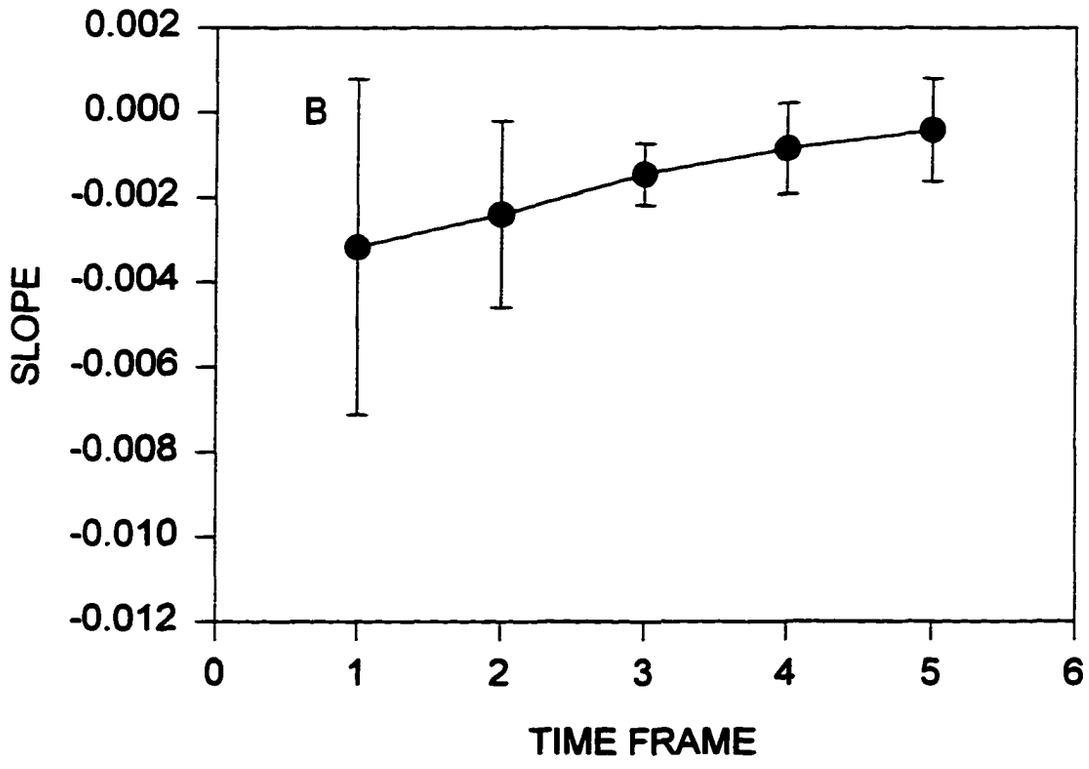
B
0.002
0.000
-0.002
-0.004
-0.006
-0.008
-0.010
-0.012
SLOPE
0
1
2
3
4
5
6
TIME FRAME

Figure 5. Control experiments with only catecholamine solution (A) and with cells without ACh stimulation (B). (A) $1.25\times10^{-3}$ M catecholamin (NE/E = 1/4) in PBS, exposure time: 500 ms, frame rate: 4.2 s/frame; (B) cells perfused with PBS only, exposure time: 150 ms, frame rate: 4.1 s/frame. O: static solution in the cell, and : flowing solution in the cell.

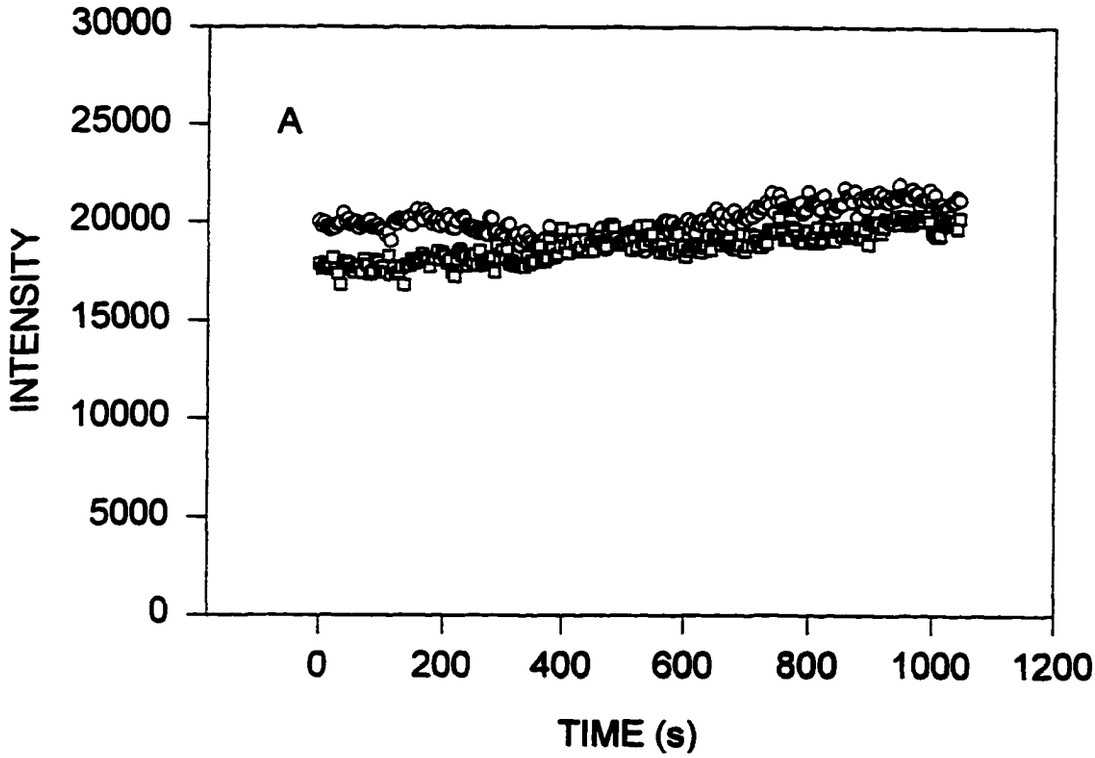
30000
25000
20000
15000
10000
5000
0
A
INTENSITY
0
200
400
600
800
1000
1200
TIME (s)

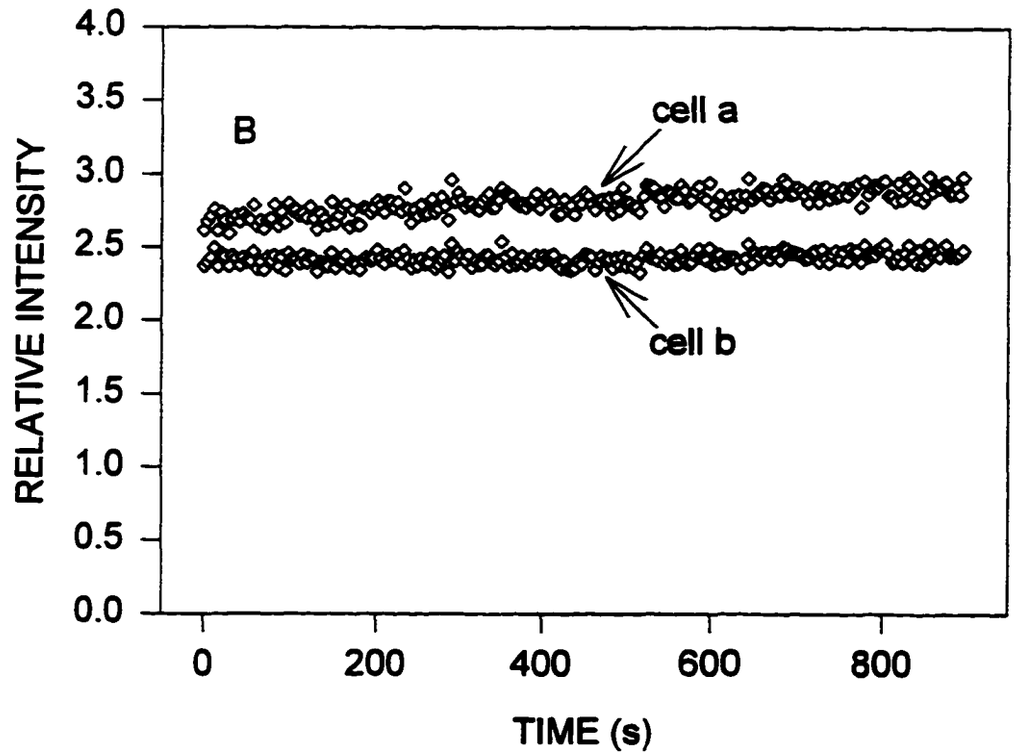
4.0
3.5
3.0
2.5
2.0
1.5
1.0
0.5
0.0
B
cell a
cell b
RELATIVE INTENSITY
0
200
400
600
800
TIME (s)

In our previous report [17], we found large local heterogeneity in serotonin release kinetics for different areas of a given astrocyte. This kind if local heterogeneity was also observed for bovine adrenal chromaffin cells here. Figure 6 shows the relative integrated intensities of 5 different regions (4×4 pixels) of the same cell (cell 1 in Fig. 3) as a function of time. Each curve in Fig. 6 was either added or subtracted by a constant to shift them apart for clarity. During a given time period, the rates of secretion at different cell regions are not the same. Amperometric detection with small diameter microelectrodes have revealed that release sites with different activities are spatially localized on endocrine cells in culture [27]. However, as in the case of mast cells [26] the degree of this heterogeneity is lower in chromaffin cells than in astrocytes [14, 17].

**Effect of UV Laser on the Cells**

In our previous study for the release of serotonin from mast cells using 305-nm laser excitation, we found that the mast cells will start to degranulate after 30 min continuous exposure to a high-intensity laser beam [26]. When using 275-nm laser excitation, this phenomena was more dramatic for adrenal chromaffin cells. In fact, when we using a longer exposure time or a higher frame rate, step-like release profiles could sometimes occur (Figure 7). Whenever such a step occurs during release process, the cell exhibiting this feature always swelled and grew in size after experiment. Furthermore, the cell can no longer exclude trypan blue. As confirmed by Fig. 5, these steps were not caused by bleaching of biomolecules by the laser. The step transition times are also different for different cells. For those cells that exhibit steps during release, the step transition times seem to be correlated with the frame rate (Figure 8), which in turn determines the total irradiation time. This highlights an important new feature of the present experimental arrangement. The use of an ICCD camera here (as opposed to a regular CCD camera in ref. 14, 17 and 26) allows the use

Figure 6. Relative fluorescence intensities from selected 4 × 4 pixel areas for cell 1 in Fig. 3. Each curves was offset by a constant to shift them apart for clarity.

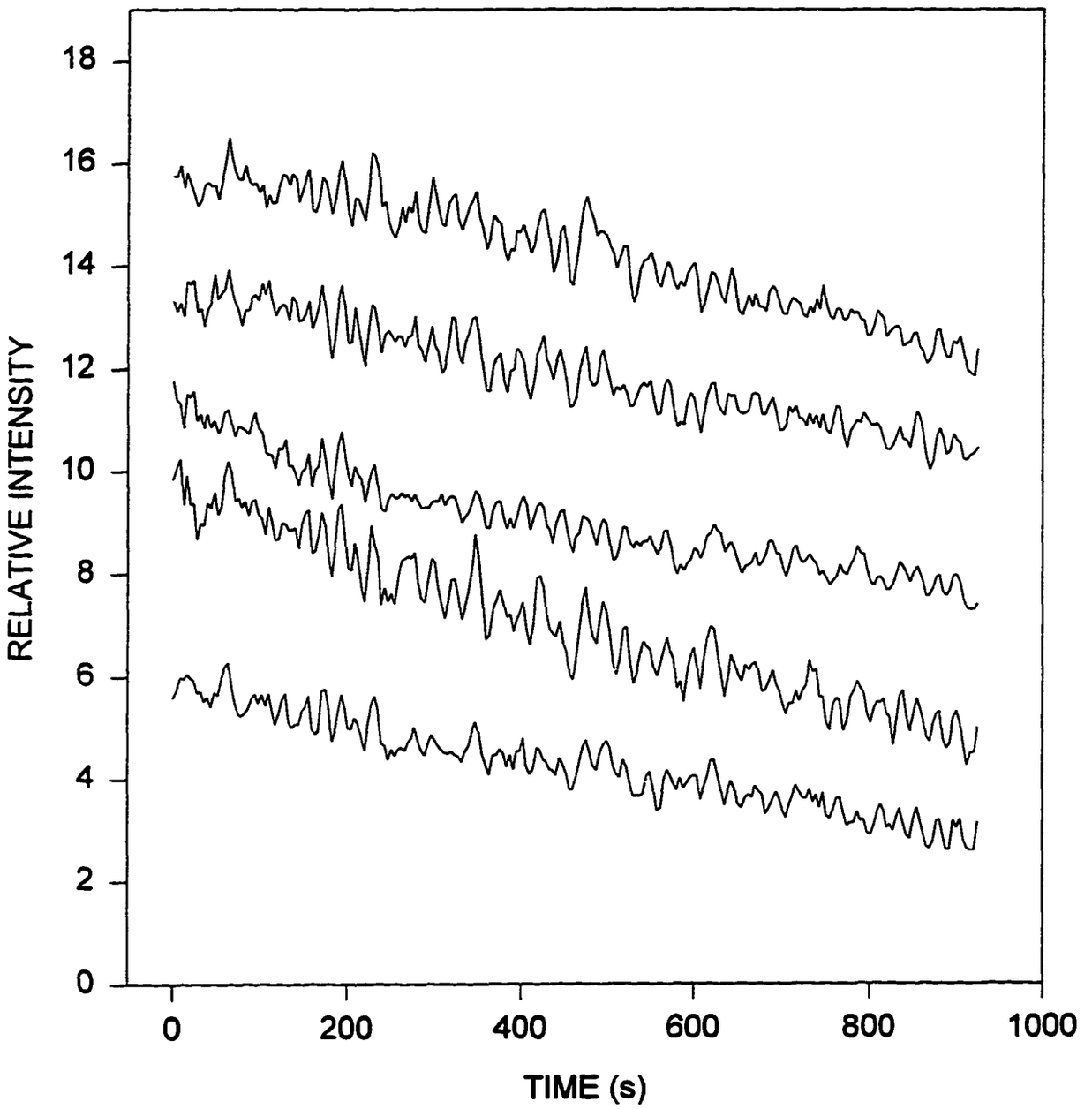
RELATIVE INTENSITY
18
16
14
12
10
8
6
4
2
0
0
200
400
600
800
1000
TIME (s)

Figure 7. Step-like release profiles that sometimes occur during long time exposure. Integrated intensities for 4 cells and for a non-cell area (bottom plot) are depicted. Exposure time: 500 ms; frame rate: 4.2 s/frame.

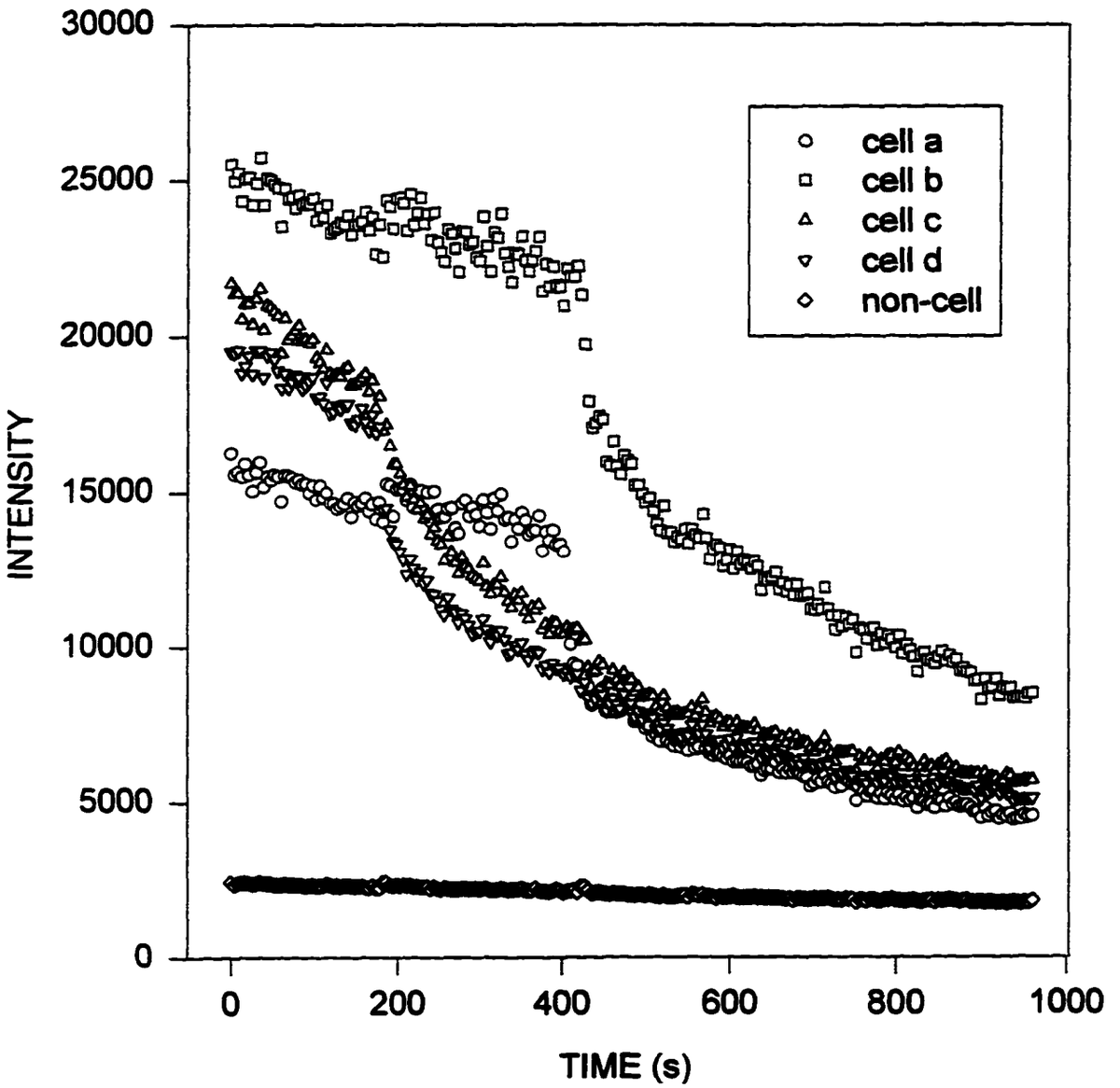
30000
25000
20000
15000
10000
5000
0
INTENSITY
0
200
400
600
800
1000
TIME (s)
cell a
cell b
cell c
cell d
non-cell

Figure 8. Correlation between the onset of the steps and the camera (exposure) frame rate.

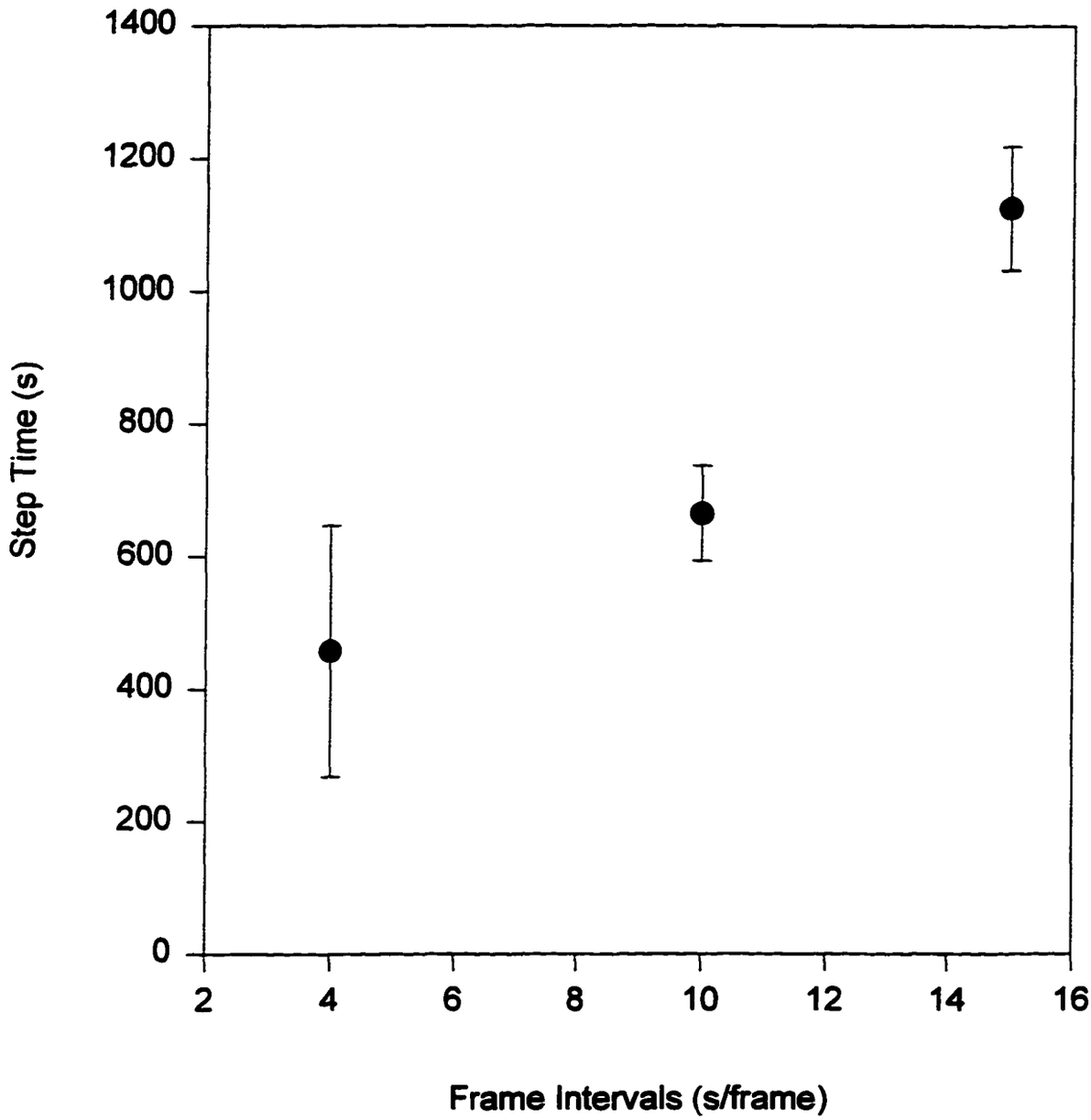
1400
1200
1000
800
600
400
200
0
Step Time (s)
2
4
6
8
10
12
14
16
Frame Intervals (s/frame)

of very low laser powers and short exposure times. The former preserves the integrity of the delicate cells here, and the latter leads to better temporal resolution.

## CONCLUSIONS

We have demonstrated that good temporal and spatial resolution can be achieved with laser-induced native fluorescence microscopy with an ICCD camera. This method is well suited for real-time monitoring of the dynamics of biochemical processes occurring in single cells because it does not depend on chemical derivatization of the biogenic species. Quantitative study of bovine adrenal chromaffin cell secretion kinetics was accomplished in this study. Large variations were found among individual cells in the amount of catecholamines secreted and the rate of secretion. Local heterogeneity in the rate of secretion during a given time period was also found. The degree of local heterogeneity is smaller in endocrine cells than that in neurons or neuroglia. Unlike CE or electrochemical methods, laser-induced native fluorescence imaging does not possess the high selectivity for confirming molecular identities of the released material. At present stage, it also does not have the ms time resolution and the sensitivity to detect single exocytotic events. This is largely limited by the frame rate of the CCD camera. However, its ability to simultaneously record spatial and temporal information is difficult to achieve with other methods such as electrochemistry, membrane capacitance, and CE. With the rapid development of video technology, native fluorescence imaging technology will continue to improve its temporal resolution and find even broader applications in biological studies.

## ACKNOWLEDGMENTS

The authors thank Drs. W. H. Hsu and T.-H. Chen for guidance in cell isolation, and Mr. R. Anderson for the generous gift of bovine adrenal glands. We also thank Dr. H.-M. Pang

for assistance with data acquisition and analysis. The Ames Laboratory is operated for the U.S. Department of Energy by Iowa State University under Contract No. W-7405-Eng-82. This work was supported by the director of Energy Research, Office of Basic energy science, Division of Chemical Sciences.

## REFERENCES

1. Burgoyne, R. D. Biochim. Biophys. Acta, 1991, *1071*, 174-202.
2. Penner, R. and Neher, E. Trends in Neurosci. 1989, *12*, 159-163.
3. Oberhauser, A. F.; Robinson, I. M. and Fernandez, J. M. Biophys. J. (A5S), 1996, *71*, 1131-1139.
4. Leszczyszyn, D. J.; Jankowski, J. A.; Viveros, O. H.; Diliberto, Jr., E. J.; Near, J. A. and Wightman, R. M. J. Biol. Chem. 1990, *265*, 14736-14737.
5. Ciolkowski, E. L.; Cooper, B. R.; Jankowski, J. A.; Jorgensen, J. W. and Wightman, R. M. J. Am. Chem. Soc. 1992, *114*, 2815-2821.
6. Tsien, R. Y. C&EN 1994, *72(29)*, 34-44.
7. Finnegan, J. M. and Wightman, R. M. J. Biol. Chem. 1995, *270*, 5353-5359.
8. Terakawa, S.; Fan, J.; Kumakura, K. and Ohara-Imaizumi, M. Neurosci. Lett. 1991, *123*, 82-86.
9. Lee, T. T. and Yeung, E. S. Anal. Chem. 1992, *64*, 3045-3051.
10. Chang, H.-T. and Yeung, E. S. Anal. Chem. 1995, *67*, 1079-1083.
11. Tong, W. and Yeung, E. S. J. Chromatogr. B 1997, *689*, 321-325.
12. Lillard, S. J. and Yeung, E. S. Anal. Chem. 1996, *68*, 2897-2904.
13. Tong, W. and Yeung, E. S. J. Neurosci. Meth. accepted.

14. Tan, W.; Parpura, V.; Haydon, P. G. and Yeung, E. S. Anal. Chem. 1995, *67*, 2575-2579.

15. Burgoyne, R. D.; Morgan, A. Biochem. J. 1993, *293*, 305-316.

16. Burgoyne, R. D. J. Physiol. Pharmacol. 1995, *46*, 273-283.

17. Tan, W.; Haydon, P. G. and Yeung, E. S. J. Appl. Spectr. accepted.

18. Schnepel, F.-H. in Fluorometric Analysis in Biomedical Chemistry, edited by Winefordner, J. D. 1991, p.69, John Wiley & Sons, NY.

19. Weiss, C.; Cahill, A. L.; Laslop, A.; Fischer-Colbrie, R.; Perlman, R. L. and Winkler, H. Neurosci. Lett. 1996, *211*, 29-32.

20. Terland, O.; Flatmark, T. and Kryvi, H. Biochim. Biophys. Acta, 1979, *553*, 460-468.

21. Winkler, H. Neurosci. 1976, *1*, 65-80.

22. Knight, D. E. and Baker, P. F. Quart. J. Exp. Physiol. 1983, *68*, 123-143.

23. Fenwick, E. M.; Fajdiga, P. B.; Howe, N. B. S. and Livett, B. G. J. Cell Biol. 1978, *76*, 12-30.

24. Holtz, R. W.; Senter, R. A. and Frye, R. A. J. Neurochem. 1982, *39*, 635-646.

25. Fenwick, E. M.; Marty, A. and Neher, E. J. Physiol. (Lond) 1982, *331*, 577-597.

26. Lillard, S. J. and Yeung, E. S. J. Neurosci. Meth. submitted.

27. Schroeder, T. J.; Jankowski, J. A.; Senyshyn, J.; Holtz, R. W. and Wightman, R. M. J. Biol. Chem. 1994, *269*, 17215-17220.

# CHAPTER 4

# SPATIAL CHARACTERIZATION OF SEROTONIN RELEASE FROM SINGLE LEECH RETZIUS NEURONS BY LASER-INDUCED NATIVE FLUORESCENCE MICROSCOPY

A manuscript in reparation to be submitted to Neuron

Wei Tong, Vladimir Parpura, Philip G. Haydon and Edward S. Yeung

## ABSTRACT

Serotonin release from single leech Retzius neurons was directly monitored by laser-induced native fluorescence microscopy. An intensified CCD camera detected the native fluorescence of serotonin in the Retzius cells excited by the 305 nm line from an Argon ion laser with simultaneous high spatial and temporal resolution. Substantially weaker fluorescence in the image of co-cultured non-serotonergic pressure sensory (P) cell compared to that of the serotonergic Retzius cell, as well as capillary electrophoresis of the Retzius cell lysate, suggested that the major native fluorescence of the Retzius cells was derived from intracellular serotonin. When extracellular $K^+$ concentration was elevated, a higher percentage of serotonin release was detected over the axon stump left from the cell isolation than the soma. The release of serotonin at the axon stump turned out to be calcium dependent. No obvious difference was found between the different regions along the axon stump in terms of the amount of serotonin released.

## INTRODUCTION

During development and regeneration a neuron can extend processes over long distances. Once at the destination the axon branches extensively to form synaptic terminals or specialized endings on the appropriate target cells. Neurons communicate with each other and with other cells in the body by releasing neurotransmitters. One of the most important neurotransmitters, serotonin, serves a variety of neuromodulatory functions in vertebrate and invertebrate species, affecting the state of alertness, hunger, strength of response, and probability of response [1]. The leech has proven to be useful for studies on many aspects of nervous system functions, including the structure and function of individual neurons, synaptic physiology, development, and behavior [2]. In the leech, the serotonergic system consists of a small number of neurons in the CNS, a major fraction of which is contained in the paired Retzius cells [3]. Retzius cells synthesize, store and release serotonin as their only classical transmitter and form a rapidly acting serotonergic synapse if co-cultured with a postsynaptic neuron [4-8]. The axon tip of the Retzius cells is a preferred region for synapse formation [7]. Electrical recordings made by loose-patch clamp show that the axon tip of the Retzius cells has the highest density of sodium channels [9, 10]. An alternative method for measuring channel distribution is optical recording [11-14] where indicator dye Arsenazo III provides a measure of changes in calcium concentration by changing its absorbance. The largest signals corresponding to the highest density of calcium channels were recorded from the axon stump left from the cell isolation procedure [13, 14]. Those methods are generally considered as indirect and do not provide the direct quantitative information about the amount of transmitter (serotonin) released and the corresponding spatial information about where the different amount of release take place. Amperometry was applied for real-time measuring the serotonin release from Retzius cells direct [15]. The amount of serotonin release from individual synaptic vesicles and the kinetics of this process were directly

determined using this method. However, electrochemical probes are inherently single-point sensors. It is difficult to obtain simultaneous temporal and spatial resolution. It will be very interesting to directly monitor the real-time release of serotonin from the Retzius cells with high spatial and temporal resolution to characterize the extent of differential releases throughout the cell.

Laser-induced native fluorescence (LINF) microscopy has proven to be a powerful direct method to image neurotransmitter distribution, uptake and releases from astrocytes, mast cells and adrenal chromaffin cells [16-18]. The native fluorescence of serotonin and catecholamines can be excited by UV beams (305 nm and 275 nm, respectively) from an $Ar^+$ laser without any derivatization and labeling. With a microscope equipped with quartz objective and optics plus the sensitive detection by intensified CCD (ICCD) camera, the power of the excitation laser and the amount of time required to obtain an image can be as low as 1 mW and a few tens of milliseconds [18]. The photodamage of the UV light to the cell and the photobleaching of the neurotransmitters can thus be minimized. In the present study, the spatial dynamics of serotonin release from single leech Retzius neurons in culture was characterized with LINF microscopy. The results shown that the extent of release was more dramatic in the axon stump region than the soma and the release was calcium dependent.

## EXPERIMENTAL

### Cell Isolation and Culture

Retzius cells were isolated from red-belly leeches (*Macrobdella*) by modification of previously reported method [19]. Desheated ganglia were exposed to a solution composed of Leibowitz's L-15 medium (no phenol red) supplemented with heated-inactivated fetal bovine serum (2% v/v), D-glucose (6 mg/mL), and gentamicin (100 μg/mL). Individual neurons

were then removed by fire-polished suction pipettes and plated into poly-L-lysine (1 mg/mL)-coated quartz-bottomed dishes. Cells were kept in culture for 1-7 days when they were used in experiments. Under these culturing conditions, cells did not develop extended neurites.

**Imaging**

An inverted microscope (Axiovert 100 TV, Carl Zeiss, Germany) equipped with a 10× quartz objective (Ultrafluar, N.A.=0.20, Carl Zeiss) was used for all imaging experiments. An ICCD camera (Princeton Instruments, Trenton, NJ) was mounted at the bottom TV port of the microscope with a C-mount adapter. The 305-nm laser line from an $Ar^+$ laser (Model 2045, Spectra Physics, Mountain View, CA) was isolated with an external quartz prism. It was directed with a pair of right-angle quartz prism (Edmund Scientific, Barrington, NJ) to the microscope sample stage from underneath without further focusing. The total laser power used was 30 mW. However, the power of the 305-nm line actually irradiating the cell was only about 4 mW. The angle of incidence was approximately 60°. An external mechanical shutter (IES004, Melles Griot, Irvine, CA) controlled by the synchronous pulse output from the ICCD controller was used to trigger the opening of the shutter. This ensured that the cells were exposed to laser light only during image data collection. The fluorescence images collected by the quartz objective passed through a WG-320 (Melles Griot) filter, two UG-1 (ESCO, Oak Ridge, NJ) filters and a UV tube lens (Carl Zeiss) before hitting the ICCD camera.

A 1-cm diameter hole was drilled at the center of a culture dish (35×10 mm). A quartz cover slide (Quartz Scientific, Fairport Harbor, OH) was glued with 5-min epoxy to seal the hole and used as the detection window of the perfusion well. The quartz cover slide was pre-coated with poly-L-lysine before plating the Retzius cells. The perfusion well was steadily

perfused at a flow rate of 10 ml/min, which exchanged the well volume about 10 times per min. The perfusion solution were normal leech Ringer (NLR), high $K^+$ leech Ringer, zero $Ca^{2+}$/EGTA high $K^+$ leech Ringer or zero $Ca^{2+}$/EGTA leech Ringer. Typically, 80 frames of images were taken with an interval of 4 s during each perfusion run. For high $K^+$ perfusion, the Retzius cells were first perfused with NLR and five images were taken. The average fluorescence intensity served as the intensity before high $K^+$ stimulation. High $K^+$ leech Ringer started to perfuse immediately after the 5th image and continued until the 30th image. After the 30th image, the cells were perfused with NLR again until the 80th image was taken. After this, the cells were allowed to recover for 5 min in NLR and another 80 frames of images were taken while perfused with NLR. These 80 frames were used as a control for photobleaching of serotonin by the laser beam and the percentage of intensity decrease in each frame was later subtracted from the corresponding frames during previous high $K^+$ perfusion. The photobleaching subtracted percentage of fluorescence intensity decrease corresponded to the percentage of serotonin released from the Retzius cells. For zero $Ca^{2+}$/EGTA high $K^+$ perfusion, the Retzius cells were first incubated in zero $Ca^{2+}$/EGTA leech ringer for 2 min and five images were taken when perfused with the same buffer. The average fluorescence intensity of these five images was used as the intensity before zero $Ca^{2+}$/EGTA high $K^+$ perfusion. Zero $Ca^{2+}$/EGTA high $K^+$ buffer then started to perfuse immediately after the 5th image and continued until the 30th image. After the 30th frame, the cells were perfused with zero $Ca^{2+}$/EGTA leech Ringer again until the 80th frame was taken. After this, the cells were recovered in NLR for 5 min and another 80 frames of images were taken when perfused with NLR. These 80 frames of images were also used as a control for photobleaching and the same subtraction was used to correct photobleaching. The photobleaching subtracted percentages of fluorescence intensity decrease during the zero $Ca^{2+}$/EGTA high $K^+$ perfusion were compared to those during high $K^+$ perfusion to determine

if the release of serotonin was $Ca^{2+}$ dependent. The percentages of serotonin released from 6×6 pixel areas at different regions of the Retzius cell were then plotted against the time, which represent the dynamics of the releases at different regions of the cell. Unless otherwise stated, the exposure time for each frame was 100 ms.

**Capillary Electrophoresis**

The home-made CE setup was similar to that described previously [20]. A 75 μm i.d., 360 μm o.d. fused-silica capillary (Polymicro Technologies, Phoenix, AZ) was used for separation and detection of serotonin and its precursors. The total length was 75 cm, and the detection window was 50 cm from the injection end. The running buffer was 20 mM Tris (pH 7.3). A high-voltage power supply (Glassman High Voltage, Inc., Whitehouse Station, NJ) was used to drive the electrophoresis at 20 kV. The same laser line with the same power as in the imaging experiments was used as the excitation source. The LINF was collected with a 10× microscope objective and passed through the same filter set as in the imaging experiment before reaching the photomultiplier tube. Electropherogram data was collected at 5 Hz with a 24-bit A/D interface (ChromPerfect, Justice Innovation, Palo Alto, CA) and stored in an IBM/PC-compatible computer.

Cultured single Retzius cells were transferred from culturing dish with the suction pipette to a dish containing 2 ml of NLR to wash away the culturing medium. The cell was then transferred to a plastic slide with a new suction pipette, washed with 20 μl of NLR and the washing buffer was removed with the pipette. 1 μl of 0.1% SDS/20 mM Tris was used to lysed the cell. Hydrodynamic injection was used to inject the cell lysate or standard solution in (0.1% SDS/running buffer). The amount of serotonin in single Retzius cells were calculated by comparing the area of the corresponding peaks in sample and standard runs.

**Reagents**

Unless otherwise noted, all chemicals were purchased from Fisher Scientific (Fair Lawn, NJ). Serotonin, DL-tryptophan, 5-hydroxytryptophan and Tris(hydroxymethyl)-aminomethan (Tris) were obtained from Sigma (St. Louis, MO). Tris running buffer was prepared by adjusting 20 mM Tris with HCl to pH 7.3. Normal leech ringer (NLR) was composed of 110 mM NaCl, 4 mM KCl, 2 mM $MgCl_2$, 2 mM $CaCl_2$ and 10 mM HEPES. The composition of high $K^+$ leech Ringer (high $K^+$) was the same as NRL except reduce the NaCl to 64 mM and raise the KCl to 50 mM. Zero $Ca^{2+}$/EGTA leech Ringer was the same as NLR but replacing $CaCl_2$ with 2 mM EGTA. Zero $Ca^{2+}$/EGTA high $K^+$ leech Ringer (zero $Ca^{2+}$/high $K^+$) was similarly prepared by reducing the NaCl to 64 mM and raising the KCl to 50 mM. All cell media was adjusted to pH 7.4 with NaOH.

## RESULTS AND DISCUSSION

**LINF Images of Retzius Cells**

Although many biogenic amines (e.g., catecholamines) and proteins will fluoresce when excited by deep UV laser, their maximum excitation wavelength is around 280 nm [21]. Most fluorescence from catecholamines and tyrosyl residues of proteins (around 310 nm) can be blocked by the 320 nm long pass filter (WG-320) used in this experiment. Possible interferences may come from the native fluorescence of tryptophan residues of cellular proteins and serotonin precursors (tryptophan and 5-hydroxytryptophan) at around 350 nm. To estimate the amount of fluorescence contributed by cellular proteins, pressure sensory cell (P cell) was imaged together with the Retzius cell (Figure 1). Histochemical fluorescence studies of the leech ganglia demonstrated that P cells are not serotonergic [3, 22]. As shown in Fig. 1, the LINF image of P cell is substantially weaker than that of Retzius cell. This

Figure 1. LINF image of co-cultured P (left) and Retzius (right) cells.

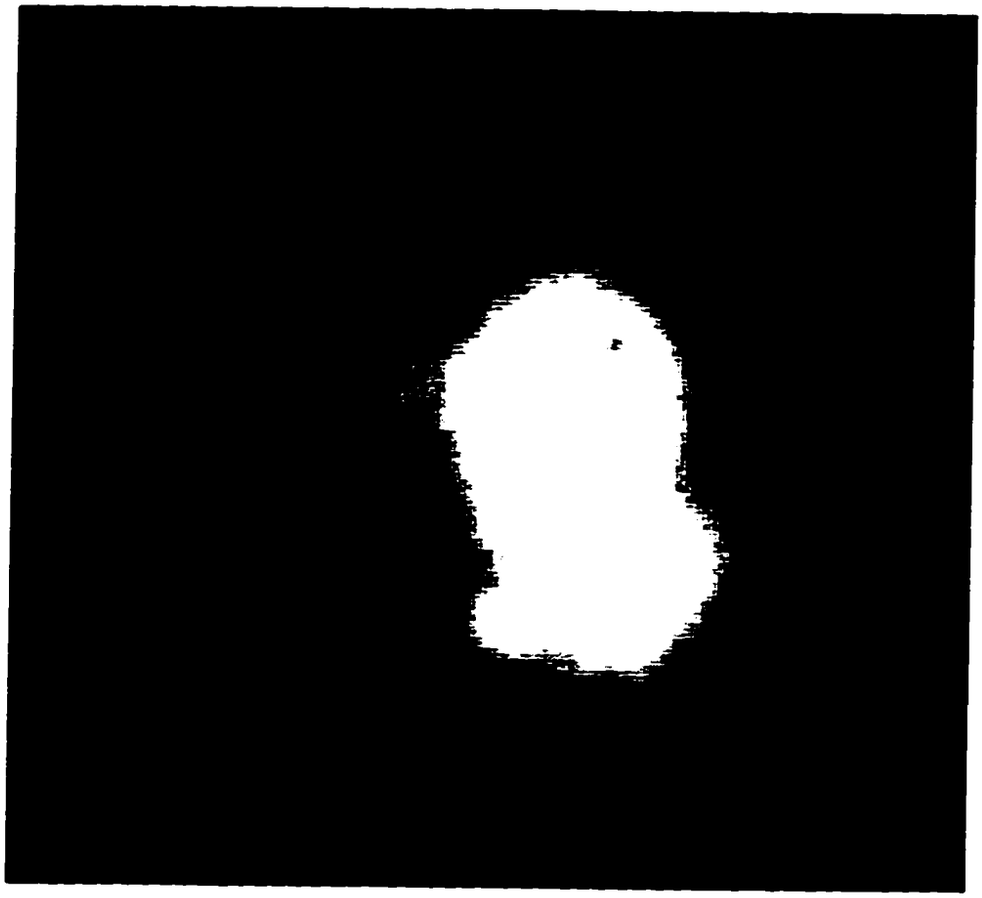

suggested that the interference of protein native fluorescence may not be an important factor. To further prove this assumption, we also did capillary electrophoresis for single Retzius cell lysate. The capillary electrophoresis results shown that only serotonin is the major native fluorescent species that exists in significant amount (Figure 2). The electropherogram for single Retzius cell also revealed three undentified minor cellular species which can not be regarded as tryptophan and 5-hydroxytryptophan (co-migrated as shown in Fig. 2A). But their fluorescences are much weaker than that of cellular serotonin. We can conclude that the native fluorescence in Retzius cell image was mainly contributed by serotonin. For 10 cells with axon stumps, the average content of serotonin in Retzius cells is 1.6±1.0 pmol. There were large variations in the serotonin content among individual cells. If we assume the Retzius cells are spherical, the average diameter measured is 82μm and the average volume is $2.9\times10^{-10}$ L. The average concentration of serotonin inside the Retzius cells is then calculated to be 5.5±3.4 mM.

**Spatial Characteristics of serotonin Release**

Previous report has demonstrated that for Retzius cells an elevation of extracellular $K^+$ concentration caused an increase in intracellular free $Ca^{2+}$ concentration ($[Ca^{2+}]_i$) and this $K^+$-induced $[Ca^{2+}]_i$ increase was completely abolished in $Ca^{2+}$-free solution [23]. Other reports shown that the highest density of calcium channels were located at the axon stump left from the cell isolation procedure [13, 14]. Using LINF imaging microscopy, we can directly measure the extent of serotonin release from different regions of the cell with high spatial resolution to determine if this release is $Ca^{2+}$ dependent. Figure 3 shows the percentages of serotonin release from axon stumps of two Retzius cells under high $K^+$ and zero $Ca^{2+}$/high $K^+$ stimulation, respectively. The images above the curves show the percentage of changes in fluorescence for the cell under high $K^+$ stimulation. When extracellular $K^+$ concentration

Figure 2. Electropherograms of serotonin. (A) $5\times10^{-7}$ M serotonin, tryptophan and 5-hydroxytryptophan in 0.1% SDS/20 mM Tris buffer, 10.3 fmol injected; (B) single Retzius cell lysed in 0.1% SDS/20 mM Tris buffer, 20.6 nL injected. Peak 1: serotonin; peak 2: tryptophan and 5-hydroxytryptophan; peak 3, 4 and 5: unidentified cellular species.

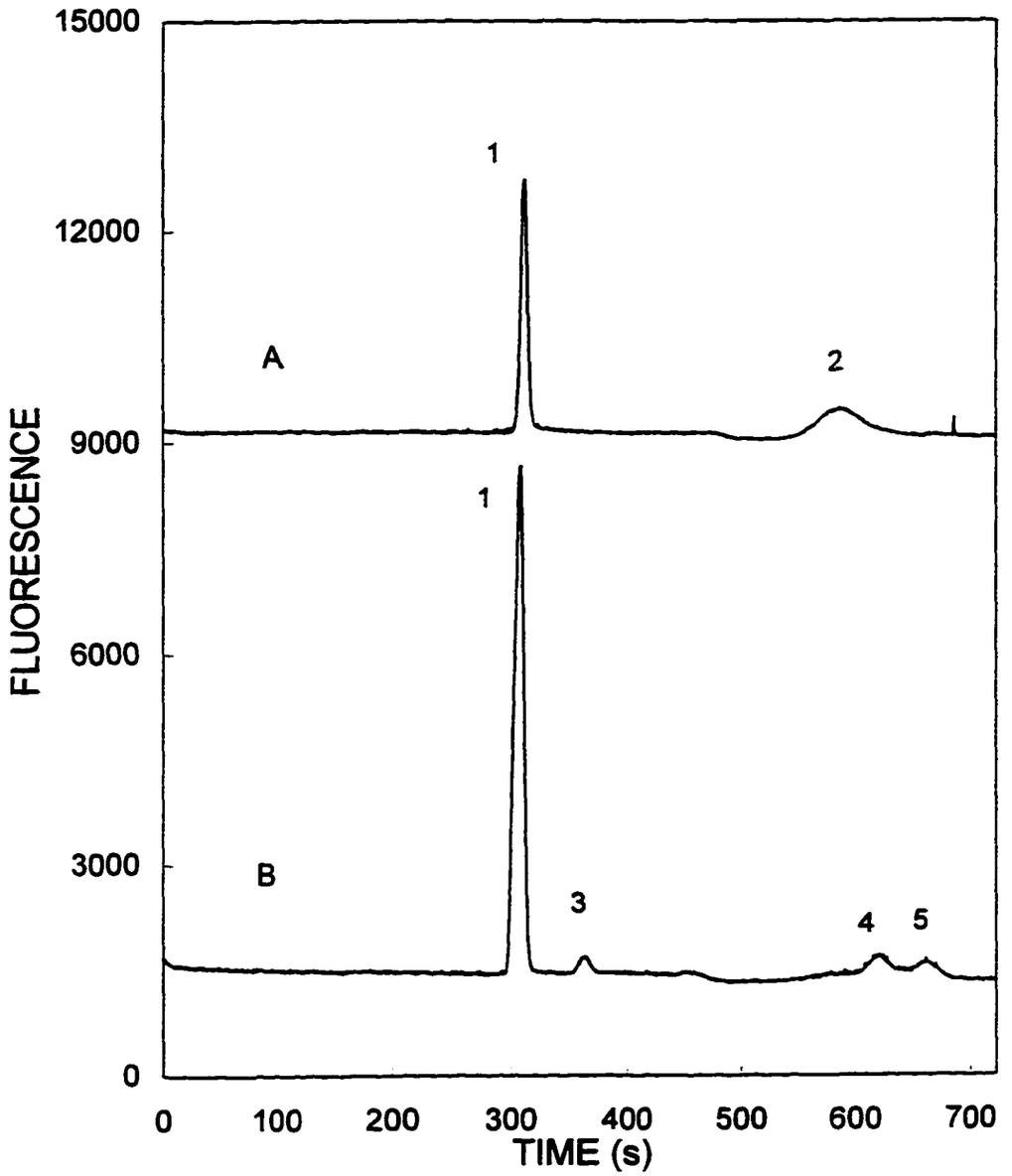
15000
12000
9000
6000
3000
0
FLUORESCENCE
A
B
1
2
1
3
4
5
0
100
200
300
400
500
600
700
TIME (s)

Figure 3. Spatial dynamics of serotonin release from single Retzius cells. The upper curve is a 6×6 pixel area at axon stump when the cell was perfused with zero $Ca^{2+}$/high $K^{+}$; the lower curve is a 6×6 pixel area at the axon stump of another cell when it was perfused with high $K^{+}$. The curves were obtained by dividing the difference between each individual frames and the average of the first five frames ($\Delta F$) with the average of the first five frames ($F_0$) multiplying 100 ($\Delta F/F_0 \times 100$). The images above the curves present the percentages of release of the cell at the 4th, 10th, 20th, 30th and 40th frames during the course of perfusion with high $K^{+}$. The images were obtained by dividing the difference between the later frames and the 1st frame ($\Delta F$) with the 1st frame ($F_0$) multiplying 100 ($\Delta F/F_0 \times 100$).

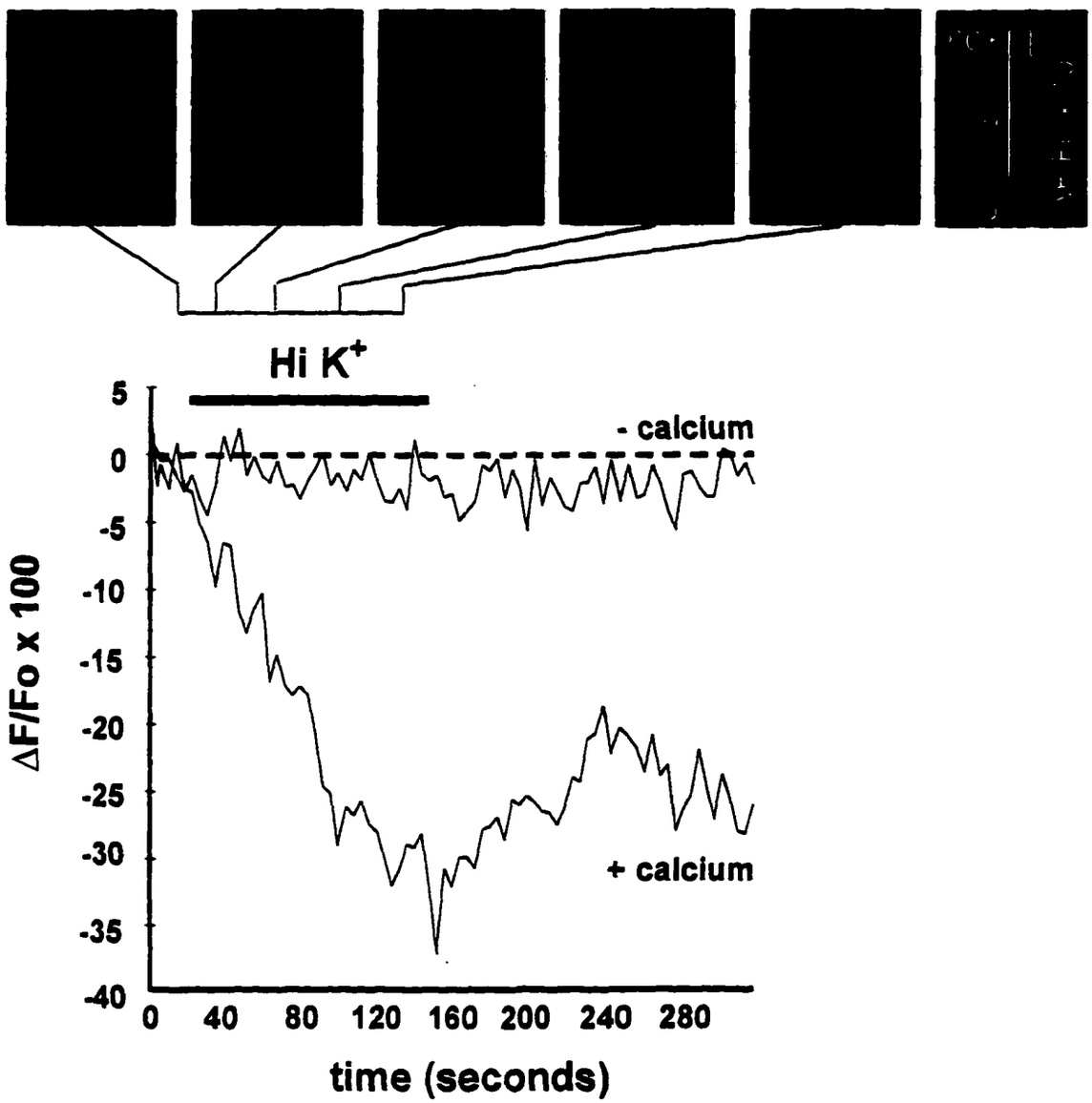
Hi K+
- calcium
+ calcium
ΔF/Fo x 100
5
0
-5
-10
-15
-20
-25
-30
-35
-40
0
40
80
120
160
200
240
280
time (seconds)

increased, there is a substantial release from the axon stump region compared to that of the soma. However, when perfused with zero $Ca^{2+}$/high $K^+$ buffer, there is no significant releases both from the axon stump and the soma. Statistic results from 6 Retzius cells also show that there is a much higher percentage of release (12.7±6.2%) from the axon stump than the soma (0.9±2.7%) (Figure 4). Comparison between the percentages of releases in the axon stump regions for 6 Retzius cells experiencing high $K^+$ and 5 cells experiencing zero $Ca^{2+}$/high $K^+$ shown that the release was almost neglectable under zero $Ca^{2+}$/high $K^+$ stimulation (Figure 5). For 4 cells with relatively long axon stump, we also examined the extent of releases from different regions along the axon stump during high $K^+$ stimulation. For 6×6 pixel areas in 1/3, 2/3 and 3/3 length regions from the axon stump tip, there was no significant difference between these different regions of the axon stump (15.5±9.3%, 11.0±3.6% and 11.9±2.5%, respectively) (Figure 6). However, all those regions shows substantial releases compared to those in the soma (Only 1.0±1.0%) (Figure 6). From these results, we conclude that a significant percentage of serotonin was released from the axon stump regions compared to that from the soma of the Retzius cells and the release is calcium dependent.

## CONCLUSIONS

We have demonstrated the application of laser-induced native fluorescence in real-time monitoring the serotonin release from single leech Retzius neurons with simultaneous temporal and spatial resolution. No chemical derivatization, which may affect the biological functions of the cell and introduce additional background, is needed for this direct detection method. In addition, the reaction kinetics of derivatization is not a concern here and this enable us to detect even faster events. Larger degrees of local heterogeneity in the extent of neurotransmitter release was found here in neurons compared to those of endocrine cells [17,

Figure 4. Comparison of serotonin releases at axon stump and soma regions for six Retzius cells under high $K^+$ stimulation.

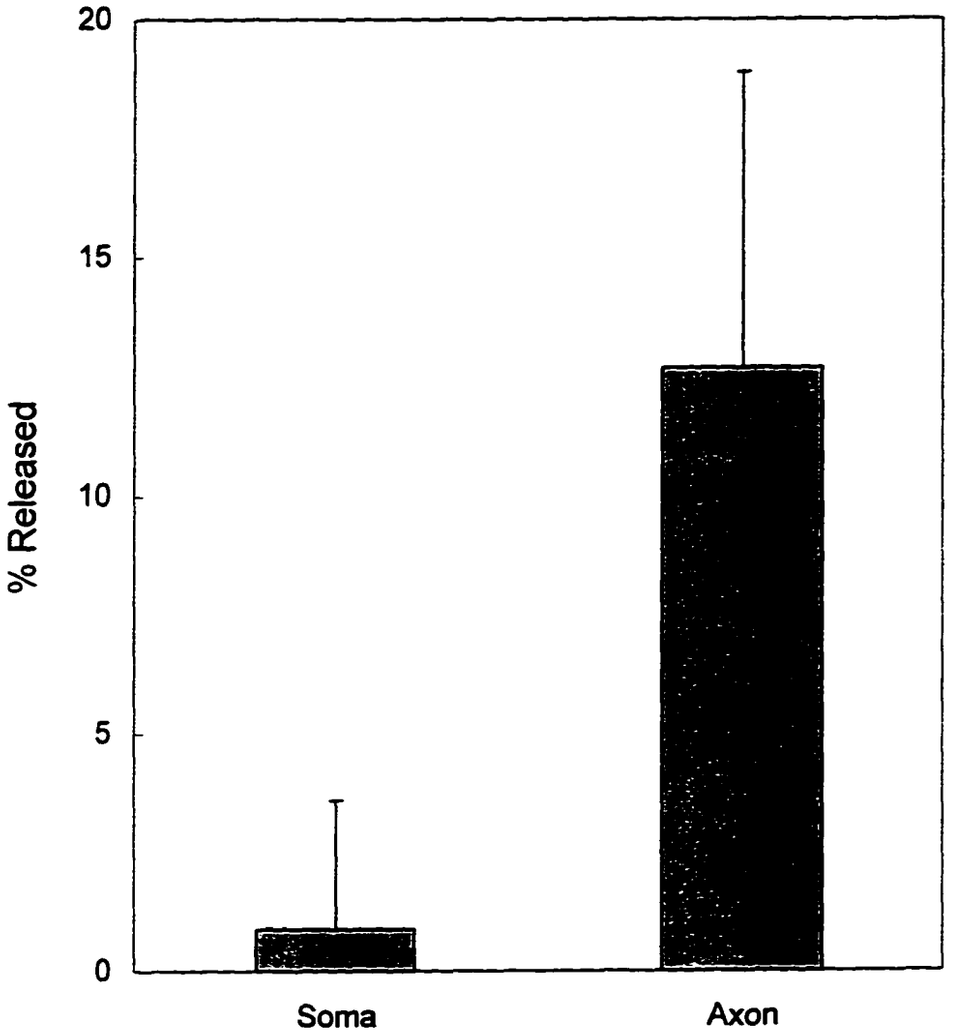
20
15
10
5
0
% Released
Soma
Axon

Figure 5. Comparison of serotonin releases at axon stump regions for Retzius cells under high $K^+$ (6 cells studied) and zero $Ca^{2+}$/high $K^+$ stimulation (5 cells studied).

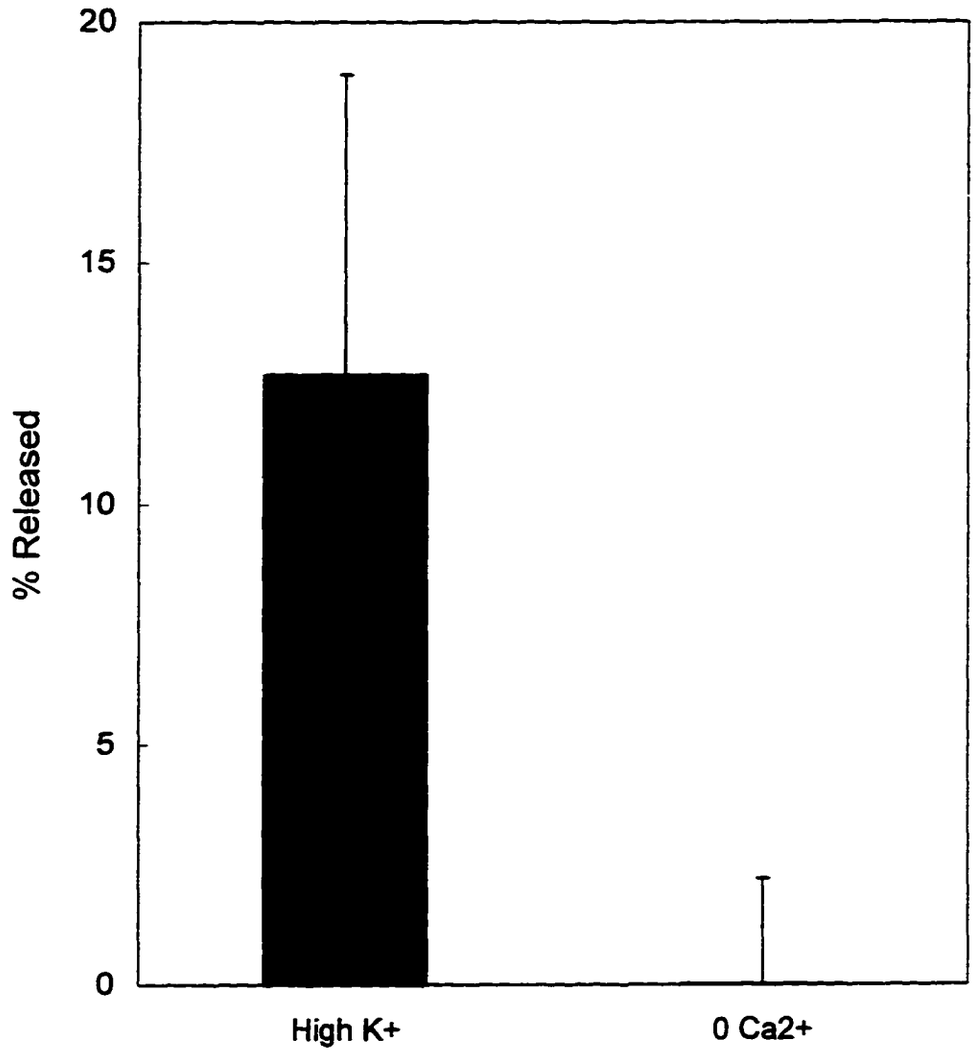
20
15
10
5
0
% Released
High K+
0 Ca2+

Figure 6. Comparison of serotonin releases from areas at the axon stumps at different distances from the axon tip and from the soma under high $K^+$ stimulation. 4 cells with relatively long axon stumps were used.

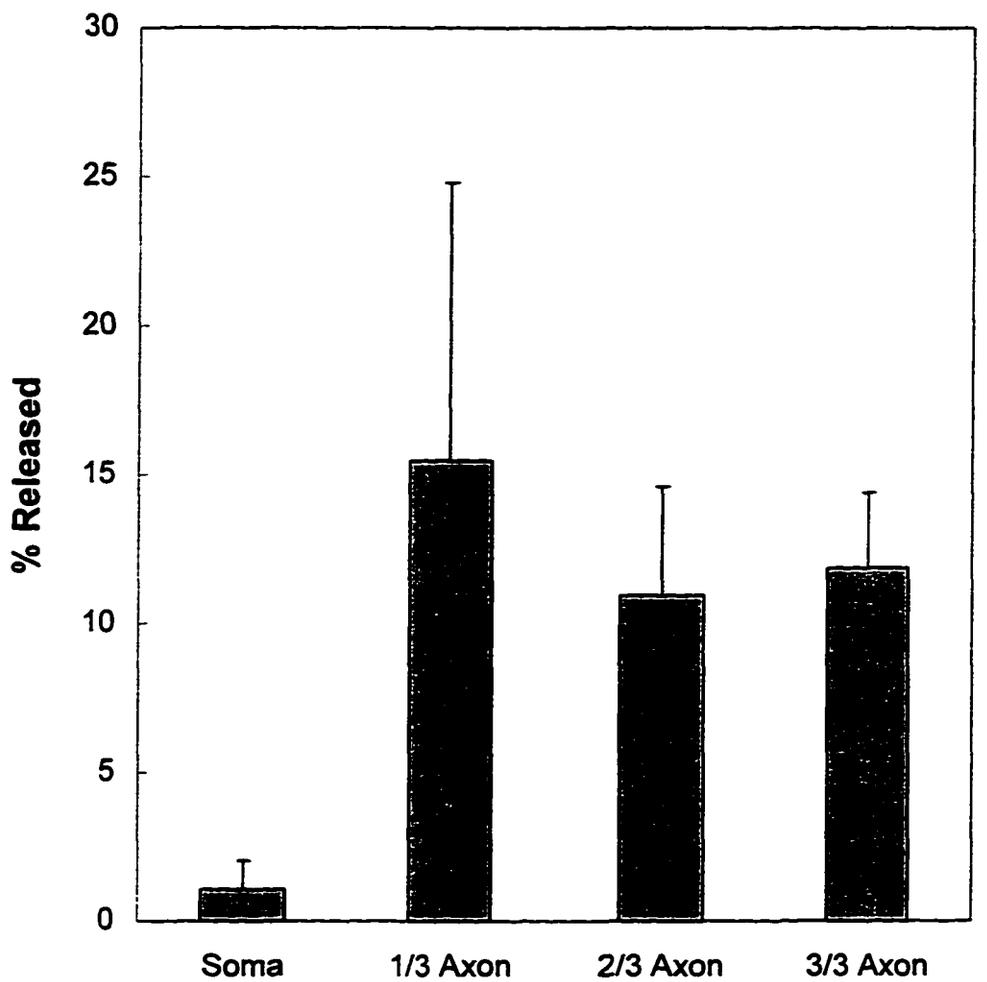
30
25
20
15
10
5
0
% Released
Soma
1/3 Axon
2/3 Axon
3/3 Axon

18]. This phenomena is also observed for astrocytes [24]. For Retzius neurons, larger percentages of serotonin release was found on the axon stump regions than on the soma. There was no significant difference in serotonin release between different regions of the axon stump. The results also shown that the release of serotonin was calcium dependent. Further work is still needed to characterize if there is any release from the soma by amperometry even though we have demonstarted here that it was very small if any. Experiments is also undergoing to measure the distribution of vesicles over the axon stump and the soma with electron microscopy and determine if the release of serotonin is due to the exocytosis of vesicles by imaging using recycling dye that fluoresce only in the vesicles and by using bafilomycin to deplete serotonin in the vesicles.

## ACKNOWLEDGMENTS

The Ames Laboratory is operated for the U.S. Department of Energy by Iowa State University under the Contract No. W-7405-Eng-82. This work was supported by the Director of Energy Research, Office of Basic Energy Sciences, Division of Chemical Sciences.

## REFERENCES

[1] Jacobs, B. L. and Fornal, C. A. 5-HT and motor control: a hypothesis. *Trends Neurosci.* 16: 346-352, 1993.

[2] Muller, K. J. and Scott, S. A. Transmission at a "direct" electrical connection mediated by an interneurone in the leech. *J. Physiol. (Lond.)* 311: 565-583, 1981.

[3] Lent, C. M., Zundal, D., Frredman, E. and Groome, J. R. Serotonin in the leech central nervous system: anatomical correlates and behavioral effects. *J. Comp. Physiol. A* 168: 191-200, 1991.

[4] Ready, D. F. and Nicholls, J. Identified neurones from the leech CNS make selective connections in culture. *Nature* 281: 67-69, 1979.

[5] Henderson, L. The role of 5-hydroxytryptamine as a transmitter between identified leech neurones in culture. *J. Physiol.* 399: 309-324, 1983.

[6] Carreta, M. The Retzius cells in the leech: a review of their properties and synaptic connection. *Comp. Biochem. Physiol.* 91A: 405-413, 1988.

[7] Nicholls, J. G. and Hernandez, U. G. Growth and synapse formation by identified leech neurones in culture: a review. *Quart. J. Exp. Physiol.* 74: 965-973, 1989.

[8] Fernandez-de-Miguel, F. and Drapeau, P. Synapse formation and function: Insights from identified leech neurons in culture. *J. Neurobiol.* 27: 367-379, 1995.

[9] Bookman, R. J., Reuter, H., Nicholls, J. G. and Adams, W. B. Loose-patch mapping of ion channel distributions in cultured leech neurons. *Society for Neuroscience Abstracts* 13: 1442, 1987.

[10] Garcia, U., Grumbacher-Reinert, S. and Nicholls, J. G. Differences in localization of $Na^+$ and $K^+$ channels in the soma, axon and growth cones of identified leech neurones in culture. *J. Physiol.* 415, 37P, 1989.

[11] Ross, W. N., Stockbridge, L. L. and Stockbridge, N. L. Regional properties of calcium entry in barnacle neurons of a barnacle ganglia. *J. Neurosci.* 4: 659-672, 1994.

[12] Ross, W. N., Arechiga, H. and Nicholls, J. G. Optical recording of calcium and voltage transients following impulses in cell bodies and processes of identified leech neurons in culture. *J. Neurosci.* 7: 3877-3887, 1987.

[13] Ross, W. N., Arechiga, H. and Nicholls, J. G. Influence of substrate on the distribution of calcium channels in identified leech neurons in culture. *Proc. Natl. Acad. Sci. USA* 85: 4075-4078, 1988.

[14] Grinvald, A., Frostig, R. D., Lieke, E. and Hildesheim, R. Optical imaging of neuronal activity. *Physiol. Rev.* 68: 1285-1366, 1988.

[15] Bruns, D. and Jahn, R. Real-time measurement of transmitter release from single synaptic vesicles. *Nature* 377:62-65, 1995.

[16] Tan, W., Parpura, V., Haydon, P. G. and Yeung, E. S. Neurotransmitter imaging in living cells based on native fluorescence detection. *Anal. Chem.* 67: 2575-2579, 1995.

[17] Lillard, S. J. and Yeung, E. S. Temporal and spatial monitoring of exocytosis with native fluorescence imaging microscopy. *J. Neurosci. Meth.* in press.

[18] Tong, W. and Yeung, E. S. Direct visualization of the secretion process of single bovine adrenal chromaffin cells by laser-induced native fluorescence imaging microscopy. *Appl. Spectr.* submitted.

[19] Dietzel, I. D., Drapeau, P. and Nicholls, J. G. Voltage dependence of 5-hydroxytryptamine release at a synapse between identified neurones in culture. *J. Physiol. (Lond.)* 372: 191-205, 1986.

[20] Hogan, B. L. and Yeung, E. S. Determination of intracellular species at the level of single erythrocyte via capillary electrophoresis with direct and indirect fluorescence detection. *Anal. Chem.* 64: 2841-2845, 1992.

[21] Schnepel, F.-H. in *Fluorometric analysis in biomedical chemistry.* edited by Winfordner, J. D. p.69, John Wiley&Sons, NY, 1991.

[22] Lent, C. M. Fluorescent properties of monoamine neurons following glyoxylic acid treatment of intact leech ganglia. *Histochemistry* 75: 77-89, 1982.

[23] Hochstrate, P., Piel, C. and Schlue, W.-R. Effect of extracellular $K^+$ on the intracellular free $Ca^{2+}$ concentration in leech glial cells and Retzius neurones. *Brain Res.* 696: 231-241, 1995.

[24] Tan, W., Haydon, P. G. and Yeung, E. S. Imaging neurotransmitter uptake and release in living astrocytes. *Appl. Spectr.* in press.

# GENERAL CONCLUSIONS

The high degree of heterogeneity of nervous and endocrine systems makes it important to study certain cellular processes at the single cell level. Laser-induced native fluorescence has proven to be a powerful direct detection method not only for measuring the intracellular components but also for monitoring the dynamic cellular processes. Capillary electrophoresis, with its compatibility with extremely small sample volumes and high separation efficiencies, has established itself as one of the most commonly used quantitative methods for single cell chemical analysis. Fluorescence microscopy features high sensitivity, high spatial and high temporal resolution making it an excellent choice for real-time monitoring of cellular processes.

This dissertation describes the advances in the direct analytical observation and measurement of pharmacokinetic responses (secretion under stimulation) at the single cell level using laser-induced native fluorescence. Capillary electrophoresis was used to quantify single or multiple neuropeptide and neurotransmitters released from individual cells. In addition to the quantitative information, temporal information was also observed. Laser-induced native fluorescence microscopic imaging was used to visualize the secretion process of individual cells directly with simultaneous high spatial and temporal resolution. These techniques can be easily extended to the study of non-fluorescent species with on-column or post-column derivatization. It is expected that interaction of small biological samples with their environments could also be studied using similar protocols to those developed in this dissertation. Drug metabolism at the cellular level may also be probed. With the development of similar imaging technologies, single molecules (e.g., HIV virus, antibody or a particular gene) may be eventually detected at single-cell level.

## ACKNOWLEDGMENT

There are so many people who gave me valuable help during my Ph. D. studies, to whom I want to extend my acknowledgment. Without them, I could not even possible to finish my study. First, I would like to thank my major professor and advisor, Professor Ed Yeung, for his guidance throughout every step of this work. His expert guidance, excellence in research, initiative ideas, encouragement, understanding and patience will benefit my whole career. It is really fortunate for me to work in his group and to learn a lot of exciting research projects going on in the group.

I would also like to acknowledge my committee members, Professors Dennis Johnson, Cheuk-Yiu Ng, Pat Thiel, James Thomas and Sam Houk, for their time in my oral examinations and reviewing my thesis.

I am also grateful to Professor Walter Hsu and Dr. Ter-Hsin Chen at the College of Veterinary Medicine for helping me preparing cells and helpful discussion. I also like to thank Professor Phil Haydon and Dr. Vlad Parpura at the Department of Zoology and Genetics for harmonic cooperation.

I would like to thank Professors Yuzhi Fang and Litong Jin, my advisors for the master degree, for the research experience in their laboratory and for their help during the early stage of my career. I also want to thank Professor Therese Cotton for introducing me of the excellent analytical chemistry program at Iowa State University during her visit in China.

I thank all Yeung group members, both past and present, for their friendship, support and cooperation, especially Qifeng Xue, Weihong Tan, Chris Smith, Sheri Lillard, Ziqiang Wang and Michael Shortreed.

Finally, I dedicate this dissertation to my wife, to may parents and to the memory of my grandparents. To my parents, I thanks you for the love, encouragement and understanding throughout my life. My greatest regret is that my grandparents, who brought me up and to

whom I am always indebted, could not share this moment with me. To my wife, Li Deng, thank you for the love, understanding and unconditional support you gave me to help me through my difficult time and to achieve my goal.

This work was performed at Ames Laboratory under Contract No. W-7405-Eng-82 with the U.S. Department of Energy. The United States government has assigned the DOE Report number IS-T 1822 to this thesis.